INSTITUTE OF INFORMATION AND
COMMUNICATION TECHNOLOGIES, ELECTRONIC
AND APPLIED MATHEMATICS (ICTEAM)

AND

INSTITUTE OF NEUROSCIENCE (IONS)

Experimental and theoretical approaches to predictive pursuit eye movements

SÉBASTIEN COPPE

Thesis submitted in partial fulfillment of

the requirements for the degree of

Docteur en Sciences de l'Ingénieur

Jury:

Prof. P. Lefèvre (Promoter), UCL, Belgium
Prof. G Masson, Aix-Marseille Univ. and CNRS, France
Prof. K. Verfaillie, KU Leuven, Belgium
Prof. M. Missal, UCL, Belgium
Dr. J.J. Orban de Xivry, UCL, Belgium
Prof. P. Van Dooren (Chair), UCL, Belgium

Acknowledgements

The work that I have achieved during the last five years would not have been possible without the involvement of several people.

My deepest considerations go to my supervisor, Professor Philippe Lefèvre for his advices and his pertinent point of view, which helped me a lot carrying out my research work. I am also very thankful to Dr. Jean-Jacques Orban de Xivry for his fresh ideas and availability during most of my projects. During my thesis, I also had the chance to actively collaborate with Dr. Demet Yüksel, Prof. Marcus Missal and Prof. Adrian Ivanoiu. This was for me an enriching experience, being a window on the neurological or clinical, but definitely non-engineering world.

I am also indebted to Prof. Paul Van Dooren for accepting to preside my thesis committee. My special thanks go the external members of the thesis jury, Prof. Guillaume Masson and Prof. Karl Verfaillie who kindly accepted to critically examine the preliminary version of the manuscript. Their comments, questions and suggestions largely enhanced its quality.

My special thanks go to my officemates Caroline Ego and Raphaël Jungers, and to my long-lasting workmate Guillaume Leclercq. I will not forget all the present and former members of the Eyelab group, with whom I shared many great moments. I would also like to thank all the members of the Euler building for the friendly working atmosphere. Thank you all for your friendship.

Finally, I wish to express my deepest gratitude to all my family for their long-lasting support. In particular, I would thank my wife Sophie, who supported me with courageous patience. The smile and the cute little face of my daughter Emilie were also a permanent source of relaxation and happiness for me.

To my loving wife Sophie
and to my smiling daughter Emilie...

Table of contents

Scope and outline of the thesis

Vision is probably our most important sense. It allows us to interact in a dynamic environment where we are surrounded by moving objects. Indeed, many aspects of our behavior are driven by visual information. One of the main functions of our brain is to accurately move the eyes in order to have a clear vision. That is why the brain has to transform visual information into accurate motor commands for the eyes. To sum up, the brain has a crucial role in deciding whether the eyes should move and in controlling the movement of our eyes. Any eye movement is therefore the consequence of neuronal activity somewhere in the brain, which is then transformed into motor commands to generate an eye movement.

Importantly, this visuomotor transformation process, with the goal of getting a clear and stabilized vision is not trivial. Indeed, objects in the external world are sometimes moving faster than the oculomotor system can react, due to some inherent delays. Therefore, the brain uses different strategies to compensate for those delays. One strategy is prediction. For instance, if you expect an object to quickly move to your right at a specific time, you will probably anticipate its movement by initiating a predictive eye movement in the expected direction. The predictive mechanisms are also crucial when the visual inputs are absent. This is the case when tracking a visual object that transiently disappears (e.g. a bird flying in the sky and briefly disappearing behind a big tree), or when you are in darkness.

This thesis focuses on the pursuit eye movements, which are required to track a moving object, i.e. to stabilize the retinal image of the moving object. In particular, predictive eye movements will be analyzed in order to better understand their mechanisms and the way they interact with visual information.

In this thesis, two different approaches are used to achieve this purpose. First, a theoretical approach consists in modeling the pursuit system, by simulating experimental data and by making hypotheses on the oculomotor behavior. This approach is then supplemented and combined with experimental studies. This thesis will show that both theoretical and experimental approaches are complementary and that each of them gives valuable information to the other.

Chapter I

This first chapter contains a general review of the literature on the pursuit and saccadic eye movements. Then, predictive eye movements are also emphasized as well as the theoretical pursuit models. Finally, a short summary of the principal neural substrates is given.

Chapter II

This chapter is devoted to the modeling of the smooth pursuit system. The novelty of this model resides in several points. First, we consider stochastic retinal inputs which are then estimated by a Kalman filter. Second, a dynamic internal representation of the target

provides an extra-retinal signal to the pursuit system. Third, these retinal and extra-retinal inputs are weighted according to their uncertainty, according to Bayesian principles. Fourth, this model is the first one capable of simulating specific experimental results linked to predictive eye movements.

Chapter III

This chapter focuses on the smooth pursuit response to biological motion, a very particular stimulus. Being able to identify people and to perceive what they are doing are essential visual abilities. Therefore, biological motion perception is probably processed differently by the visual system than other kinds of motion. Here, we show that biological motion also influences the motor response by facilitating the smooth pursuit response.

Chapter IV

The acknowledged fact that biological motion influences the smooth pursuit system raises the question of how this specific influence is achieved by the brain. We use a theoretical model to make predictions of the possible influence of biological motion on smooth pursuit eye movements during and after the transient blanking of the stimulus. Experimental data show that biological motion influences the visuomotor processing.

Chapter V

In this chapter, we analyze the involvement of the frontal lobes of the brain on the oculomotor response. We record the eye movements of patients with a mild frontal degeneration and compare their oculomotor behavior to control subjects and Alzheimer's Disease patients, which is another form of dementia. We show that the frontal patients are impaired in predictive timing, which is not the case for Alzheimer's Disease patients. This difference is so important that it could lead to a new biomarker to distinguish those two pathologies in the early stages of the disease.

Chapter VI

This last chapter discusses some implications of the results presented in the previous chapters and proposes some new theoretical and experimental perspectives.

Outcomes of the thesis

Journal papers

- Orban de Xivry J.J., Coppe S., Missal M., Lefèvre P., "Biological motion drives perception and action". Journal of Vision 10(2):6, 1-11, 2010.

- Coppe S., Orban de Xivry J.J., Missal M., Lefèvre P., "Biological motion influences the visuomotor transformation for smooth pursuit eye movements". Vision Research, 50(24):2721-2728, 2010.

- Coppe S., Orban de Xivry J.J., Yüksel D., Ivanoiu A., Lefèvre P., “Dramatic impairment of prediction due to frontal lobe degeneration”. Journal of Neurophysiology, 2012 (in press).

Conference paper

- Coppe S., Orban de Xivry J.J., Lefèvre P., Missal M., "Biological motion input to the oculomotor system". Proceedings of the 4th European Congress of Biomedical Engineering, 2008.

Articles in preparation

- Coppe S., Orban de Xivry J.J., Blohm G., Lefèvre P., “Kalman filtering accounts for visually-guided and predictive smooth pursuit dynamics”.

- Coppe S., Orban de Xivry J.J., Yüksel D., Ivanoiu A., Lefèvre P., “Smooth pursuit impairment is linked to frontal lobes degeneration: a longitudinal patient study”.

- Coppe S., Orban de Xivry J.J., Blohm G., Lefèvre P., “A model of saccade pursuit interactions based on Kalman filtering of noisy inputs”.

Conference communications

- Coppe S., Orban de Xivry J.J., Missal M., Lefèvre P., "Smooth pursuit of biological motion". Society for Neuroscience, Annual Meeting, Washington DC, 2008.

- Coppe S., Orban de Xivry J.J., Missal M., Lefèvre P., "Biological Motion boosts the oculomotor response". 28th Benelux Meeting on Systems and Control, Spa, 2009.

- Coppe S., Yüksel D., Ivanoiu A., Lefèvre P., "Predictive oculomotor behavior in patients with frontotemporal lobar degeneration". Society for Neuroscience, Annual Meeting, Chicago 2009.

- Coppe S., Orban de Xivry J.J., Blohm G., Lefèvre P., "Modeling orienting eye movements". 29th Benelux Meeting on Systems and Control, Heeze, 2010.

- Coppe S., Orban de Xivry J.J., Blohm G., Lefèvre P., "Modeling saccade pursuit interactions". Society for Neuroscience, Annual Meeting, San Diego, 2010.

- Coppe S., Orban de Xivry J.J., Blohm G., Lefèvre P., "A non-deterministic model of visual tracking". 30th Benelux Meeting on Systems and Control, Lommel, 2011.

- Coppe S., Orban de Xivry J.J., Yüksel D., Ivanoiu A., Lefèvre P., "Recording the eye movements can help to diagnose some kind of dementia". 10th National Day on Biomedical engineering, Brussels, 2011.

- Coppe S., Orban de Xivry J.J., Blohm G., Lefèvre P., A model with uncertainty to reproduce the saccade-pursuit synergies". 16th European Conference on Eye Movements, Marseille, 2011.

- Coppe S., Orban de Xivry J.J., Yüksel D., Ivanoiu A., Lefèvre P., "Predictive pursuit eye movements are degraded with frontotemporal lobar degeneration". Society for Neuroscience, Annual Meeting, Washington DC, 2011.

Seminars

- "Modeling of the interaction between smooth pursuit and saccadic eye movements". Seminar in Systems and Control (CESAME), Louvain la Neuve, May 25, 2010.

- "Predictive pursuit eye movements are degraded with frontotemporal lobar degeneration". Symposium on Memory in normal aging and preclinical dementia: Insights from cognitive studies, Brussels, September 16, 2011.

Chapter I
Introduction

Visually-guided eye movements

Vision is one of the most important senses for humans. In everyday life, having a clear vision is crucial to gather the required information to evolve in our environment. This information can then be processed and interpreted by the brain in order to generate an appropriate motor action, e.g., grasping an object, stopping at a red traffic light, hitting a tennis ball, smiling to a familiar face, etc.

Although we have the feeling that we can process the whole visual field in one single look, it is actually not the case. Basically, when the image of the visual scene is projected onto the retina, only a small part is perceived with high visual acuity. Indeed, primates have a high concentration of photoreceptors in the center of the retina, called the fovea, where the visual acuity is maximum. As the eccentricity angle increases, visual acuity rapidly decreases (Anstis, 1974).

For this reason, having accurate eye movements is crucial for humans to place and stabilize the image of the target close to the fovea in order to view the moving target optimally. This visual tracking is achieved by three types of orienting eye movements: saccades,

smooth pursuit and vergence. Two types of gaze stabilizing eye movements are added to these three gaze-shifting mechanisms: the vestibulo-ocular reflex (VOR) and the optokinetic reflex (OKN). Hereafter, we will describe these eye movements with emphasis on two important eye movements, i.e. saccades and smooth pursuit.

Saccades

The goal of the saccades is to bring the image of an object of interest onto the fovea. Therefore, saccadic eye movements are very fast jumps from one eye position to another (Fig. I.1). Saccades can reach velocities larger than 500 deg/s (since the eyes are rotating, degrees of visual angles are used to measure eye movements) and can be made towards different types of target, e.g. towards auditory or tactile stimuli (Jay and Sparks, 1984; Groh and Sparks, 1996). Saccadic eye movements have very stereotyped durations and velocity trajectories that vary systematically with saccade amplitude. The amplitude is linearly proportional to the saccade duration (for saccades larger than 5 deg) while the maximum velocity depends on saccade amplitude in a non-linear saturating way. These relationships have been called the “main sequence” of saccades (Bahill et al., 1975). Because of their short durations (30-80 ms), saccades are performed in open-loop, i.e. they cannot be controlled by visual feedback since the visual delay is around 100 ms. For that reason, it was long assumed that saccades were ballistic, i.e. their trajectory is programmed prior to the movement. However, it is not the case, since saccades can be modified in mid-flight by factors presented before

the eye starts to move (Viviani et al., 1977; Van Gisbergen et al., 1987; Smit and Van Gisbergen, 1990; Schreiber et al., 2006).

The main input used by the saccadic system to program a saccade is the distance between the target and the current eye position, i.e. the position error. The saccadic system usually undershoots the target position by about 10% (Becker, 1991). This is illustrated in Fig. I.1, where the first saccade undershoots the target. A second catch-up saccade is then triggered to realign the target on the fovea. Saccades to moving targets are also accurate. Therefore, the saccadic system also uses the target velocity as input (or more precisely the retinal slip, i.e. the velocity difference between the target and the eye) (Keller and Johnsen, 1990; Gellman and Carl, 1991; de Brouwer et al., 2001; Eggert et al., 2005; Orban de Xivry and Lefèvre, 2007). However, these two saccadic system inputs (position error and retinal slip) are not synchronized. Indeed, the first part of a short-latency saccade is only influenced by the position error while the second part of this saccade is also affected by the retinal slip. This asynchrony between position and motion signals can yield some curved saccades with two peaks in their velocity profile (instead of one usually). These saccades are referred to as “double-peaked saccades” (Schreiber et al., 2006).

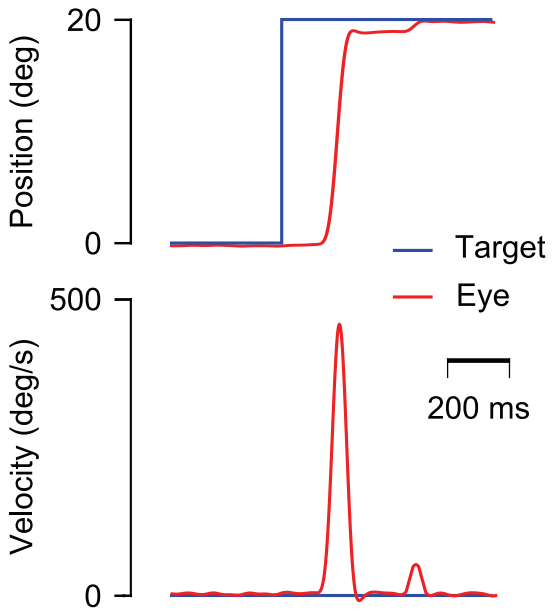

Figure I.1: Typical example of a saccadic eye movement (red traces). The upper panel represents position vs. time while the lower panel represents velocity vs. time. Target is shown in blue traces.

Saccadic latency, i.e. the time between target onset and the initiation of the eye movement, can range from 80 to 300 ms with a mean of 200 ms (Westheimer, 1954; Robinson, 1965). This saccadic reaction time toward a visual stimulus can be reduced to less than 100 ms in some conditions (Paré and Munoz, 1996; Findlay, 1998; Schiller et al., 2004). For instance, if the fixation point is extinguished 200 ms before the target appears (we say there is a “gap” period with no visible stimulus), the probability to observe a short-latency saccade is high (Fischer and Boch, 1983; Fischer and Ramsperger, 1984). Carpenter and Williams (1995) proposed a model to explain the general saccade latency distribution. The main idea is that the decision to trigger a saccadic eye movement is taken when a decision

signal reaches a threshold level. The constant rate of rise of this decision signal is randomized between trials, following a Gaussian distribution. This linear “rise to threshold” model is called the LATER model (Carpenter and Williams, 1995).

To sum up, saccades bring the image of an object of interest onto the fovea and are most of the time followed by visual fixation. In many situations, however, objects move relative to the viewer and this is where smooth-pursuit eye movements come into play.

Pursuit

Smooth pursuit eye movements stabilize the image of the moving target on the fovea, thereby supporting high-acuity analysis of the tracking target. The high visual acuity of a moving target is the consequence of minimal retinal image motion on the fovea. It has been shown that vision is degraded if the retinal slip (i.e. the velocity error) exceeds a speed of 3-4 deg/s (Westheimer and McKee, 1975; Barnes and Smith, 1981; Demer et al., 1994).

Pursuit eye movements are slower movements than saccadic eye movements. Meyer et al. (1985) measured the maximum pursuit velocity in human subjects. Pursuit gain (i.e. the ratio between eye velocity and pursuit velocity) was usually larger than 0.9 when tracking stimuli moved at a constant velocity up to 100 deg/s, but declined for larger velocities. Despite the fact that pursuit is a voluntary response, it is impossible to initiate a pursuit eye movement without a visual moving target (Rashbass, 1961) or the expectation of a moving target (Kowler and Steinman, 1979a). Indeed, most

subjects initiate saccadic eye movements when trying to elicit a pursuit eye movement of a target whose image is stationary on the retina (Morris and Lisberger, 1987). Figure I.2 illustrates an example of smooth pursuit eye movement response to a moving target. After a position step to the left, the target moves at constant velocity to the right. This paradigm (Rashbass, 1961) is often used to obtain a pursuit initiation without any saccades. The smooth pursuit latency is usually between 100 and 150 ms but can be reduced in particular conditions, e.g. after a gap period (Knox, 1996, 1998; Krauzlis and Miles, 1996a) or when a distractor moves in the same direction (Ferrera and Lisberger, 1995). Pursuit acceleration depends on the retinal slip, but saturates for large retinal slips (Lisberger et al., 1981; Lisberger and Westbrook, 1985; Tychsen and Lisberger, 1986; Carl and Gellman, 1987; Barnes, 1993).

The first part of the smooth pursuit response is considered as “open-loop”, since the pursuit is not driven by the compensatory eye movements. After around 100 ms, pursuit velocity can be adjusted online to compensate for the retinal slip. This is achieved by adding an extra-retinal feedback of the ongoing eye velocity (i.e. the efference copy) to retinal slip (i.e. evaluated ~80 ms earlier).

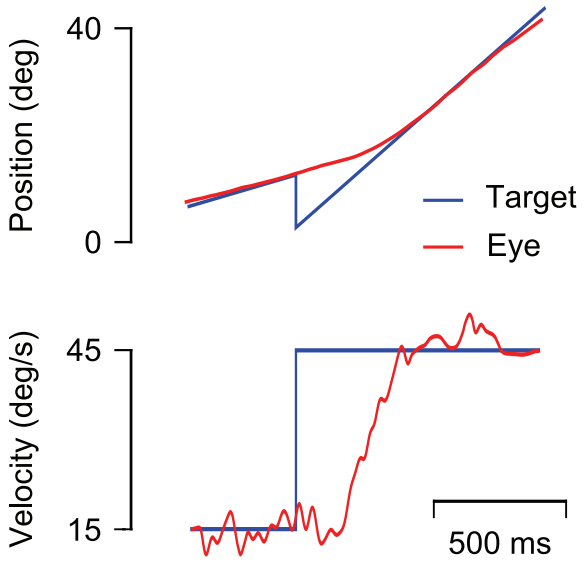

Figure I.2: Typical example of smooth pursuit eye movement (red traces). The upper panel represents position vs. time while the lower panel represents velocity vs. time. Target is shown in blue traces.

Pursuit velocity reaches the target velocity between 200 and 400 ms after target onset, depending on the initial retinal slip. Eye velocity usually overshoots target velocity (typically by 5% to 20% of the target velocity, (Robinson, 1965; Mrotek et al., 2006)) and then often shows a transient oscillating response attributed to uncompensated delays in the feedback loop.

While saccades can be guided by a large variety of signals (visual, auditory, etc.), smooth pursuit is primarily driven by visual motion (Rashbass, 1961). However, position input is also taken into account by the pursuit system, since a briefly flashed target during ongoing pursuit induces smooth pursuit eye movements in its

direction (Blohm et al., 2005). This view is supported by a recent study showing tuned changes of the post-saccadic pursuit velocity driven uniquely by a position error (Schütz and Souto, 2011).

Vergence and gaze stabilizing eye movements

Vergence is considered to be the third type of orienting eye movement, and is needed for binocular vision. It results from the simultaneous movement of both eyes in opposite directions, to get or to maintain single binocular vision. Therefore, if the tracking target moves in depth (away or toward the eyes), it certifies that the system keeps both eyes aligned with this target.

In addition to these orienting eye movements, there are also two types of stabilizing eye movements. The vestibulo-ocular reflex (VOR) is a reflex eye movement that stabilizes the image of the visual scene on the retina during head movement. It receives information about the head rotation from the semicircular canals and generates an eye movement in the direction opposite to the head movement. The VOR is important to ensure perception of a stable world during locomotion. The optokinetic reflex (OKN) is an eye movement that counteracts large-field visual motion. It compensates the speed and direction of the visual world compared to the retina.

Saccade-pursuit interactions

Because there are important time delays in visual motion processing, the oculomotor system develops mechanisms to avoid large position errors and then keep a good visual acuity, as detailed in the previous subsections. However the pursuit system acceleration and velocity are limited. For instance, a pursuit eye movement alone cannot follow an abrupt change of the tracking target position and velocity (Fig. I.3). In this situation, a catch-up saccade will be triggered to realign the gaze and the target, “helping” the smooth pursuit system. However, these catch-up saccades should be minimized because vision is degraded during saccade execution (Bridgeman et al., 1975; McConkie and Zola, 1979). Triggering a saccade is therefore the result of a trade-off situation: the benefit (the target is on the fovea, leading to a pursuit with high acuity) should be larger than the cost to make a saccade (decreased vision during saccade).

A good collaboration between the pursuit and saccadic systems is then required to deal with the sensory and motor delays (Orban de Xivry and Lefèvre, 2007). This is accomplished by sharing the visual inputs (retinal slip and position error) and some information about the “trigger decision” (i.e. the decision to trigger a saccade or not).

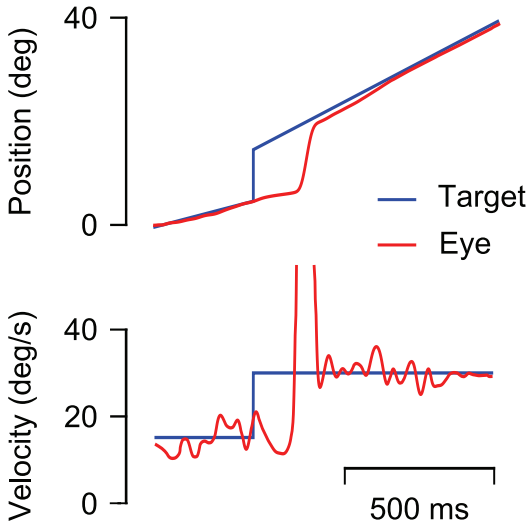

Figure I.3: Typical example of a catch-up saccade triggered during ongoing pursuit (red traces). The upper panel shows position vs. time while the lower panel shows velocity vs. time. Target moved abruptly (position and velocity step) and is represented in blue traces.

In some conditions, the tracking target can move in a predictable way. For instance, it is the case for repetitive or periodic stimuli. In this situation, the oculomotor system has developed some predictive mechanisms in order to anticipate target movement. These predictive eye movements will be detailed in the following sections.

Other types of stimuli

In our everyday life, we have to face more complex objects than those often studied in a lab. For instance, objects usually have complex contours and the motion of their edges must be

distinguished from the background (which can also be moving), and selectively integrated to retrieve the correct object motion. The transition from processing local motion cues (provided by the edges in this example) to global motion might influence pursuit eye movements. For instance, tilted lines (or “type II diamonds”, see Masson and Stone, 2002) evoke a pursuit eye movement that is initially biased toward the direction orthogonal to the line orientation and that is only later corrected towards the object’s global motion (Pack and Born, 2001; Masson and Stone, 2002; Wallace et al., 2005; Born et al., 2006; Montagnini et al., 2006, 2007). These studies illustrate that perception and pursuit integrate local motion information similarly. The transformation of 1D local motion to 2D or 3D object motion involves different stages of motion processing (Masson, 2004). The use of “barber pole stimuli” or “uni-kinetic plaids” has shown that the early component of the eye velocity is driven by 1D local motion signals whereas later stages are driven by 2D motion information, suggesting a parallel processing of 1D and 2D visual motion signals (Masson et al., 2000; Masson and Castet, 2002). It is therefore obvious that higher-level visual and perceptual mechanisms play a crucial role in the control of pursuit eye movements (see Hafed and Krauzlis (2010); Masson et al. (2010) for reviews).

Another example of complex motion is biological motion. Biological motion stimuli have often be studied in a lab, by using point-light animation techniques created by a computer (Cutting, 1978) or by motion-capture technology (Vanrie and Verfaillie, 2004). In this case, the stimulus information is reduced to the motion of a small number of points. However, these biological motion stimuli still provide abundant information about the human shape and the type of the actions performed (for a review see Verfaillie (2000); Blake and

Shiffrar (2007)). Therefore, the visual system could process biological motion stimuli differently than other types of stimuli (Grezes et al., 2001; Grossman and Blake, 2002; Peuskens et al., 2005; Billino et al., 2009). However, there was yet no evidence that perception of biological motion could influence the motor action. Chapter III focuses on the eye movements elicited in response to biological and non-biological stimuli. Results show for the first time that motor action can be facilitated by biological motion, and thus that the biological motion perception network is also an essential input to the pursuit system.

Predictive eye movements

In many situations, the brain can use some cues to predict the future movement of the object of interest, or at least the timing of its motion onset. For instance, a good tennis player uses the opponent's body part kinematics to predict the future direction of the ball after it has been hit by his opponent (Singer et al., 1996; Shim et al., 2005; Huys et al., 2008; Mark Williams et al., 2009; Yarrow et al., 2009). By anticipating the tennis ball motion, position error and retinal slip are smaller when the player gets the visual feedback (i.e., ~100 ms after the ball has been hit by his opponent), leading to a better vision and better conditions for the future tracking.

In everyday life, the oculomotor system often uses prediction to anticipate the future target trajectory during pursuit eye movements. An internal representation of the future target trajectory can be computed by using past history, periodicity in its movement or by the physical laws, e.g. target acceleration induced by gravity (Angelaki et al., 2004; Indovina et al., 2005).

Anticipatory eye movements illustrate the internal storage of velocity information by the brain. For instance, at the first presentation of a moving target, the eyes initially lag behind this target. The repeated presentation of the identical motion target (e.g. constant velocity ramps) leads to an increase of pursuit velocity well before (usually 100 to 200 ms) target motion onset (Kowler and Steinman, 1979a, 1979b; Barnes and Asselman, 1991; Kao and Morrow, 1994; Barnes et al., 1997). Predictive smooth pursuit velocity is influenced by the target velocity of the preceding trial. This is often called the “history effect”, and has been first shown for small (<0.5 deg/s) anticipatory pursuit velocities (Kowler, 1989) and later with larger predictive eye movements (Jarrett and Barnes, 2002; Poliakoff et al., 2005). This history effect influences the latency of the anticipatory response as well (Heinen et al., 2005; Badler and Heinen, 2006). More generally, the anticipatory response is influenced by the expected velocity after the change of target motion (Boman and Hotson, 1992; Barnes and Schmid, 2002). Anticipatory pursuit velocity can also be influenced by a cue that scales the value of the predictive eye movement to the expected stimulus velocity (Poliakoff et al., 2004, 2005). Directional cues can also elicit anticipation in the correct direction (Jarrett and Barnes, 2002). Even if these studies used different types of cue (i.e. audio, visual - e.g. using the gap paradigm, when a time delay is present between fixation point disappearance and target appearance and motion - or even sometimes tactile), the type of cue does not seem to affect the results (Barnes and Donelan, 1999). In all studies, these cues are very important to predict the timing of target motion. However in reality cue time itself may be variable. Therefore, the timing of anticipatory pursuit can also vary in its distribution (de Hemptinne et al., 2007).

When there were two possible cues (early or late) occurring at random, monkeys initiated both early and late anticipatory pursuit movements (de Hemptinne et al., 2006). An example of anticipatory eye movement elicited by a 300 ms gap paradigm is illustrated in Fig. I.4. Two typical trials are represented, one with a catch-up saccade triggered when visual feedback was available to correct for the position error (red traces) and one with a very large anticipatory pursuit eye movement, sufficient to catch the target without any saccade (green traces).

Similarly, anticipatory eye movements can also be observed before the (predictable) termination of target motion and be influenced by the previous target motion (Boman and Hotson, 1988; Wells and Barnes, 1999; de Hemptinne et al., 2010).

After the collision of a ball by a launcher target, inducing the movement of the ball, predictive eye movements were observed in the causal direction (i.e. the same direction than the launcher target) (Badler et al., 2010). Interestingly, the ball could move either in the direction predicted by the collision or in its orthogonal direction. This causality perception could be seen as a cue signal, cueing the future direction of the ball in the causal direction.

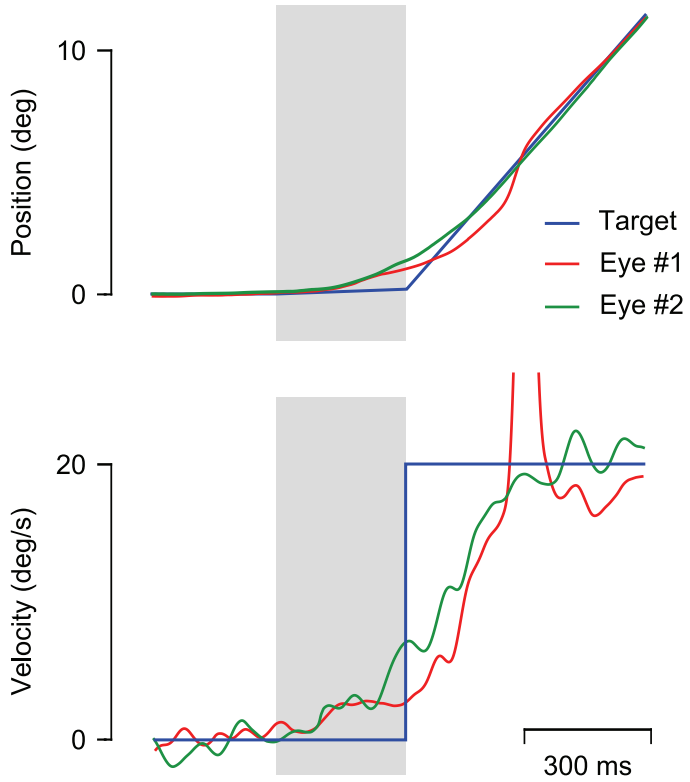

Figure I.4: Typical anticipatory eye movements (gap paradigm). In some trials, anticipatory pursuit is sufficient to anticipate the abrupt motion of the target (blue traces) and no saccade is triggered (green traces). However, most trials show a small visually-guided catch-up saccade triggered to realign the gaze and the target (red traces). The upper panel shows position vs. time while the lower panel shows velocity vs. time. Gap period (no visible target) is represented by the grey area.

Pursuit eye movements also use predictive mechanisms in response to periodic stimuli, like a sinusoidally moving target. Indeed, it has been shown that pursuit eye movements in response to a

sinusoidal stimulus compensate almost fully for the time delays in visual processing after one or two cycles (Dallos and Jones, 1963; Bahill and McDonald, 1983a; Barnes and Asselman, 1991; Barnes et al., 2000). By contrast, the eye would always lag behind the target without any predictive mechanisms. When tracking a sinusoidal stimulus at high frequencies (>0.5 Hz), the eye velocity gain is decreased and the eye lags behind the target, causing a phase shift (Barnes et al., 1987; Barnes and Ruddock, 1989). Moreover, because of the pursuit velocity saturation, the decrease of the pursuit gain with frequency is even larger when the amplitude of target displacement increases (Wyatt and Pola, 1983; Barnes, 1993). However, the saccadic system compensates for most of the decrease in pursuit velocity up to frequencies of 1 Hz.

Prediction mechanisms are also highlighted when the tracked target (moving at constant velocity) transiently disappears (Mitrani and Dimitrov, 1978). During the blanking period, the oculomotor system has to handle without any sensory (i.e. retinal) information. After target disappearance, the pursuit eye movement velocity decreases exponentially for about 300 ms (Becker and Fuchs, 1985). If the target is expected to reappear, pursuit velocity is stabilized at a residual velocity, which is usually between 40 and 60% of the target velocity. Subjects are able to maintain smooth pursuit up to 4 s after the disappearance of the target. In contrast, when the target is not expected to reappear, eye velocity is not maintained but falls exponentially towards zero. The decrease in pursuit velocity during blanking can vary from trial to trial for a single subject.

If the timing of target reappearance is known by the subject (e.g. when the same target movement is repeated, what is often called “blocked trials”), pursuit velocity can increase before the end of

the blanking (Bennett and Barnes, 2003). This predictive eye acceleration is also called the “predictive recovery”. Pursuit velocity at reappearance can be scaled to the expected target velocity (Bennett and Barnes, 2004; Orban de Xivry et al., 2006). Figure I.5 shows different predictive eye movements of a human subject when tracking a target that transiently disappears. During the first presentation of the target (black traces), the subject had no prediction about the timing of the target reappearance (i.e., there is no predictive recovery). After some consecutive presentations of the same stimulus (red, blue and green traces respectively represent the oculomotor response for the 7^{th}, 8^{th} and 9^{th} trials), the subject was able to anticipate the target reappearance, and exhibited a predictive recovery. This is shown for these three traces by a global predictive pursuit acceleration between 200 ms before target reappearance and 80 ms after this reappearance (i.e., before any influence of the visual feedback). In contrast, the black trace shows no predictive acceleration but a visually-guided increase of pursuit velocity about 100 ms after target reappearance. As for the residual pursuit velocity during blanking, the predictive reacceleration is variable from trial to trial.

During the blanking period, the position error accumulates since pursuit eye velocity decreases. However, the saccadic system compensates for the variability of this decrease on a trial by trial basis, i.e. the larger the pursuit velocity decrease, the larger the saccadic amplitude (Orban de Xivry et al., 2006, 2008). To correct for this eye velocity decrease during blanking, saccades have been shown to place the eye ahead of the target (Bennett and Barnes, 2003, 2006a). This is also illustrated in Fig. I.5. In contrast to visually-guided saccades, the triggering of the predictive saccades (i.e. the

timing of their execution) does not seem to be influenced by the performance of the smooth pursuit response during target blanking (Orban de Xivry et al., 2009). Monkeys are also able to trigger saccades to the expected position of the invisible target (Barborica and Ferrera, 2004) and can also approximately predict target position of the invisible target (Filion et al., 1996). All these evidences show that even when the target is blanked, the oculomotor system has access to accurate information about the invisible target movement. Moreover, this internal representation of the target movement is dynamic. Indeed, subjects are able to track an invisible target moving along a circular path, which shows that subjects have a dynamic internal representation of the target motion evolving with time (Orban de Xivry et al., 2008).

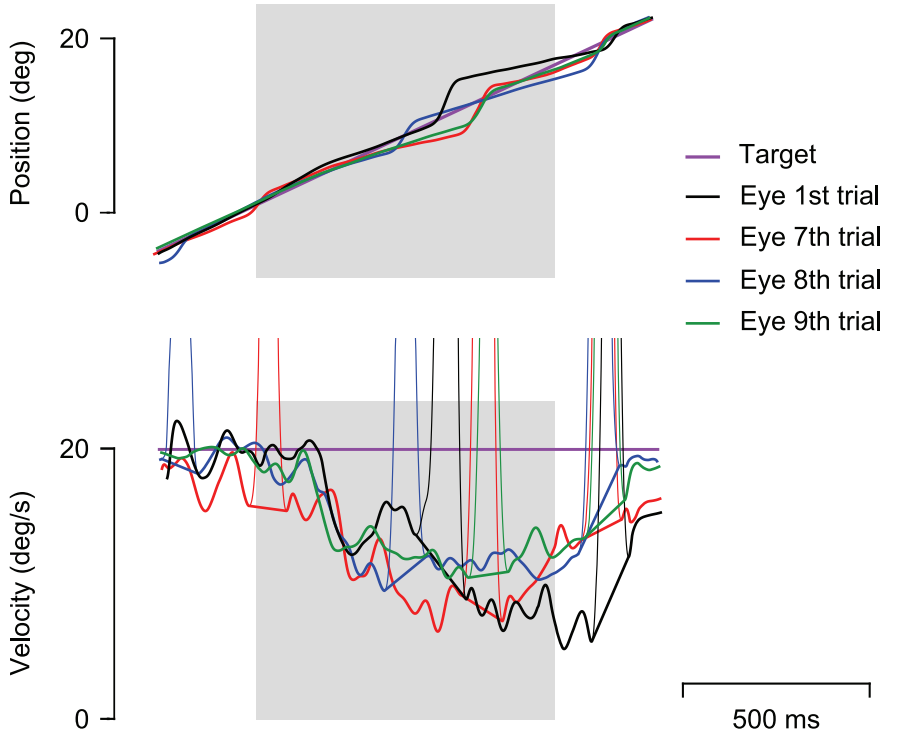

Figure I.5: Typical predictive eye movements during blanking of the pursuit target. Oculomotor response for the first presentation of the target is shown in black (subject had no prediction about target reappearance). Red, blue and green traces respectively represent the eye movement response for the 7th, 8th and 9th consecutive presentation of the same target (and same blanking period). Target is shown in purple traces. The upper panel shows position vs. time while the lower panel shows velocity vs. time. Blanking period (no visible target) is represented by the grey area. Smooth pursuit eye movements are represented in continuous traces (for the velocity panel, pursuit velocity during saccades was linearly interpolated) and the thin traces represent saccadic eye movements.

Models

Modeling eye movement has significant implications for understanding the oculomotor system and investigating the neural basis for eye movements. Typically, models describe the oculomotor system by a relationship between the inputs (retinal and extra-retinal) and the outputs (the production of the motor command sent to the eye muscles). The development of those quantitative models has historically highlighted unresolved issues and identified data that provide important evidences on the organization of the neural system. Obviously, the oculomotor system is extremely complex and not perfectly understood yet. Therefore, some simple and sometimes more global (and complex) models must be developed and validated with experiments in order to explain the oculomotor behavior. Here, we focus on the pursuit system and rapidly review the history of pursuit models. Chapter III illustrates the benefit of using a simple model to make theoretical predictions and then facilitates the interpretation of new experimental results

Basically, there were two classes of pursuit models for visually-guided eye movements: “internal feedback” models and “image motion” models. These were followed by the appearance of pursuit models explaining some predictive mechanisms of the pursuit system. A chapter of this thesis is devoted to a new pursuit model, integrating both retinal and extra-retinal inputs to the pursuit system on a weighted and natural manner (Chapter II).

The first pursuit models try to replicate the dynamics of the visually guided pursuit eye movements generated in response to a step-ramp target motion (Young et al., 1968; Robinson et al., 1986). This class of models is referred to as internal feedback models since

the internal feedback loop determines the dynamics of the sustained eye velocity (Fig. I.6). These models principally focused on the initial pursuit acceleration and on the oscillations in eye velocity during sustained pursuit. The latter model of Robinson et al. (1986) attempted to fit data from human subjects. They used two distinct mechanisms to control the initiation and the maintenance phases of pursuit. Visual inputs determined the trajectory of eye velocity at the initiation of pursuit while an internal feedback loop was used to explain the frequency of oscillations during prolonged pursuit of target motion (Fig. I.6). Different time delays are located before, after and within the positive feedback loop and explain the frequency of those oscillations and the dynamics of pursuit.

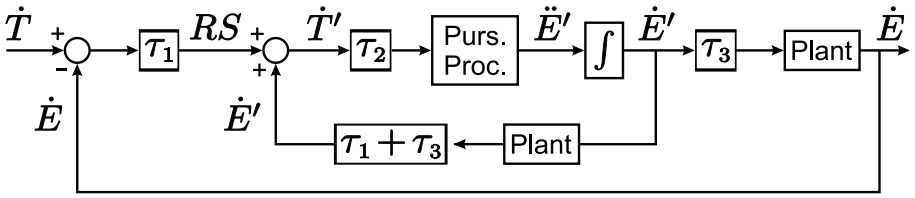

Figure I.6: Schematic diagram of an “internal feedback” model. Retinal slip (RS) is computed as the difference between target velocity and eye velocity. RS is then added to an efference copy of eye velocity $(\dot{E}')$ (output of the internal feedback loop) to give an estimation of the target velocity $(\dot{T}')$. This signal is then processed (an estimation of eye acceleration $(\ddot{E}')$ is computed), integrated and sent to the eye plant. τ_1, τ_2 and τ_3 are internal delays. Adapted from Robinson et al. (1986).

The second class of models achieves similar objectives by using visual input signals that are associated to motion onset transient, image acceleration as well as image velocity (Lisberger et al., 1987; Krauzlis and Lisberger, 1989, 1994; Churchland and Lisberger, 2001a). While the internal feedback models implement the pursuit processing mainly with saturating functions on pursuit acceleration and velocity, for the second class of models, the acceleration signal $(\ddot{E}')$ is provided by three feed-forward pathways (Fig. I.7). This last class is usually referred to as “image motion” models since the dynamics of the eye velocity is determined directly by the processing of visual inputs. Each of the three pathways is made of a non-linear saturating function (except for the velocity motion which has a linear function) which transforms the amplitude of the input signal, a second-order filter that adjusts the time course of the input signal and a gain factor to weight the signal according to its relative importance (Fig. I.7). Motion transient pathway is switched on only for 20 ms following the detection of a velocity step, to give a brief pulse of image velocity. The image velocity pathway outputs an acceleration signal proportional to the retinal slip (but this pathway is inhibited for the 20 ms following the detection of a velocity step). Finally, the image acceleration pathway provides an acceleration signal proportional to the derivative of the retinal slip. In a first version of the model (Krauzlis and Lisberger, 1994), these three outputs were added and integrated by a perfect integrator (Fig. I.7).

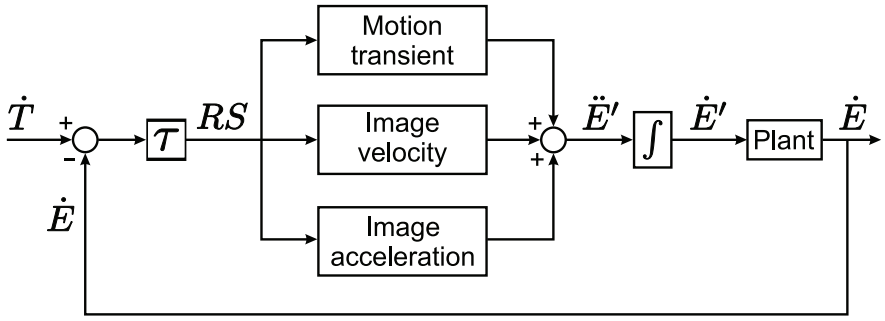

Figure I.7: Schematic diagram of an “image motion” model. Retinal slip (RS) is computed as the difference between target velocity and eye velocity. RS is then sent to three parallel pathways of visual processing to give acceleration signals $(\ddot{E}')$. These signals are then added and integrated. Adapted from Krauzlis and Lisberger (1994).

However, this model was not able to simulate some pursuit mechanisms as pursuit offset for instance. Later, Krauzlis and Miles suggested that the onset and offset of pursuit can be mediated by a single mechanism (Krauzlis and Miles, 1996b). Therefore, in a new model presented in Fig I.8, the perfect integrator was substituted by a "leaky” integrator. This leaky integrator (Fig I.8) consisted of a filter H_i with a single time constant (leading to an exponential decay) and a gain G_e. The outputs from the parallel pathways are then summed with a copy of the eye velocity coming from the positive efferent feedback loop. Then the resulting signal is modulated by a second input signal (labeled “Gain”) in a multiplicative junction that affects similarly the signal coming from the visual inputs and the signal coming from the positive efferent feedback (Fig I.8). This model can simulate pursuit onset, steady-state pursuit and pursuit offset (with or

without overshoot depending on the parameters). We will see later than this model can also simulate some predictive mechanisms.

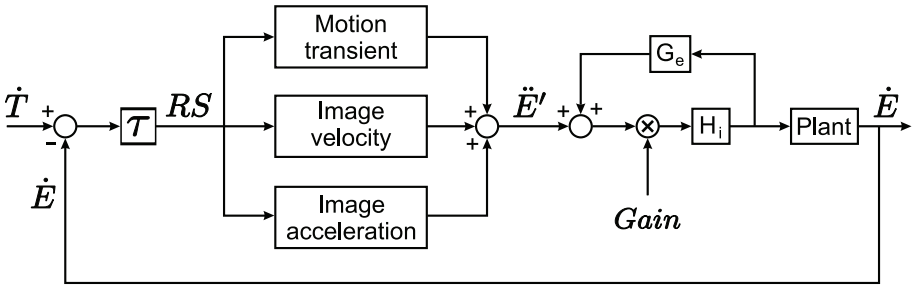

Figure I.8: Schematic diagram of an “image motion” model with a positive efferent feedback. The visual inputs are processed similarly by the three parallel pathways, but their outputs are here sent to a (leaky) integrator H_i. This integrator is modulated by a positive efferent feedback loop through gain element G_e and another multiplicative gain element. Adapted from Krauzlis and Miles (1996b).

Image motion and internal feedback models can correctly simulate experimental data observed during pursuit initiation and pursuit maintenance when tracking a target moving at constant velocity. Nevertheless, these models are not able to explain other characteristics of the pursuit system such as the influence of perception, the predictive mechanisms, the sensory processing. For instance, sensory processing allow us to extract the direction and velocity of a moving target, and then to anticipate its future trajectory (e.g. humans are able to follow a target moving sinusoidally with zero phase lag between eye and target).

Different models have integrated predictive mechanisms in order to simulate sinusoidal pursuit. For that purpose, prediction of the future target motion is needed. For instance, two studies proposed a simple pursuit model, similar to the one presented in Fig I.6, but inserted a “predictor” before pursuit processing (Deno et al., 1995; Shibata et al., 2005). As the name suggests it, the predictor predicts the upcoming target velocity, based on its current velocity. By doing this, the eye starts moving before the target, and therefore overcomes the sensorimotor delays. Basically, these two studies (as others) extrapolate the velocity of the moving target into the future, based on the current target motion (Bahill and McDonald, 1983b; Deno et al., 1995; Kettner et al., 1997) and on a component of the current target acceleration (Soechting et al., 2010). However, these models are not able to simulate the response to transient blanking of the target. Barnes and Asselman (1991) proposed to combine the “predictor” with a short term memory that holds velocity. In their model, they assume that two independent processes are involved for predictive mechanisms: the short term storage of premotor drive information and the estimation of periodicity (or timing). In this model, the drive for eye velocity can be influenced by both retinal and extra-retinal inputs.

Barnes et al. presented different versions of this model (Barnes and Asselman, 1991; Barnes and Wells, 1999; Bennett and Barnes, 2003, 2004, 2006b; Barnes and Collins, 2008a) to simulate the predictive pursuit eye movements in response to sinusoidally moving object or to a transient blanking of the target. To get a general idea of the model, a schematic representation is shown in Fig. I.9. An extra-retinal input coming either from a direct efference copy loop (shown in red) or an indirect predictive loop (shown in blue) is added

to an eye velocity command computed with the visual inputs. The direct loop represents the ongoing efference copy, which perpetuates the eye motion when there is only a weak expectation regarding the upcoming stimulus characteristics. The indirect loop acts as a short-term memory (MEM), represented as a local feedback loop. It contains an integrator that cumulatively adds the error within the local feedback loop until the error is zero.

The decision to switch between the direct and the indirect loop depends on the strength of the subject's expectation regarding to the timing and motion characteristics of the upcoming target. For instance, at the first occurence of a new stimulus of unknown characteristics, subject generates a reactive response, while the short-term memory loop is charging. Then, after several presentations of the same target movement, subject initiates a predictive response prior to target onset, driven by the output of the short-term memory.

In the case of target blanking, the β gain (initially equal to 1 and presented in Fig. I.9) is decreased to a positive value comprised between 0 and 1 if the target is expected to reappear, or to zero if there is no expectation regarding the target reappearance. This β gain can be reinstated to its initial value before target reappearance, leading to a predictive recovery, since a static value of the target motion is held in the memory. The $\alpha(t)$ gain is actually time-dependent, representing the multiple levels of motion information that may be stored in the memory (e.g., when following a target that accelerates (see Bennett and Barnes, 2006b)). However, this short-term memory approach is not dynamic (even with the use of the artificial $\alpha(t)$ gain, which should be adapted manually based on the context). In other words, this model is not able to simulate predictive

pursuit of a blanked target when the initial eye velocity is zero. In the same way, a change in target motion during blanking (e.g., a target moving along a circular path in 2D; Orban de Xivry et al., 2008) would not be easy to simulate and it would require a constant adaptation of the $\alpha(t)$ gain.

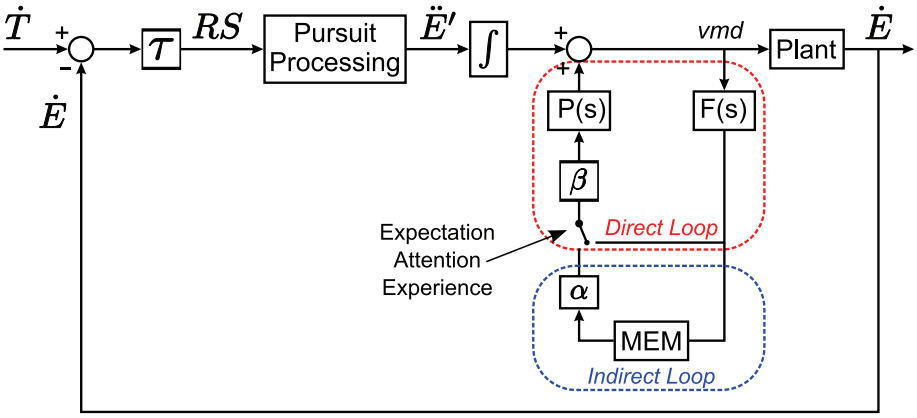

Figure I.9: Schematic diagram of a pursuit model with a memory loop (MEM). Retinal inputs provide an eye velocity motor command which is added either with the output of the direct efference copy (reflexive) loop or with the output of the indirect predictive (cognitive) loop. Adapted from Bennett and Barnes (2006b).

Finally, different studies used a model similar to the one presented in Fig. I.8 (adapted from Krauzlis and Lisberger, 1994; Krauzlis and Miles, 1996b) to simulate the pursuit response during a target blanking (Churchland et al., 2003; Madelain and Krauzlis, 2003). Indeed, while the initial purpose of the “Gain” located in the leaky integrator (Fig. I.8) was to simulate pursuit offset (by an abrupt decrease to zero), it can also reproduce the decay of pursuit velocity

during target blanking. For instance, Madelain and Krauzlis (2003) temporarily decreased its value after target disappearance, leading to the well-known exponential decay of pursuit velocity and a residual pursuit velocity. However, this model is not able to reproduce anticipatory pursuit or the predictive recovery observed before target reappearance. Indeed, since the visual processing is no longer producing any acceleration signal $(\ddot{E}')$, any decrease of the stored velocity in the leaky integrator can not be reinstated (unless the Gain is increased to a value higher than 1, leading to unstable simulations).

Chapter II presents a new pursuit model, based on some hypotheses presented above. However, this new pursuit model also brings some new hypotheses about the functioning of the pursuit system. The presented model deals with a general noise representation, as the brain does, thanks to Kalman filtering. Even if this technique has often been proposed to deal with noise and uncertainty in multisensory integration in other fields of neurosciences (e.g. for proprioception and vision signals in reaching arm movements), it has never been used in any oculomotor model to explain the interaction between retinal and extra-retinal inputs. This new way to explain the pursuit system therefore estimates the sensory (retinal) and internal (extra-retinal) signals based on previous estimations and current measure on the retina. Moreover, the evaluation of the uncertainty of the estimations, also given by the Kalman filter, allows us to combine these two signals in an optimal way. In order to have some optimal estimation, the noises present in the system have to be Gaussian and non-correlated. The weighting of these two signals, depending on their reliability, is also a new way to consider the combination between the retinal and extra-retinal signals. The key is therefore to have the larger confidence in the

signal. Last but not least, the extra-retinal signal used in this new model is based on a dynamic internal representation of the target, which can explain different oculomotor behaviors. This model is the first one able to simulate both anticipatory pursuit, pursuit during target blanking and pursuit in response to a sinusoidal moving target. To date, different model organizations were needed to simulate those three examples of predictive pursuit eye movements.

Neurophysiological substrate

This section will briefly describes the anatomical structures involved in saccadic eye movements before focusing on the neurophysiology of visually-guided and predictive pursuit eye movements. Giving a full description of all the brain areas involved in the generation and execution of eye movements is not the objective. The purpose is rather to present a general description of the most important areas.

Saccadic eye movements

Visual information is initially projected from the retina to the primary visual cortex (V1). In V1, the position of a visual stimulus is coded in retinal coordinates (Leigh and Zee, 2006). This means that different parts of this cortical map correspond to different positions on the retina. The goal of the saccadic system is then to transform this retinotopic representation of the target location into a motor command that will be sent to the extra-ocular muscles. The difficulty is that the

motor command is encoded by the motoneurons in terms of discharge frequency and duration. Therefore, this sensorimotor transformation must transform the stimulus, which is “place-coded”, into the saccadic command which is “temporally-coded”. This sensorimotor transformation involves a large number of brain areas.

Neurons from area V1 project to the parietal cortex, which contains the lateral intraparietal area (LIP) which is involved in visuospatial integration and in reflexive saccade triggering (Andersen et al., 1990; Pierrot-Deseilligny et al., 1991; Gaymard et al., 1998) and to the frontal eye fields (FEF). FEF are involved in visuomotor planning and target selection (Schall, 2001) and are connected with the supplementary eye fields (SEF). Patients with a lesion affecting the left SEF had problems with the chronology of memory-guided saccade sequences, suggesting that SEF selects saccade plans from spatial working memory (Gaymard et al., 1990, 1993; Petit et al., 1996; Heide et al., 2001).

Frontal and parietal cortical areas both project to the superior colliculus (SC), which is probably one of the most important areas for saccade programming (Scudder et al., 2002; Sparks, 2002; Leigh and Zee, 2006). SC consists of seven layers, the superficial layers responding more to visual stimuli (and encodes the position error of the stimuli on a retinotopic map of the visual field) whereas the deeper layers are more related to motor events. The motor command from the SC is then sent to the Pontine Nuclei and to the Cerebellum. Cerebellum has an important role for saccade accuracy, dynamics and trajectory in both online and long-term characteristics. Finally, the brainstem circuit forms the final output commands and sends them to the extra-ocular muscles (Keller and Missal, 2003). A simplified view

of the saccadic system (adapted from Krauzlis, 2004) is represented in Fig. I.10A.

Smooth pursuit eye movements

Smooth pursuit eye movements also involve a large number of cortical areas. Again, the objective here is not to be complete, but to give a rough overview of the most important areas implicated in smooth pursuit generation (see Krauzlis (2004); Thier and Ilg (2005) for reviews). This includes the middle temporal (MT) and medial superior temporal (MST) areas and subregions of the LIP, FEF, SEF and the cerebellum (Fig. I.10B). Therefore, many of the same cortical areas are concerned by the control of both pursuit and saccadic eye movements. However, each cortical area contains separate subregions for the two different types of movements (Tian and Lynch, 1996a, 1996b; Heinen and Liu, 1997; Krauzlis and Miles, 1998), even if these subregions are probably interconnected (Krauzlis, 2004, 2005; Orban de Xivry et al., 2007). The schematic representation of the functional organizations of the pursuit and saccadic system illustrates the similarities between these two systems (Fig. I.10).

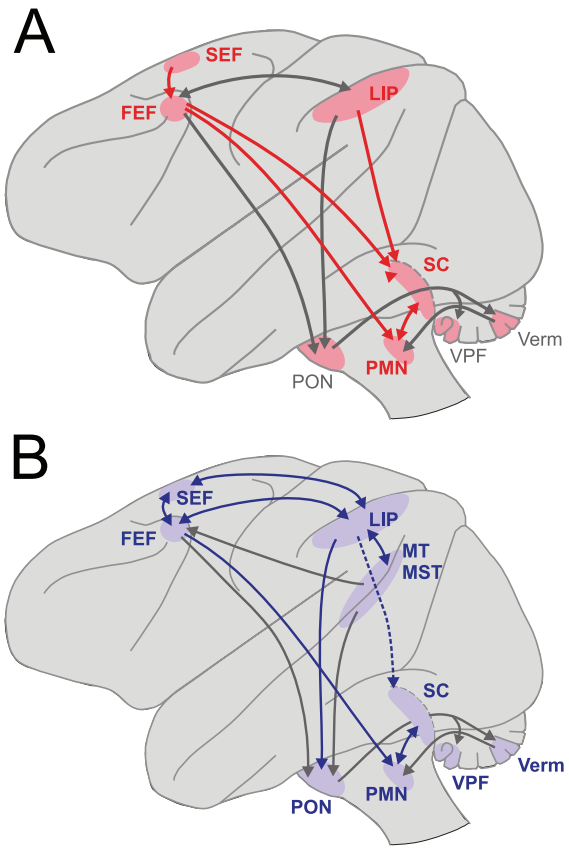

Figure I.10: Schematic representation of the central nervous system areas implicated in saccadic (A) and pursuit eye movements (B). Diagram depicts a lateral view of the monkey brain. Shaded regions indicate specific areas within the cerebral cortex, cerebellum, and brain stem, and arrows indicate the anatomical connections between these areas. FEF: frontal eye field. SEF: supplementary eye field. LIP: lateral intraparietal cortex. MT: middle temporal area. MST: medial superior temporal area. SC: superior colliculus. PON: precerebellar pontine nuclei. PMN: brain stem premotor nuclei. VPF : ventral paraflocculus (cerebellum). Verm: vermis (cerebellum). Adapted from Krauzlis (2004).

For the brain, the first step to generate an eye movement is the processing of the retinal inputs. The heart of visual motion processing is located in the middle temporal area (MT) and medial superior temporal area (MST) (see Ilg (2008) for a review). However, MST neurons differ from MT neurons by taking into account the ongoing eye and head movements (Komatsu and Wurtz, 1988; Thier and Erickson, 1992; Ilg et al., 2004). This means that MST has access to an efference copy of the eye and head movement commands to estimate the target motion during smooth pursuit (as opposed to retinal slip in MT). Many studies have shown the crucial role of area MT on the visual processing (see Born and Bradley (2005) for a review). For instance, lesion in area MT or MST impaired motion perception (Newsome and Paré, 1988; Rudolph and Pasternak, 1999). However, motion perception of a large moving pattern seems to be improved after the temporary and virtual disruption of area MT by transcranial magnetic stimulation (TMS) (Tadin et al., 2011). Similarly, motion perception of second order stimuli has been reported in the absence of any MT response (Ilg and Churan, 2004). This can be explained by the fact that MT neurons represent local (and not global) motion signals (Majaj et al., 2007). Chemical lesions in area MT shows its importance for guiding pursuit (Newsome et al., 1985; Dursteler and Wurtz, 1988). Similarly, stimulation of MT alters smooth pursuit: an increase of pursuit velocity was observed toward the side of the brain being stimulated and a decrease in the opposite direction (Komatsu and Wurtz, 1989). Indeed, MT neurons were found to encode both target velocity and acceleration (Lisberger and Movshon, 1999; Churchland and Lisberger, 2001b; Priebe et al., 2003; Priebe and Lisberger, 2004; Price et al., 2005).

MT and MST areas are directly interconnected with the frontal eye fields (FEF), which also receive inputs from the parietal cortex. FEF is probably the main cortical area involved in the control of pursuit gain (Tanaka and Lisberger, 2001). First, FEF contains neurons that display direction selective pursuit response during pursuit eye movements (MacAvoy et al., 1991; Tanaka and Lisberger, 2002). Also, the analysis of the dynamic variations of both neural and pursuit responses in FEF showed that a few FEF neurons are sufficient to drive pursuit eye movements at any time (Schoppik et al., 2008). Moreover, lesion or inactivation of the FEF has dramatic effects on pursuit (Keating, 1991; Shi et al., 1998).

MST also sends projections to SEF, which is interconnected with FEF. In monkeys, SEF neurons were shown to be active during pursuit and even after target disappearance (Heinen, 1995). Moreover, stimulation of SEF can increase the pursuit velocity when applied during pursuit initiation, but it has little effect when stimulated during the fixation period (Tian and Lynch, 1995; Missal and Heinen, 2001). In the latter study, saccades latency was increased during stimulation, even if their accuracy was not affected.

LIP, which is interconnected with FEF and SEF, is also involved in the control of both pursuit and saccades. Many LIP neurons show direction specific activity during pursuit (Bremmer et al., 1997), and the activity is sustained after target disappearance (Sakata et al., 1983). Since pursuit activity of LIP neurons seem to be influenced by the eye position and other extra-retinal signals, LIP area may be involved in the representation of space in a nonretinopic reference frame (Schlack et al., 2003). More generally, the posterior parietal cortex (PPC) is a region where a large variety of signals converge, coding visual stimuli and spatial goals in diverse

coordinates, from retinotopic to non-retinotopic reference frames (depending on the specific area of the PPC).

All the previously cited cortical areas project to the pontine nuclei. Then oculomotor signals generated by the pontine nuclei are sent to the cerebellum. Two different parts of the cerebellum are really essential for the control of pursuit: the ventral paraflocculus (VPF; Rambold et al., 2002) and the cerebellar vermis (Krauzlis and Miles, 1998; Robinson and Fuchs, 2001). Indeed, some Purkinje cells from the vermis were found to be sensitive to eye velocity whereas other Purkinje cells discharged proportionally with the retinal slip (Kase et al., 1979; Suzuki et al., 1981). The presence of two populations of Purkinje cells in the vermis is also important for the cerebellum to control the pursuit velocity during head-unrestrained eye movements (Suzuki and Keller, 1988a, 1988b). Finally, the cerebellum directly projects towards the premotor neurons, which control the eye muscles and cause the eye movement.

Predictive pursuit eye movements

Many evidences highlight the importance of the frontal lobes for the predictive mechanisms used by the oculomotor system. fMRI studies showed some modification in activation during predictive pursuit in three different regions of the frontal lobes: FEF, dorsolateral prefrontal cortex (DLPFC) and supplementary motor area (SMA; including SEF). The activity in the FEF was either maintained or increased during blanking of a moving target (Lencer et al., 2004;

Nagel et al., 2007; Ding et al., 2009) and was correlated with the difference in velocity between the eye and the target during target blanking (Nagel et al., 2006). The DLPFC was less activated during a smooth pursuit task with predictable than with unpredictable target trajectories (Schmid et al., 2001) but it was more activated during a blanking period than during visually-guided pursuit (Ding et al., 2009). The correlation between the BOLD signal from this area and from the FEF suggests that DLPFC could modulate FEF activity in function of target visibility (Ding et al., 2009). Oculomotor tasks that require predictive eye movements elicit a larger activation of the SMA (Schmid et al., 2001; Lencer et al., 2004).

Stroke patient studies also demonstrated that anticipatory and visually-guided smooth pursuit eye movements are impaired when frontal areas are damaged (Morrow and Sharpe, 1995; Heide et al., 1996; Lekwuwa and Barnes, 1996), especially when the target moves towards the side of the lesion (see Sharpe (2008) for a review of the effects of lesion in the human brain on the pursuit system). In addition, the latency of the motor response to a predictable event is often longer in these patients. For instance, increased phase lag between target and eye velocities, attributed to impaired target prediction, was found in patients with a lesion located in the prefrontal cortex, particularly with a right-sided lesion (Lekwuwa and Barnes, 1996). Moreover, TMS over the SEF and the FEF differently impaired predictive pursuit eye movements, suggesting that they have different contribution to the predictive mechanisms of pursuit eye movement (Gagnon et al., 2006; Drew and van Donkelaar, 2007).

Different studies in monkeys also highlight these predictive mechanisms in the frontal lobes. For instance, stimulation of SEF facilitates anticipatory pursuit, when the expectation of the target

motion is high (Missal and Heinen, 2004). Finally, as extra-retinal signals were also observed in FEF neurons activity, predictive pursuit may be linked to an internal representation of invisible target motion located in FEF (Fukushima et al., 2002; Barborica and Ferrera, 2003, 2004; Xiao et al., 2007; Ferrera and Barborica, 2010).

Other cortical areas may have a role for the predictive pursuit eye movements, by dealing with extra-retinal signals. To test if the discharge of MT and MST neurons were related to an extra-retinal input related to the pursuit movement itself (and not only by the visual stimulation of the target motion on the retina), Newsome et al. (1988) used a target blanking paradigm. When the target transiently disappeared, the MT responses disappeared as well. In contrast, many neurons in MST showed a sustained activity during target blanking (Newsome et al., 1988; Kawano et al., 1994; Ono and Mustari, 2006). Similar results were found during pursuit of an imaginary target (Ilg and Thier, 2003). Neurons in area MST were also activated during anticipatory pursuit (Ilg, 2003). fMRI studies have also shown that the MT/MST complex is active during blanking of the target (Nagel et al., 2006), as well as LIP and the superior parietal cortex (Lencer et al., 2004).

Extra-retinal signals have also been found in the cerebellum. Some Purkinje neurons showed responses during sinusoidal or circular pursuit (Leung et al., 2000), showing that internal models are represented in the floccular complex of the monkey cerebellum (for review, see Lisberger, 2009). For instance, the activity of Purkinje cells recorded in cats was maintained during the transient blanking of the target, reflecting an internal model of the target movement based on previous movements (Cerminara et al., 2009). Angelaki et al.

(2004) also showed that the cerebellum produces an internal representation of the physical laws of the world.

In sum, different parts of the brain are involved in predictive mechanisms needed for predictive pursuit eye movement. Indeed, the frontal lobes (including FEF, SEF, DLPFC), LIP, MST and some parts of the cerebellum contain extra-retinal signals and probably provide input which describes target movement in an external frame of reference.

Chapter II
Kalman filtering accounts for visually-guided and predictive smooth pursuit dynamics

Introduction

When you look at the ball your child is gently throwing to you, your visual system is analyzing the ball's trajectory. This interpretation of the ball motion will evoke an appropriate smooth pursuit eye movement that will minimize retinal image motion and maintain a good acuity. Smooth pursuit eye movements require visual motion signals, which are often noisy signals (Osborne et al., 2005, 2007). Therefore, the brain integrates stimulus information over time across large populations of neurons (Georgopoulos et al., 1986; Treue et al.,

2000) in order to improve the reliability of sensory signals (Snowden and Braddick, 1991; Perrett et al., 1998; Gold and Shadlen, 2003).

Now, if the moving target instantly disappears, people are able to estimate its movement (Barborica and Ferrera, 2003; Ilg and Thier, 2003). This prediction represents another important input to the pursuit system. It allows humans or monkeys to track the ball in the absence of retinal signals (Becker and Fuchs, 1985; Pola and Wyatt, 1997; Bennett and Barnes, 2003; Orban de Xivry et al., 2006). Those predictive movements are also observed before the onset of a predictably moving target (Dallos and Jones, 1963; Barnes and Asselman, 1991).

Different models have analyzed the pursuit system. Some of them focused on visually guided pursuit (Robinson et al., 1986; Krauzlis and Lisberger, 1989, 1994; Krauzlis and Miles, 1996b) while others accounted for predictive mechanisms (Barnes et al., 1995; Bennett and Barnes, 2003; Madelain and Krauzlis, 2003; Barnes and Collins, 2008a; Soechting et al., 2010). Unfortunately, none of them did combine the visually-guided and predictive smooth pursuit responses without using a switch mechanism. In addition, those models were deterministic while the brain deals with noisy sensory signals. Therefore, previous models did not account for pursuit variability.

Kalman filtering has been often used in other neuroscience fields which are dealing with multiple input signals, but not yet in the oculomotor field. For instance, when the brain has access to two different noisy sources of information, several papers proposed that the brain combines these two signals, weighted by the confidence about each source (Körding and Wolpert, 2004). In case of linear systems, this can be achieved with Kalman filtering. In the oculomotor

system, two main sources of information are available; retinal and extra-retinal signals. The key property of a Kalman filter is the ability to combine some internally generated estimation with some estimation obtained from sensory feedback. Therefore, Kalman filtering has been implemented in recurrent networks for computing sensorimotor transformations (Haykin, 2001; Rao, 2004; Denève et al., 2007).

In this paper, a pursuit model uses Kalman filtering (Kalman, 1960; Kalman and Bucy, 1961) to estimate both retinal and extra-retinal (internal) noisy inputs. Basically, the Kalman filter uses the current observation (of the retinal slip, i.e. the velocity error, for instance) to improve its estimation and compute the associated variability. Therefore, the Kalman filtering approach makes the hypothesis that the brain incorporates a measure of uncertainty about these sensory (and predictive) predictions. This measure of uncertainty of both sensory and predictive signals will be used to combine those signals in a statistically optimal way (Ernst and Banks, 2002; Vaziri et al., 2006; Ronsse et al., 2009).

Until now, previous pursuit models with a predictive component always used a static memory. This static memory made some prediction at a fixed horizon (Soechting et al., 2010) or used static images of velocity motion (Bennett and Barnes, 2003, 2006b; Churchland et al., 2003; Madelain and Krauzlis, 2003). In contrast, our model incorporates a dynamic internal representation of target motion (Orban de Xivry et al., 2008) that is also based on Kalman filtering in order to learn from previous experience. This model is therefore able to reproduce different predictive mechanisms and to learn about the past target motion in order to improve the estimation of future target trajectory.

Methods

Global Structure

The model aims at estimating the actual retinal slip through two different mechanisms: Kalman filtering of noisy sensory inputs and prediction of future retinal slip. In Kalman filtering, noisy sensory inputs are combined with the previous estimate of retinal slip (RS) in order to refine this estimation. Noisy sensory inputs are delayed by 80 ms. The predicted retinal slip is obtained from an efference copy of eye velocity and an internal representation of target motion (if available). Estimated and predicted values of the retinal slip are then combined and processed similarly as in previous models.

More specifically, the block diagram of the model is shown in Fig. II.1. The model takes target velocity as its input and eye velocity as its output. The model consists of three main parts: 1) Visual processing processes the noisy retinal inputs and gives an estimation of the sensory retinal slip ($\hat{RS}_{sens}$) and its associated uncertainty (Σ_{sens}); 2)The internal representation block computes a prediction of the estimated retinal slip ($\hat{RS}_{\text{int}}$) and its uncertainty (Σ_{int}) from past sensory information (past values of $\hat{RS}_{sens}$) and the current estimation of the eye velocity (coming from efference copy); 3) The motion pathway produces the motor command, using both sensory and predicted retinal slips, weighted by their uncertainty.

The processing of the motor command is a simplified version of a previous model (Krauzlis and Lisberger, 1994). It is transmitted to the premotor system, which includes a pathway with a gain element T_1 and a second parallel pathway with a neural integrator. Its output is finally sent to the eye plant to give the eye velocity signal.

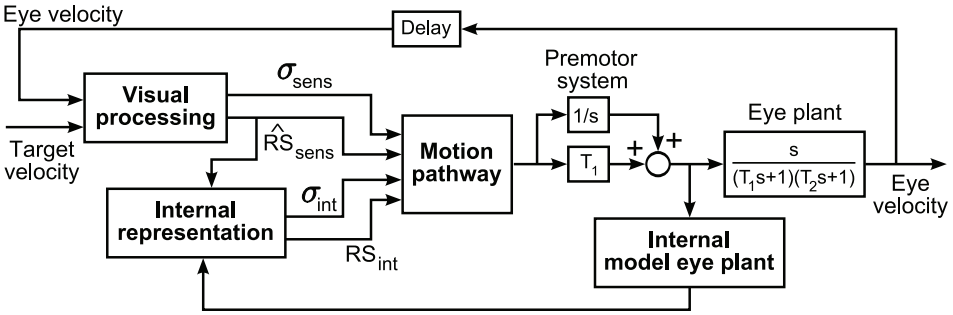

Figure II.1: Global structure of the model. Visual processing computes the noisy target velocity and eye velocity (which is delayed by 80 ms) in order to give an estimation of the sensory retinal slip ($\hat{RS}_{sens}$) and its uncertainty (Σ_{sens}). The internal representation block constructs a prediction of the estimated retinal slip ($\hat{RS}_{\text{int}}$) and its associated uncertainty (Σ_{int}) from past sensory information (past values of $\hat{RS}_{sens}$) and the current estimation of the eye velocity (coming from efference copy). Motion pathway generates the motor command, using both sensory and internal retinal slips. This command is sent to the premotor system and then to the eye plant, and finally gives the eye velocity signal.

The eye plant function approximates the dynamics of the eyeball, the extraocular muscles and the tissues that surround them. Its transfer function is composed by a second order function, with time constants T_1 and T_2 fixed to 170 ms and 13 ms (Robinson, 1976; Zee and Robinson, 1979; Robinson et al., 1986). There is no noise added to the eye plant (no motor noise simulated).

Details of the visual processing: Kalman filtering

Retinal slip is estimated from the slip of the image of the target on the retina, i.e. by subtracting eye velocity from target velocity (Fig. II.2). However, these signals are represented in the brain by noisy signals (Stein et al., 2005; Osborne et al., 2005, 2007; Osborne and Lisberger, 2009; Gold and Watanabe, 2010). Moreover, there are many non-linearities in the brain signals. For instance, the sensory inputs coming from the retina are clearly not linear, since a measure on the fovea is much more reliable than a measure on the retinal periphery.

Therefore, we wanted to have a general noise configuration that can explain a broad range of noise signals. Consequently, additive and multiplicative noises were added to the basic retinal slip signal.

Then the noise observed in the signal will be mainly due to additive noise for small values of RS, whereas multiplicative noise will explain most of the noise for large values of RS:

$$RS_{noisy} = RS_{\det}\left(1+\delta_{mult}\right)+\delta_{add} \qquad \text{Eq. II.1}$$

with $RS_{\det}$ the deterministic value of RS, $\delta_{add} \sim \mathrm{N}(0,\mathrm{Sens}_{\mathrm{add}})$ and $\delta_{mult} \sim \mathrm{N}(0,\mathrm{Sens}_{\mathrm{mult}})$. This noisy signal was then filtered by the brain before being used by the pursuit system.

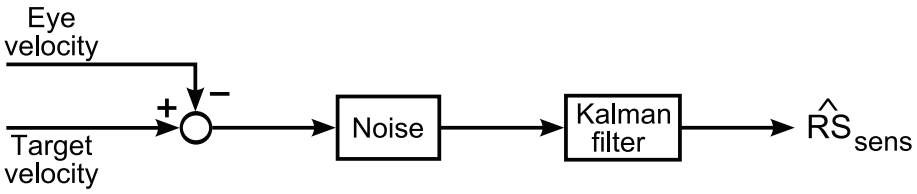

Figure II.2: Visual Processing system. Eye velocity and target velocity are compared to give the retinal slip. Some multiplicative and additive noises are then added, before a Kalman filter estimates the sensory retinal slip $\hat{RS}_{sens}$.

An estimation of the sensory retinal slip ($\hat{RS}_{sens}$) signal was computed from this noisy signal using the Kalman filtering technique. The assumption is made that the estimated RS at time k will be used to predict RS at time k+1 and is modeled by a random walk.

Therefore, the system dynamics is:

$$\hat{RS}_{sens_k} = \hat{RS}_{sens_{k-1}} + \theta_k \qquad \text{Eq. II.2}$$

where $\hat{RS}_{sens_k}$ represents the last estimate of the retinal slip and θ_k is an additional process noise with $\theta_k \sim \mathrm{N}(0,\mathrm{Q})$ representing the state variability.

Because the system does not know how $\hat{RS}_{sens}$ will evolve, it considers that $\hat{RS}_{sens}$ evolves as a random walk. This prediction will then be refined by the observed values of RS. The observation could be written as:

$$RS_k^{Obs} = \hat{RS}_{sens_{k-1}} + \gamma_{k-1}\hat{RS}_{sens_{k-1}} + v_{k-1} \qquad \text{Eq. II.3}$$

where γ_k and v_k are the multiplicative and additive measure noises with $\gamma_k \sim \mathrm{N}(0,\mathrm{D})$ and $v_k \sim \mathrm{N}(0,\mathrm{R})$.

In the Kalman filtering, the extrapolated value of $\hat{RS}_{sens}$ is updated with the observation from the last time step and yields an estimation of the sensory retinal slip $\hat{RS}_{sens}$:

$$\hat{RS}_{sens_k} = \hat{RS}_{sens_{k-1}} + K_k\left(RS_{k-1}^{Obs} - \hat{RS}_{sens_{k-1}}\right) + \eta_t \qquad \text{Eq. II.4}$$

with RS_k^{Obs} the noisy signal (called RS_{noisy} on Eq. II.1) of RS observed at time k on the brain (i.e. the signal measured on the

retina, delayed by 80 ms), η_t is the internal noise of the estimation (done by other neurons) with $\eta_t \sim \mathrm{N}(0,\Omega_n)$.

Following Kalman theory, and because the different noises are Gaussian and not correlated, the optimal value for K_k can be computed as:

$$K_k = \Sigma_{sens_k}\left(\Sigma_{sens_k} + R + D\left(\Sigma_{sens_k} + \hat{RS}_{sens_k}\ \hat{RS}_{sens_k}^{\ T}\right)D^T\right)^{-1} \quad \text{Eq. II.5}$$

$$\Sigma_{sens_k} = Q + \Omega_n + \left(1 - K_k\right)\Sigma_{sens_{k-1}} \quad \text{Eq. II.6}$$

with Σ_{sens} the estimation error variance. This estimation will be used to assess the uncertainty associated with the estimation $\hat{RS}_{sens}$.

Internal Representation

In some circumstances (e.g. blanking of the target), visual information is not available and $\hat{RS}_{sens}$ cannot be computed. In other circumstances (e.g. sinusoidal target motion), the brain can predict the future target motion and anticipate it in order to reduce the time lag between eye and target motion (Dallos and Jones, 1963; Barnes et al., 1987; Barnes and Ruddock, 1989; Barnes et al., 2000). Based on experience, the brain could use internal representations and prediction in many situations in order to predict the future target trajectory (Barborica and Ferrera, 2003; Ilg and Thier, 2003).

By combining this knowledge of future target motion with the efference copy of the actual eye velocity, the retinal slip can be predicted ("internal RS": $\hat{RS}_{\text{int}}$):

$$\hat{RS}_{Int_k} = TV^{\text{Pr}ed}_{Int\,\text{Re}\,pr_{k+150}} - \dot{e}^{Est}_{Eff\ copy_k} \qquad \text{Eq. II.7}$$

where $TV^{\text{Pr}ed}_{Int\,\text{Re}\,pr_{k+150}}$ represent the predicted target velocity 150 ms into the future (time step k+150 ms) and $\dot{e}^{Est}_{Eff\ copy_k}$ the estimated value of current eye velocity (at time step k) as estimated by an internal model of the eye plant (Skavenski and Robinson, 1973; Robinson, 1981). The value of 150 ms will be discussed later and an alternative will be suggested.

The accuracy of the $TV^{\text{Pr}ed}_{Int\,\text{Re}\,pr_{k+150}}$ prediction can be estimated later by comparing it to the actual target trajectory. The difference between the predicted and actual target trajectory will determine the confidence in the internal signal $\hat{RS}_{\text{int}}$. Again, a Kalman filter was used to assess the uncertainty linked to $\hat{RS}_{\text{int}}$.

For the prediction of target velocity, the dynamics of the system is represented by:

$$TV_{k+1} = TV_k + B_{\text{int}}\, u_k + \alpha_k \qquad \text{Eq. II.8}$$

where TV is target velocity and $u_k = \Delta(TV)^{\text{Pr}ed}_{Int\,\text{Re}\,pr}$ represents the known change in velocity from k to k+1, $\alpha_k \sim \text{N}(0, \text{Q}_{\text{int}})$ the process noise.

The dynamics of TV has an additional term compared to the dynamics for RS (see Eq. II.2). The main difference between RS and TV systems is that the brain knows how TV evolves over time whereas this evolution is unknown for RS. The control signal u_k (and thus the whole internal representation of target motion) can be obtained by several ways such as extrapolation based on previous target motion yield the series of u_k (Soechting et al., 2010), memory of previous target motion or computation through the law of physics.

In this model, observation of the actual TV is delayed by 150 ms, so the observation equation is:

$$TV_k^{Obs} = TV_{k-150} + \varphi_k \, TV_{k-150} + \beta_k \qquad \text{Eq. II.9}$$

The internal representation of TV is then refined thanks to the observation:

$$\hat{TV}_k = \hat{TV}_{k-1} + B_{\text{int}} \, u_{k-1} + K_{\text{int}_{k-1}} \left(TV_{k+150}^{Obs} - C_{\text{int}} \, \hat{TV}_{k-1} \right) + \varepsilon_t \qquad \text{Eq. II.10}$$

$$K_{\text{int}_k} = \Sigma_{\text{int}_k} \left(\Sigma_{\text{int}_k} + R_{\text{int}} + M \left(\Sigma_{\text{int}_k} + \hat{TV}_k \, \hat{TV}_k^{\,T} \right) M^T \right)^{-1} \qquad \text{Eq. II.11}$$

The uncertainty Σ_{int} will be given by:

$$\Sigma_{\text{int}_k} = Q_{\text{int}} + \Omega_e + \left(1 - K_{\text{int}_{k-1}}\right)\Sigma_{\text{int}_{k-1}} \qquad \text{Eq. II.12}$$

with $\hat{TV}_k$ the predicted target velocity at time k for target velocity at time k+150 computed by the Kalman filter, $\beta_k \sim \mathrm{N}(0, \mathrm{R}_{\text{int}})$ the measure noise, $\varphi_k \sim \mathrm{N}(0, M_{\text{int}})$ the multiplicative measure noise and $\varepsilon_k \sim \mathrm{N}(0, \Omega_{\mathrm{e}})$ the internal noise.

Given, this 150 ms prediction time horizon, the estimated $\hat{TV}_k$ cannot be used to refine the internal representation of target motion within a trial. However, it will be used when consecutive trials will be simulated. As a result, the model can learn and improve its internal estimation of target trajectory. In this case, the output of the Kalman filter at trial j is used as the internal representation of target motion at trial j+1, with some noise:

$$\left(TV_{k+150}\right)_{Trial\ j+1} = \left(TV_k^{\Pr ed}\right)_{Trial\ j}\left(1 + \delta_{Int_{mult}}\right) + \delta_{Int_{add}} \qquad \text{Eq. II.13}$$

with $\delta_{Int_{mult}} \sim \mathrm{N}(0, \mathrm{Int}_{\text{mult}})$ and $\delta_{Int_{add}} \sim \mathrm{N}(0, \mathrm{Int}_{\text{add}})$. Therefore, this value $\left(TV_{k+150}\right)_{Trial\ j+1}$ will be used as the $TV_{Int\,\mathrm{Re}\,pr_{k+150}}^{\Pr ed}$ signal (Eq. II.7) for the next trial. In contrast, the accuracy of the prediction Σ_{int} will be used in the motion pathway (see below).

Motion Pathway

The inputs of the motion pathway are coming from two different sources of information (Fig. II.3): these are sensory (i.e. retinal) and internal signals (i.e. extra-retinal). These two sources of information are weighted in function of their estimated variability (Σ_{sens} and Σ_{int}). The optimal weighting of such stochastic variables (Ernst and Banks, 2002; Vaziri et al., 2006) is given by:

$$\hat{RS} = \frac{\Sigma_{\text{int}}}{\Sigma_{\text{int}} + \Sigma_{sens}} \hat{RS}_{sens} + \frac{\Sigma_{sens}}{\Sigma_{\text{int}} + \Sigma_{sens}} \hat{RS}_{\text{int}} \qquad \text{Eq. II.14}$$

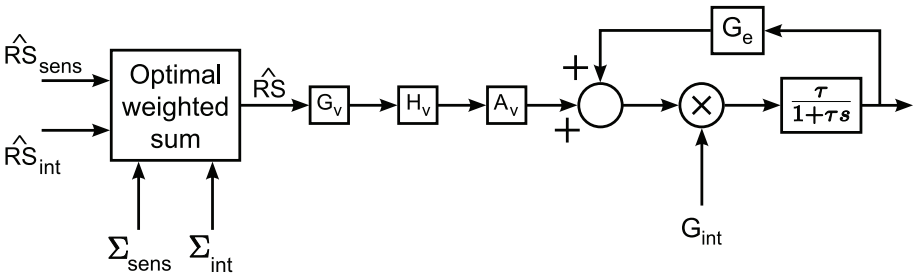

Figure II.3: Motion pathway. Sensory and internal RS are weighted according to their uncertainty and give the estimated RS ($\hat{RS}_{sens}$). This signal is processed by a part of a classical pursuit model (velocity motion pathway from Krauzlis and Lisberger, 1994). The output is then sent to a (leaky) integrator.

The model needs an “a priori” for the uncertainty of the sensory and internal signals. This a priori is based on previous experiences. At movement onset, the visual feedback will be favored if the internal representation is absent or inaccurate (Σ_{int} is large). This is implemented by increasing the value of Q_{int} (the process noise), which will increase the noise of the internal representation and then favor the sensory information. Forcing the initial conditions given to the sensory variance (e.g., after target disappearance $\Sigma_{sens} = \infty$ as a result of the absence of retinal feedback) will also lead to an abrupt change of weighting.

The weighted $\hat{RS}$ signal is then sent to a pathway similar to the « image velocity motion pathway » from Krauzlis and Lisberger (1994). This velocity motion pathway (Fig. II.3) contains a linear function (G_v), a second-order filter (H_v) and a gain element (A_v). The parameters used in these functions were close to those from the original functions and were equal to:

$$G_v(u) = 7\,u \qquad \text{Eq. II.15}$$

$$H_v(s) = \frac{35^2}{s^2 + 2\,0.8\,35\,s + 35^2} \qquad \text{Eq. II.16}$$

$$A_v = 0.9 \qquad \text{Eq. II.17}$$

The output goes to a (leaky) integrator (called “positive efferent copy feedback loop” in Krauzlis and Miles (1996b)) that is characterized by two variables: G_{int} and τ. G_{int} determines the gain

of pursuit system (gain ~ $G_{\text{int}}{}^2$). It is set to $\sqrt{G_{\text{int}}}$ during visually-guided smooth pursuit, to zero when the target stops moving or disappears and is modulated around an intermediate value when the target disappears but is expected to reappear (transient blanking). τ represents the time constant of the integrator that is required to maintain eye velocity when RS=0 ($\tau = 100ms$). The linear gain element was set to $G_e = \frac{1}{\tau}$.

In the present model, the memory used for prediction stores a memory of target motion, which is dynamically updated by the Kalman filter based on past information. This contrast with models where short-term memories stores copies of eye motor commands that are replayed to replace the retinal information for predictive pursuit (Krauzlis and Miles, 1996b; Bennett and Barnes, 2003; Madelain and Krauzlis, 2003). Therefore, the motion pathway is not only active during visually guided pursuit but also in the absence of retinal signals.

Simulation parameters

We used a fixed step size of 0.001 s to run all simulations. The blocks and equations were numerically integrated using the 4th order Runge-Kutta method from Simulink (Matlab).

We used the following values for noise parameters (Eq. II.1 and II.13): $\text{Sens}_{\text{add}} = 20$, $\text{Sens}_{\text{mult}} = 1$, $\text{Int}_{\text{add}} = 1$, $\text{Int}_{\text{mult}} = 0.01$. Unless otherwise specified, parameters of the visual processing (Eq. II.2 to

Eq. II.4) Q, D, R and Ω_n were respectively equal to 1, 1, 20 and 0.1. For the internal representation (Eq. II.8 to Eq. II.10), parameters B_{int}, Q_{int}, R_{int}, M_{int} and Ω_e were respectively equal to 0.5, 1, 20, 0.1 and 0.1. Initial conditions of noise variance were set to $\Sigma_{sens} = 1$ and $\Sigma_{\text{int}} = 1$. All these parameters did not change during a simulation.

For all trials where no predictions were available (Fig. II.4, Fig. II.5, first half-cycle in Fig. II.6, first pursuit trial in Fig. II.8), the noise added to the dynamics of the internal system (Eq. II.8) was quite important ($Q_{\text{int}} = 1$), because the lack of predictability of future target trajectory.

For other trials where some prediction could be made on future target trajectory (Fig. II.6 for all half-cycles except the first one, Fig. II.7, Fig. II.8 for all pursuit trials except the first one, Fig. II.9 and Fig. II.10), the noise added to the dynamics of the system (Eq. II.8) was less important ($Q_{\text{int}} = 0.1$).

In Fig. II.4A, target motion was 20 deg/s after a fixation period. In Fig. II.4B, the target underwent a velocity step, ranging from -50 deg/s to 50 deg/s. For each velocity step, 30 simulations were achieved, and we measured the mean acceleration of the pursuit initiation (between 80 and 180 ms after pursuit onset). We compared these simulation data with experimental data, where the acceleration was measured similarly. These data were re-analyzed from the dataset of de Brouwer, Missal, Barnes and Lefèvre (2002).

In Fig. II.5, 30 simulations were done for each velocity step of the target (5, 10, 20 and 30 deg/s). For each target motion, the

average of the 30 associated simulations was performed and shown in red in Fig. II.5.

In Fig. II.6, the target moved sinusoidally (maximum peak velocity of ±6.7deg/s).

In Fig. II.7, pursuit gain for a half cycle was computed (for a given interval centered around target peak velocity) as the peak eye velocity divided by the peak target velocity. The phase was obtained as the difference in time (expressed in angular degree) between those two peaks. Data were obtained by averaging 30 different simulations (same kind than in Fig. II.6), over 3 half-cycles (from the 4th to the 6th half-cycles).

To induce anticipatory pursuit (gap paradigm, Fig. II.8), a 300 ms gap period (transient blanking of the target) is used before target motion. During this period, G_{int} is set to 0.6 until visual feedback of the moving target was available (80 ms after target motion). Then, G_{int} was set to 1. From the 2nd trial onwards, the internal representation of target motion ($TV_{Int}^{\text{Pr}ed}{}_{\text{Re}\,pr_{k+150}}$ in Eq. II.7) is the output of the Kalman filter of the previous trial ($\hat{TV}_k$ in Eq. 10) with an advance of 150 ms and some added noise (Eq. II.13).

In Fig. II.9, G_{int} was set to 1 when the target was visible, and then instantly decreased to 0.6 during target blanking. This sudden change in G_{int} produced the typical exponential decay of eye velocity (Becker and Fuchs, 1985; Bennett and Barnes, 2003; 2004; 2005). To simulate predictive recovery of eye velocity, G_{int} was increased linearly from a time T that was randomly chosen between 50 and 250

ms before target reappearance. The slope of this increase was equal to $\frac{(1-G_{\text{int}})}{2T}$. By doing this, G_{int} was inferior to 1 when the target reappeared. It was reinstated to 1 when visual feedback of the target was available (i.e., 80 ms after target reappearance). When the target was blanked, because there was no more visual input to the sensory system, we set $\Sigma_{sens} = \infty$. Therefore, we have $\hat{RS} = \hat{RS}_{\text{int}}$ during this period of time. During blanking, the noise values for $\hat{TV}_k$ (Eq. II.13) increased linearly as the estimation of the target became more uncertain with time evolving. At time X (in s after target disappearance), Int_{mult} and Int_{add} were both multiplied by $(1+X)$. Target was moving at 20 deg/s for both panels. Varying the gain G_{int} illustrates the range of variability of the residual velocity during the blanking (Fig. II.12B). In this figure, we changed the value of G_{int} during the blanking period for the different simulations, varying from 0.9 to 0.4.

For Fig. II.10, after a fixation period, the target underwent a velocity step of 10 deg/s and instantly a constant acceleration of 8 deg/s² for 2s.

In Fig. II.11, parameters were the same than for Fig. II.7. When the target was blanked (80 ms after its disappearance), G_{int} was set to 0.6 until 80 ms after target reappearance (when sensory information was available). Then, it was reinstated to its initial value of 1.

For Fig. II.12, after a fixation period, the target underwent a velocity step of 5 deg/s and instantly an acceleration of 300 deg/s² for

100 ms. After those 100 ms, the target moved at constant velocity of 35 deg/s for 1 s. For the simulations in Fig. II.12C, during the blanking period G_{int} was set either to 0.7 (green simulations for the “occluded” condition) or to 0.5 (red simulations for the “blinked” condition).

Results

Simulations on visually-guided pursuit: comparison with human data

The model performance in response of the sudden motion of a visible target is illustrated on Fig. II.4A. After a fixation period (~500 ms), the target underwent a “step ramp” motion (20 deg/s). Different simulations are shown in red traces, showing the variability of the model output response.

The pursuit acceleration predicted by the model was analyzed by simulating different target velocity steps. We compared the simulated results with experimental results from human subjects (data were re-analyzed from dataset used in de Brouwer et al, 2002). This comparison is shown in Fig. II.4B. We measured the acceleration as the mean acceleration in the interval between 80 and 180 ms. Note that this model did not contain a specific saturation function for pursuit acceleration, as it was the case for some previous models (Bennett and Barnes, 2003; 2006). The model prediction closely matched

smooth pursuit acceleration in humans for “normal” values of retinal slip (<50 deg/s).

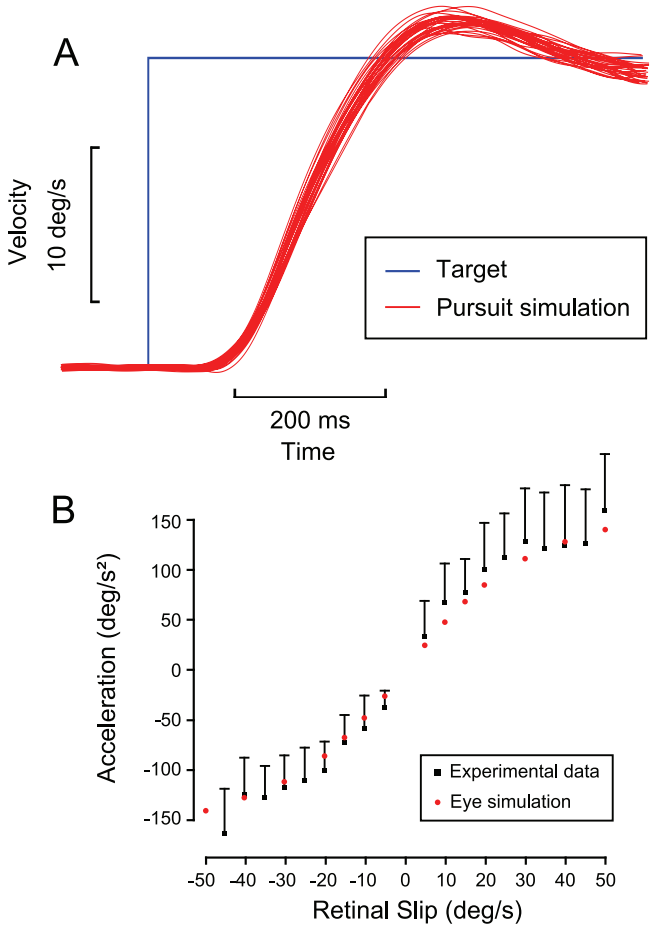

Figure II.4: Simulations of visually-guided pursuit initiation. A) Simulations of pursuit velocity (in red). Target velocity is represented in blue. B)Relationship between sensory retinal slip and mean eye acceleration in the interval between 80 and 180 ms after pursuit onset. Black squares correspond to experimental data, red dots correspond to simulation data. Standard deviation is shown with vertical bars.

The mean latency of the pursuit response is 120 ms +/- 14 ms. The value is similar to those measured in Tarnutzer et al. (2007), Rasche and Gegenfurtner (2009). The standard deviation observed when initiating pursuit at 20 deg/s is around 2 deg/s (10%). This value is similar to those observed in previous studies (Osborne et al., 2005; Rasche and Gegenfurtner, 2009).

Simulations on visually-guided pursuit: comparison with previous models

A comparison with velocity traces simulated from previous models has shown little difference (Fig. II.5). Simulations of pursuit initiation to a target moving at a constant velocity generated with the pursuit model made by Robinson, Gordon and Gordon (1986) were very similar to those produced with the pursuit model of Krauzlis and Lisberger (1994). Here, we can observe than the pursuit acceleration and the overshoot at the end of the initiation phase are comparable. However, the model did not reproduce the 4 Hz oscillations visible during sustained pursuit.

It is worth noting that the current pursuit model does not contain an “image acceleration motion pathway”, as it was the case in previous models (Krauzlis and Lisberger, 1994; Krauzlis and Miles, 1996). This “image acceleration motion pathway” was previously used to promote persistent oscillations of eye velocity during sustained pursuit and to avoid large overshoot at the end of the initiation of

pursuit. In the present model, the internal system will increase its weight compared to the sensory system after pursuit initiation. It will therefore help to avoid a large overshoot at the end of pursuit initiation (since the predictive system works with an estimation of the retinal slip with an advance of 150 ms, predictive pursuit velocity will never overshoot target velocity) .

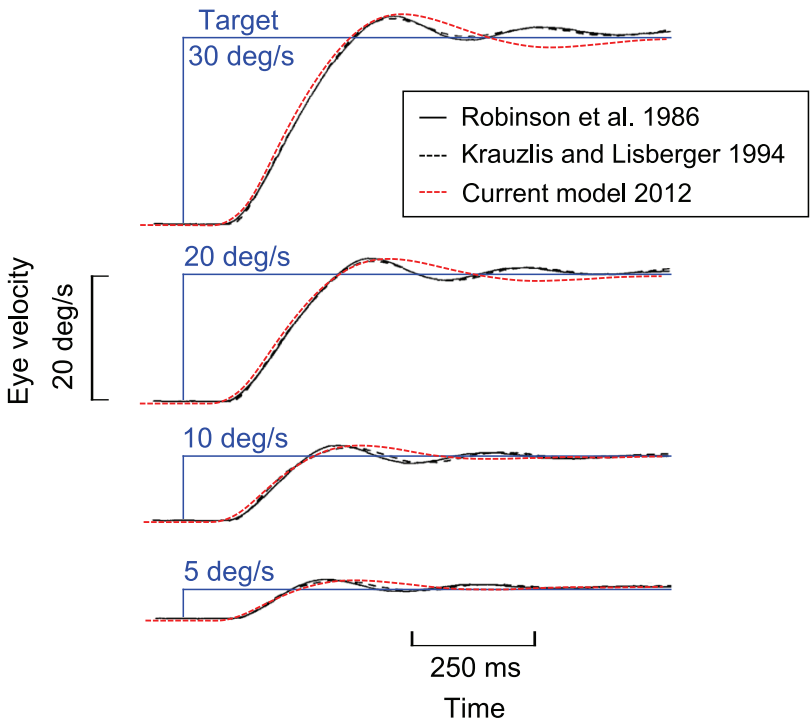

Figure II.5: Comparison with previous models. Initiation of the pursuit system in response of targets moving at 5, 10, 20 and 30 deg/s. Target velocity is represented in blue, simulations coming from the model of Robinson et al. (1986) are shown in continuous black traces, simulations coming from the model of Krauzlis and Lisberger (1994) are shown in dashed black traces and the simulations from our model are shown in red.

Simulations of smooth pursuit in response to a sinusoidally moving target

Tracking a sinusoidally moving target is often performed with small phase lag (Dallos and Jones, 1963; Yasui and Young, 1984; Barnes et al., 1987; Barnes and Ruddock, 1989; Barnes et al., 2000). The Kalman model can achieve this by using the memory acquired during half a cycle as the internal representation of target motion for the next half-cycle (Fig. II.6). Initially, the subject had no internal representation of future target motion (1st half-cycle). During this period, the model relies solely on sensory signal ($\hat{RS}_{sens}$), with a sensorimotor delay of 80 ms and lags behind the target (Fig. II.6). Then, target motion estimated during this period is used as the internal representation of target motion for the second half-cycle. For all ensuing half-cycles, the estimated target motion obtained during one half-cycle is obtained during the next one. The use of this internal representation decreases the phase lag to realistic levels (inferior to 10 deg for low frequencies (<0.4Hz), see Barnes (2008) for a review) and the gain is close to one.

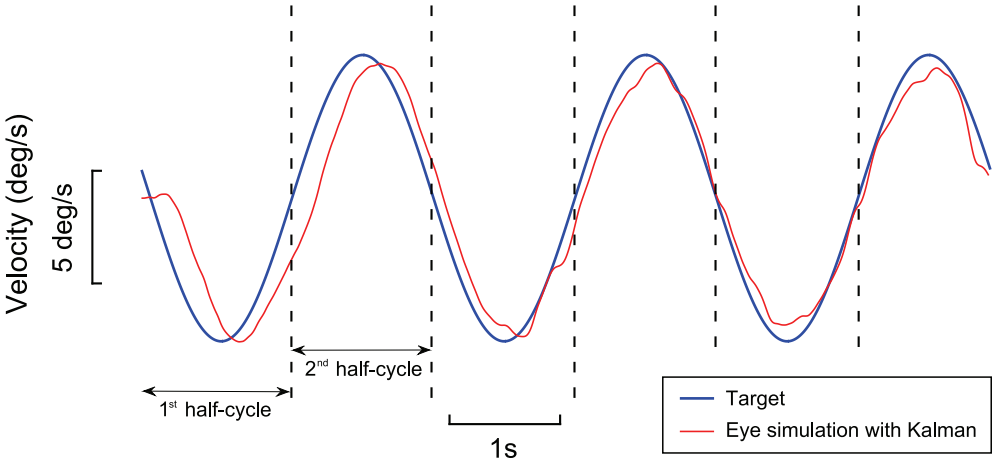

Figure II.6: Simulation of smooth pursuit velocity (in red) when tracking a small target (in blue) moving with a sinusoidal velocity, with peak displacement of ± 6.7 deg/s and a frequency of 0.4 Hz.

After several such cycles, phase lags and pursuit gains reach similar levels as obtained in human subjects. Figure II.7 presents experimental data from Barnes, Donnelly and Eason (1987). The parameters measured are the gain and phase, for a sinusoidal moving target (maximum velocity of 5 deg/s). We can observe the similarity of the model prediction for the different frequencies of the moving target.

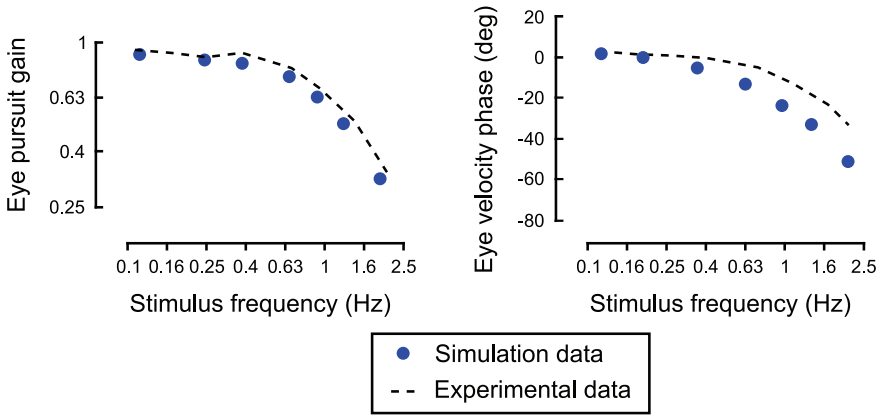

Figure II.7: Gain and phase as a function of frequencies of the sinusoidal waveform. Black dashed traces depict the gain and phase recorded in normal subjects tracking a sinusoidal moving target. Model predictions (see Simulation parameters) are represented by the blue dots and can be compared to the experimental data. Experimental data are adapted from Barnes, Donnelly and Eason (1987).

Simulations of anticipatory eye movements before target motion onset

Building an internal representation of target motion from past experience is advantageous for tracking sinusoidally moving target but also for anticipating target motion onset. Indeed, it is well known that when direction of target motion and the timing of its onset are known, subjects are able to move their eyes before target onset

(Kowler and Steinman, 1979a, 1979b). Similarly, after a few trials, the model exhibits anticipation of target motion. Namely, the eyes start moving before target motion onset. Figure II.8A illustrates a pursuit response with visually guided eye movements and Fig. II.8B to Fig. II.8D show anticipatory eye movements using the prediction of the future target velocity (coming from the previous estimation of the internal Kalman filter 150 ms in advance). The increase in anticipatory eye movements is visible over the course of trials.

In addition, the update of the internal representation of target motion after each trial will naturally lead to a type of "history effect" (Kowler et al., 1984). This effect is observed when target motion varies from trial-to-trial. Therefore, anticipatory eye velocity will be stronger after two consecutive trials with fast target motion than after one trial with low and one trial with fast target motion (Poliakoff et al., 2005).

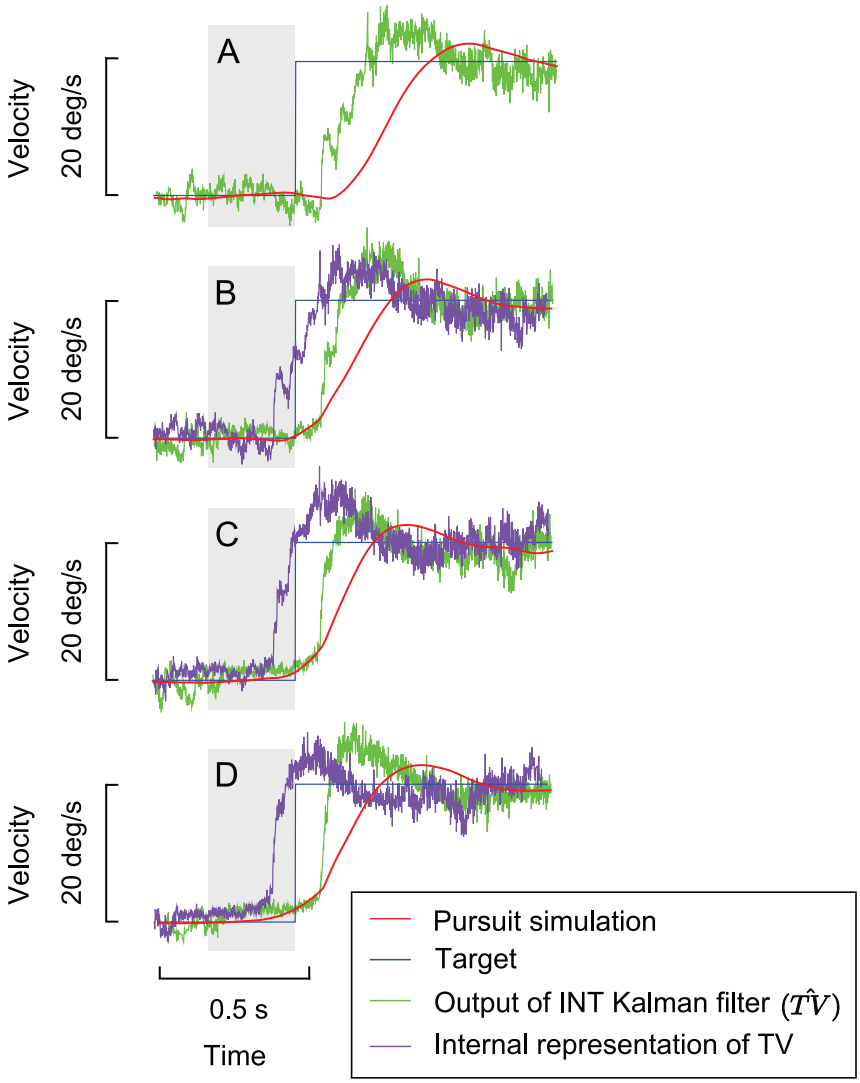

Figure II.8: Anticipatory pursuit eye movement based on the learning of past target trajectories. Target velocity is shown in blue, the estimation of target velocity given by the internal Kalman filter ($\hat{TV}$) is shown in green, the internal representation of the target velocity is shown in purple and the simulated pursuit eye movement in red. Grey areas represent periods when target was blanked (gap periods).

A) No prediction available: a visually-guided pursuit eye movement is initiated (red trace) and an estimation of target velocity is computed (green trace). B) The previous estimation of target motion is used as the internal representation (purple trace), but the associated uncertainty is quite important. Then, the anticipation is quite small. However, the estimation of target velocity is improved for next trial (green trace). C) The anticipatory eye movement is more important, and the estimation is still refined. D) The anticipation begins earlier and is more prominent, due to the larger reliability of the estimation of the target velocity.

Simulations of smooth pursuit during target blanking

Predictive smooth pursuit eye movements are similarly highlighted when the moving target is blanked for several hundreds of milliseconds. In this case, the model reproduces the smooth pursuit eye movement observed during the blanking of a target moving at constant velocity (Fig. II.9A).

As in human subjects, simulated eye velocity decreases after target blanking. Both τ and G_{int} (presented in the motion pathway, Fig. II.3) determine the rate at which pursuit velocity decays towards the residual velocity plateau (Becker and Fuchs, 1985). The time constant is $\frac{\tau}{1-G_{\text{int}}}$, so that its value will be around 200 ms for $\tau = 100ms$ and $G_{\text{int}} = 0.5$. This time constant is similar to the one

measured in previous studies (see e.g. Becker and Fuchs (1985) or Orban de Xivry et al., (2008) for different time constant values).

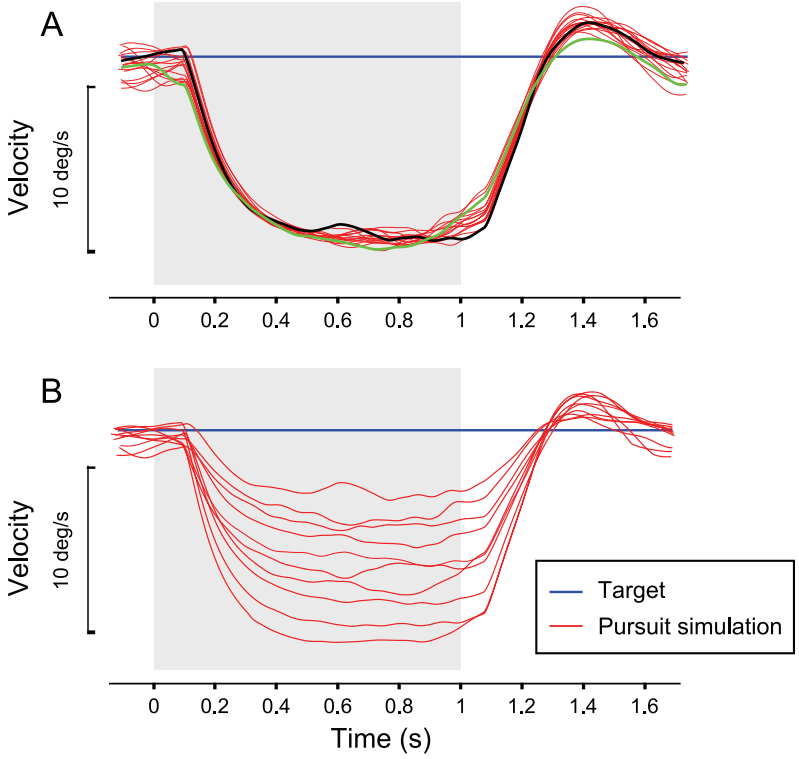

Figure II.9: Smooth pursuit simulations with target blanking. Simulated pursuit traces (red traces) when target disappeared behind an invisible occluder (blanking period; grey area). Target velocity is 20 deg/s and is shown in blue. A) Two typical simulations are highlighted (green and black traces) with respectively a large and no predictive recovery. B) Simulations of smooth pursuit eye movements with different levels of residual velocity.

For the simulations, we kept $\tau = 100ms$ constant, G_{int} was set to 0.6 during blanking periods (see Simulation parameters section). In general, the smooth pursuit response is variable, even during the blanking period despite the fact that the gain G_{int} was kept constant for all trials. This variability is coming from the noisy $\hat{RS}_{\text{int}}$.

Two different simulations are highlighted in black and in green (Fig. II.9A). The black trace illustrates a trial where there is no predictive recovery (or a very small one). On this trial, we can see that the large acceleration occurring after target reappearance is due to sensory signal (visually guided acceleration). However, on many trials, we can observe a clear predictive acceleration before the target reappeared, as we can see on the green trial.

If we now change the value of G_{int}, we will obtain different values of residual velocity (Becker and Fuchs, 1985). This phenomena is often observed in experimental data, even in consecutive trials for a single subject (see Fig. I.5 or Fig. 8 from Orban de Xivry et al., (2006) where respectively 3 and 4 trials coming from a single (different) subject are shown). Similarly, there is variability in the beginning of pursuit reacceleration, even for a single subject knowing the timing of target reappearance. In Fig. II.9B, each simulation has a different value of G_{int}. Again, the timing of the onset of the predictive recovery, that could be observed clearly in most simulations, begins at different timing (see Simulation parameters).

Given that the model possesses a dynamic internal representation of target motion (Orban de Xivry et al., 2008), it is able to reproduce the behavior during the blanking of an accelerating target (Fig. II.10; Bennett and Barnes, 2006; Bennett et al., 2007) or a

sinusoidally moving target (Fig. II.11; Whittaker and Eaholtz, 1982; Kveraga et al., 2001; Fukushima et al., 2002). When the target is accelerating during the blanking period, the residual eye velocity is slightly increasing, as it is the case in human recordings (Fig. II.10). Note that in our simulations, the value of G_{int} was constant during the occlusion while other models with a static internal representation increased the value of the gain to obtain the eye acceleration during the blanking (Bennett and Barnes, 2006b).

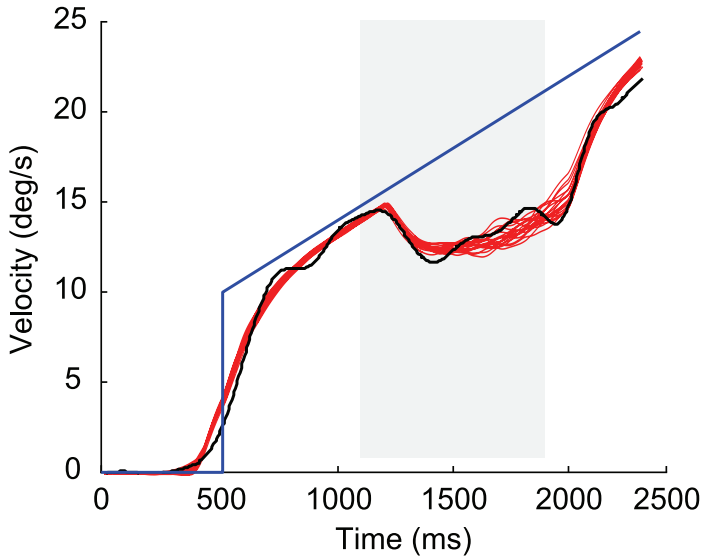

Figure II.10: Anticipatory eye movement and tracking of an accelerating target. Simulations (in red) are compared with experimental data (black trace) with the same target conditions (target velocity is shown in blue). The target was blanked for 800 ms (grey area). Experimental data are adapted from Bennett and Barnes (2006).

However, this can not work anymore if the eye velocity is zero when the target is blanked. In this case, a pursuit model with a static memory will not be able to increase its pursuit velocity, since there is no more retinal information and no velocity stored into the short-term memory. A simple example is shown in Fig. II.11 where the sinusoidally moving target disappears a bit before the peak amplitude of its movement (i.e., when eye velocity is zero).

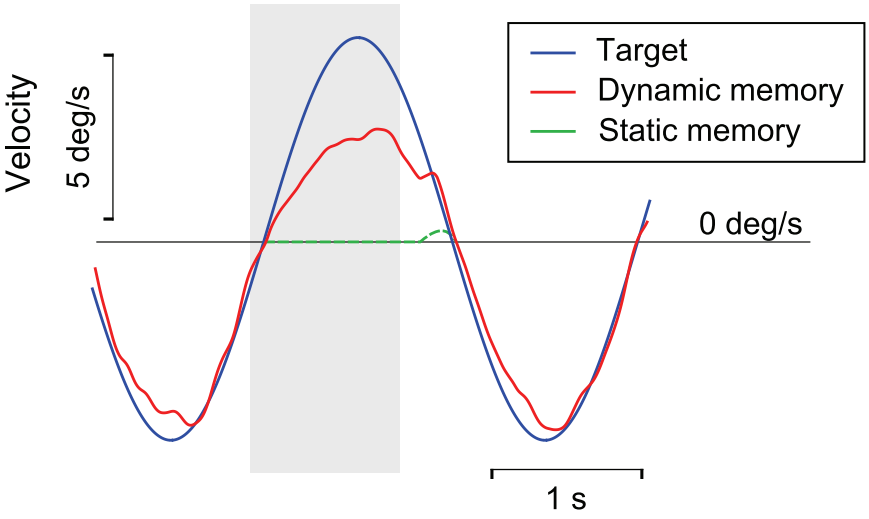

Figure II.11: Blanking of a sinusoidally moving target. After a normal predictive pursuit of the sinusoidally moving target, the target is blanked. The grey area represents the blanking period. However, the dynamic representation of the future target motion is able to increase the pursuit velocity and therefore to continue tracking the invisible moving target. Target velocity is shown in blue. Simulated pursuit response with the dynamic memory is shown in red. Simulation with a static memory gives no eye velocity during blanking (green dashed trace). The horizontal black line shows zero velocity.

When the visual feedback of target disappearance is available (80 ms after its disappearance), the eye velocity is then equal to zero. After target blanking, the pursuit velocity increases with the dynamic representation. During the blanking period, the mean pursuit gain is not as large as before (due to a decrease of G_{int} from 1 to 0.7 during the blanking period), but the pursuit is clearly superior to zero and synchronized with the target motion, meaning that the dynamic representation of the target motion (i.e. based on past information of the target motion) update correctly the retinal slip information. In comparison, a static memory will predict zero eye velocity during the blanking period (Fig. II.11, green dashed trace). To the best of our knowledge, this model is the first capable to simulate this kind of situation.

We were also interested in reproducing the experiments of Churchland et al. (2003), where target was extinguished about 100 ms after pursuit onset (during pursuit initiation). However, this experiment was performed on monkeys and was never done on humans. Therefore, we had to adjust target parameters. In particular, the delay between target motion and its extinction. This delay was less than 120 ms for monkeys (Fig. II.12A and Fig. II.12B). In our simulations, target was blanked 230 ms after its motion onset (Fig. II.12C). Monkeys performed the task in two conditions; the moving target could disappear behind a visible occluder (“occluded” condition) or behind an invisible occluder (“blinked” condition). In this latter condition, the pursuit velocity decrease was more important, since the monkeys were not 100% sure that the target was going to reappear. In the occluded condition, monkeys knew that the target was going to reappear shortly and were therefore motivated to continue the tracking.

To simulate these experimental data, we made the hypothesis that the difference between “occluded” and “blinked” conditions can be explained by a difference in the decrease of the G_{int} gain. Therefore, we simulated the “occluded” condition by setting G_{int} to 0.7, whereas G_{int} was set to 0.5 for the simulations in the “blinked” condition.

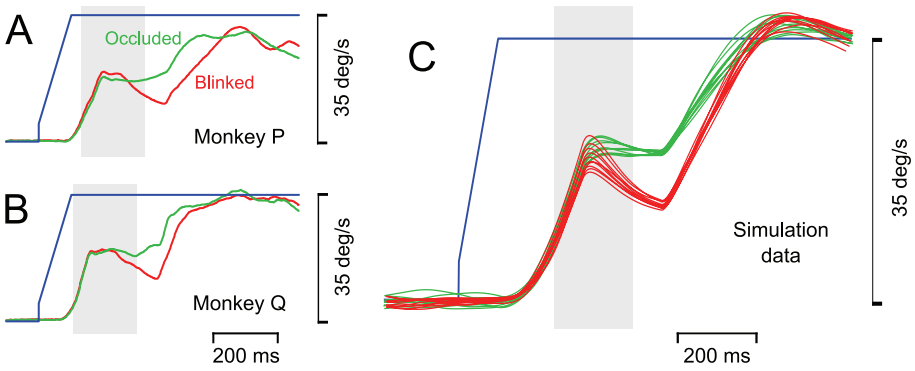

Figure II.12: Blanking of the target during the initiation of the pursuit. A) and B) Experimental data, recorded in two monkeys, adapted from Churchland et al. (2003). Target velocity is shown in blue, pursuit velocity for trials when the target was occluded (visible occluder on the screen) is shown in green and pursuit velocity for trials when the target was blanked (invisible occluder) is shown in red. The grey area represents the blanking period. C) Simulations on the expected behavior of a human subject tracking the same target (velocity shown in blue). The two different conditions (occluded vs blinked) have been simulated by a difference in the G_{int} parameter (G_{int} was equal to 0.7 for the “occluded” condition whereas it was equal to 0.5 for the “blinked” condition).

We can observe that the simulations are similar to the monkey behavior. Since this experiment has not been conducted on human subjects yet, these simulations are a prediction of the potential human oculomotor behavior.

Parameters sensitivity

Changing the value of the noise present in the system is obviously influencing the pursuit response. But changing the noise can also be interpreted differently if one assumes that the brain is aware of this change or not. If one increases the noise present in the system ($\mathrm{Sens}_{\mathrm{add}}$ and $\mathrm{Sens}_{\mathrm{mult}}$ in Eq. II.1) and the estimated noise by the brain (D and R in Eq. II.3) in the same way, then the pursuit response will become slower, with a lower acceleration (see Fig. VI.2). However, if one now changes the system noise (Eq. II.1) without adjusting the estimated noise, the story is different. In this case, the brain does not estimate correctly the noise present in the system, leading to suboptimality (Beck et al., 2012).

Figure II.13 illustrates how much a suboptimal estimation of the noise can impact the pursuit response. If the noise is overestimated, the variability of the response is decreased and the pursuit response is slightly decreased as well (Fig. II.13, green traces). In contrast, the variability is dramatically amplified when the brain underestimates the noise present in the system. Moreover, the mean pursuit velocity is also affected by this suboptimal estimation.

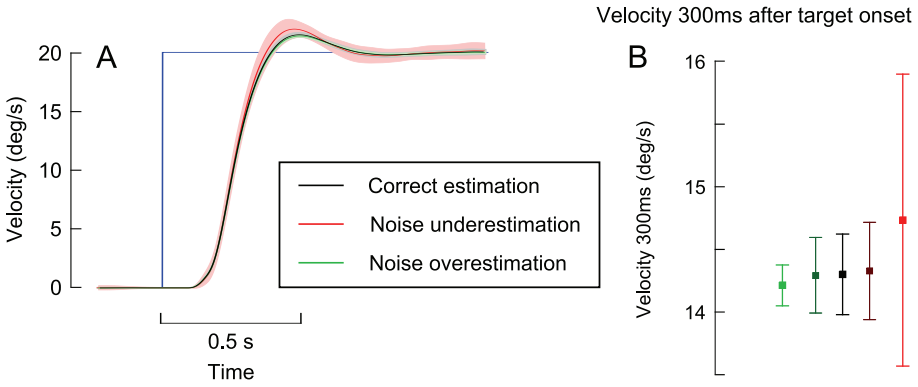

Figure II.13: Illustration of suboptimal noise estimation. A) Simulation responses to a 20 deg/s moving target, represented in blue. Black trace shows the normal simulation. Green trace shows the pursuit response when the system noise is overestimated by the brain (3 times noise overestimation). Red trace shows the pursuit response when the brain underestimates the noise present in the system (3 times noise underestimation). Areas surrounding the traces represent the standard deviation of the mean. B) Pursuit response evaluated 300 ms after target onset for the three simulations. The left green (resp. right red) thick bars show 3 times noise overestimation (resp. underestimation), whereas the center black thick bar represents the normal simulation and the two other thin bars show 10% noise deviation from the normal noise level, shown in black). Squares represent the mean and the spreads show the standard deviation.

Discussion

The model proposes a way to deal with noisy inputs. The Kalman filtering estimates these retinal and extra-retinal inputs, and also computes their associated uncertainty. Therefore, sensory and internal inputs are weighted as a function of their uncertainty. This combination of retinal and extra-retinal inputs allows the pursuit system to improve itself with time evolving (or from previous experience, like past trials), depending on the context (i.e., the reliability of sensory and/or internal inputs). For instance, the dynamic internal representation of the target motion becomes more accurate if the target moves in the same direction as previously. This will lead to an increase of confidence in the internal signal and therefore to a predictive pursuit eye movement.

Pursuit initiation and sensory noise

Previous studies (Osborne et al., 2005, 2007) have highlighted the importance of the noise in the sensory signals, explaining most of the variability in the initiation of pursuit eye movements. Moreover, the nervous system lowers the impact of noise on the sensory estimation (Gold and Shadlen, 2003). In the present model, the noise on retinal inputs induces variability on pursuit latency and acceleration during its initiation phase, with Kalman filtering

representing the nervous system reducing the noise and enhancing the sensory signals with time evolving.

However, a crucial question is to know whether or not the brain has an accurate estimation of these sensory noises. In this model, the hypothesis is made that the brain correctly estimates the sensory noise. It also has an estimation of the system dynamics noise, i.e. the uncertainty of the system (values of all these noises are kept constant for the simulation). Yet, if the noise estimation is not correctly computed by the nervous system, it can lead to a suboptimal estimation of the signal (Beck et al., 2012). This suboptimal estimation would therefore amplify the sensory noise present in the system. As a consequence, pursuit variability would be due in a large part to this suboptimal estimation.

When the target of interest is a more complex stimulus than used in this paper, like random dot patterns or a biological motion stimulus (BM), the associated noise level could be more important and could differ from one stimulus to another. For instance, a smaller noise level could be perceived when following a BM stimulus in comparison with tracking a random control stimulus. This difference in noise estimation in the nervous system could explain the larger pursuit acceleration observed in Coppe et al. (2010) in response of BM, compared to a random control stimulus.

Kalman filtering to estimate retinal and extra-retinal inputs

Kalman filtering is widely used in other contexts than smooth pursuit. It is used in optimal motor control (Wolpert et al., 1995; Todorov and Jordan, 2002; Körding and Wolpert, 2006; Wu et al., 2006; Denève et al., 2007; Izawa and Shadmehr, 2008), for decision making situations (Mrotek and Soechting, 2007) or even to train neural networks (Kramer and Stubberud, 2006). Kalman filtering might represent a natural way for the brain to treat noisy sensory inputs, coming from a large population of neurons. For instance, as it was shown for monkeys (de Hemptinne et al., 2007), a larger uncertainty about the future target movement (or the timing of its motion onset) is directly correlated to a smaller anticipatory pursuit eye movement (less confidence put in the internal system).

Moreover, the manner how the retinal (sensory) and extra-retinal (predictive) signals are implemented together in previous models is not always so clear. However, experimental studies have shown that the predictive signals are not simply turned-off during randomization of the expected target parameters (Kowler and McKee, 1987; Kao and Morrow, 1994; Heinen et al., 2005). Indeed, anticipatory pursuit velocity remains when target velocity or its motion onset was randomized. Here, the weighting of the sensory and internal retinal slip estimations according to their uncertainty is continuous; it do not change abruptly as an “on-off” mechanism can do. Moreover, we know that this weighting is optimal (Vaziri et al., 2006), if the noise present in the system is correctly estimated by the brain (Beck et al., 2012).

Using a dynamic representation of the expected target motion

In the present model, Kalman filtering was also used to construct a dynamic memory from past information. The dynamic nature of the memory can explain different situations, where some information about the future target movement can be retrieved in order to improve the internal representation of this future target trajectory. This information can be extracted from several sources.

First, past history of target motion can be employed to predict the future target motion. This is the case when tracking a sinusoidally moving target or a similar periodic pattern (Dallos and Jones, 1963; Barnes et al., 1987; Barnes and Ruddock, 1989), when anticipating the timing of target motion (Barnes and Asselman, 1991; Wells and Barnes, 1998; Barnes and Donelan, 1999; Barnes et al., 2000) or when scaling the anticipatory eye velocity with the previous target velocity (Barnes and Collins, 2008a).

Second, information about future target motion can be found from current evidence, as symbolic precues help the subject about target direction (Kowler, 1989; de Hemptinne et al., 2006), target velocity (Jarrett and Barnes, 2001, 2002) or about the onset of target motion (Wells and Barnes, 1998; Badler and Heinen, 2006).

Third, information can be extracted from physical laws of motion. It has been shown that some neurons compute internal models of these natural laws (Angelaki et al., 2004). Another example of physical consequence occurring often in our everyday life is causality of an event. For instance an object will move after being

struck by another object. When viewing the situation, the expectation of the future collision will elicit anticipatory pursuit eye movements in the direction of the second object motion before the collision (Badler et al., 2010).

The hypothesis made about the dynamic representation of the target is also supported by target blanking experiments, in which saccadic eye movements compensate for the decrease of pursuit gain (Orban de Xivry et al., 2006). This means that an internal representation of the expected target trajectory is available, and could be compared with an internal representation of eye position to compute the amplitude of the required saccade. In our model, knowledge about this dynamic representation allowed us to simulate pursuit responses when tracking an accelerative target motion or a sinusoidally moving target, even when this target transiently disappeared when pursuit velocity is equal to zero deg/s.

To the best of our knowledge, this model is also the first one able to reproduce both anticipatory pursuit, pursuit during target blanking and pursuit in response to a sinusoidal moving target. Until now, different model mechanisms were used to simulate those three examples of predictive pursuit eye movements. This model shows therefore that these three types of predictive pursuit eye movements may include similar mechanisms.

For the internal representation of the expected target motion, we chose 150 ms as an arbitrary prediction time horizon. This 150 ms time period allows the pursuit system to react in function of the expected target motion. Yet, we do not believe in a discrete time value at which a prediction is made. This prediction on the future target velocity is probably done continuously from evidence or past history. We could imagine having a more complex model where there

will be many predictions of the future target motion for different time horizons. An uncertainty could therefore be associated with each prediction made on the future target motion. The combination of all these predictions, weighted according to their uncertainty, could then replace our discrete prediction made on this arbitrary 150 ms timing. For instance, in the visible occluder example (Fig. II.12, green traces), the border of the occluder acts as a strong clue to estimate the timing of target reappearance. Therefore, at target disappearance, the uncertainty linked to the 200 ms time period estimation could be less important than the 100ms time period estimation. This uncertainty difference concerning different time horizons can also explain some of the differences observed between a visible or invisible occluder.

Model limitations

The present model allows us to simulate several neurophysiological data. However, some behavioral data are currently hard to be simulated. For instance, the pursuit response of a moving tilted bar is known to be initially biased in the orthogonal direction to the line orientation (Masson and Stone, 2002; Masson, 2004). In order to have correct simulations of this bidimensional visual motion integration process, the model should contain a supplementary “perception box” in the early “visual process”. By adding a “perception stage” in the computation of the RS signal, the model would have some transient RS direction error (due to the initial perception bias) and then would be able to correctly simulate the pursuit eye movements often described with the aperture problem. This would be an interesting way to combine both Bayesian models

(e.g., Montagnini et al., 2007) and smooth pursuit models in a single model.

Neural substrate of the model

Middle temporal area (MT) is thought to play a main role in the perception of motion (direction and velocity) and the integration of local motion signals. Moreover, MT neurons appear to filter noise coming from motion processing (for a review, see Born and Bradley (2005)). Sensory variability has been found in MT neurons (Law and Gold, 2008). In the present model, sensory Kalman filtering can be achieved by the large neuron population in MT. Indeed, Osborne et al. (2004, 2007) found some similarity of information accumulation for pursuit eye movements and MT neuron discharges. Osborne et al., 2004 also indicate that some information could be extracted from the first spikes of the MT neurons response.

The dynamics of neurons present in MT might therefore reflect the iterative computation of the Kalman filter (Pack and Born, 2001; Osborne et al., 2004). However, MT neurons did not seem to discharge when blanking the target, whereas neurons from the medial superior temporal area (MST) did continue to discharge (Newsome et al., 1988). Later, Ilg and Thier (2003) showed that neurons in the frontal eye field (FEF) and in MST were active during transient disappearance of the tracking target. These neurons therefore receive some extra-retinal input in addition to the common retinal input of the image motion. Neurons from the supplementary eye field

(SEF) also provide an extra-retinal drive to the pursuit system (Missal and Heinen, 2004).

We could imagine having area MT involved in sensory motion integration and neurons from areas MST/FEF/SEF involved in the prediction of the future target motion. It also seems that there is a neural mechanism present in the dorsal medial superior temporal area (MSTd) managing a form of statistical inference. This mechanism might predict behavioral cue weighting in an optimal way (Fetsch et al., 2012). The weighting of sensory and predictive signals could take place in MSTd area.

Chapter III
Biological motion drives perception and action

Abstract

Presenting a few dots moving coherently on a screen can yield to the perception of human motion. This perception is based on a specific network that is segregated from the traditional motion perception network and that includes the superior temporal sulcus (STS). In this study, we investigate whether this biological motion perception network could influence the smooth pursuit response evoked by a point-light walker. We found that smooth eye velocity during pursuit initiation was larger in response to the point-light walker than in response to one of its scrambled versions, to an inverted walker or to a single dot stimulus. In addition, we assessed the proximity to the point-light walker (i.e. the amount of information about the direction contained in the scrambled stimulus and extracted from local motion cue of biological motion) of each of our scrambled stimuli in a motion direction discrimination task with manual responses and found that the smooth pursuit response evoked by those stimuli

moving across the screen was modulated by their proximity to the walker. Therefore, we conclude that biological motion facilitates smooth pursuit eye movements, hence influences both perception and action.

*This chapter has been published : "**Orban de Xivry J-J, Coppe S, Lefèvre P, Missal M**. Biological motion drives perception and action. Journal of Vision 10: 6.1-11, 2010"*

Introduction

Humans are able to perceive human motion and infer a person's intentions from it (Blake and Shiffrar, 2007). This ability is often studied by showing human subjects a movie of the movement of dots attached to the body joints of a human actor or an animal performing a particular action, referred to as biological motion (e.g., walking, Johansson, 1973). Due to its particular importance, biological motion is probably processed differently by the visual system than other kinds of motion stimuli (Oram and Perrett, 1994; Decety and Grezes, 1999; Giese and Poggio, 2003; Billino et al., 2009). Indeed, several electrophysiological (Perrett et al., 1985; Jellema et al., 2004) and imaging studies (Grossman et al., 2000, 2005; Grezes et al., 2001; Grossman and Blake, 2001, 2002; Pelphrey et al., 2003; Saygin et al., 2004; Saygin, 2007) support the hypothesis of one or several specific neural pathways for biological motion perception. Indeed, biological motion perception is subserved by a bottom-up and a top-down mechanism (Blake and Shiffrar, 2007; Troje, 2008). Some authors believe that biological motion perception

is determined by local motion cues and probably originates in early areas of the visual pathway (Johansson, 1973; Mather et al., 1992; Troje and Westhoff, 2006). In contrast, others consider that biological motion perception is mostly based on configural processing, hence on structure-from-motion mechanisms (Bertenthal and Pinto, 1994; Thornton et al., 1998; Neri et al., 1998; Beintema and Lappe, 2002).

In several instances, perception and smooth pursuit eye movements have been shown to share motion integration mechanisms (Krauzlis and Stone, 1999). For example, perception of motion direction and steady-state pursuit eye movements (>300 ms after stimulus onset) exhibited similar directional thresholds (Beutter and Stone, 1998; Stone et al., 2000; Stone and Krauzlis, 2003). In the same vein, pursuit and perception variability are similar during steady-state pursuit (Rasche and Gegenfurtner, 2009). During the open-loop phase of the pursuit response (<300 ms with respect to stimulus onset), pursuit exhibits a directional bias that is similar to perception (Masson and Stone, 2002; Masson, 2004), but with much less sensitivity to speed (Rasche and Gegenfurtner, 2009). In sum, the link between pursuit and perception evolves over time. During initiation, pursuit is very sensitive to low-level motion cues whereas it becomes more sensitive to higher-level motion later, i.e. after the first catch-up saccade (Wilmer and Nakayama, 2007). Speed and direction of motion are essentially processed in the middle temporal area (MT; Born & Bradley, 2005), which is one of the main inputs to the smooth pursuit system (Orban de Xivry and Lefèvre, 2007; Ilg and Thier, 2008; Lencer and Trillenberg, 2008).

The above-mentioned studies focused on the link between motion perception and smooth pursuit. In this study, we investigated whether biological motion perception that is not processed by the

conventional motion processing network (Vaina et al., 1990; McLeod et al., 1996), influenced smooth pursuit eye movements. To do so, we proceeded in three different steps. First, we compared smooth pursuit eye movements elicited by a point-light walker and by some control stimuli. We hypothesized that the biological motion stimulus might either decrease smooth pursuit latency or increase eye velocity. Both scrambled or inverted point-light walkers were used as control stimuli as they disrupt different aspects of biological motion perception (i.e., local motion is preserved in the scrambled stimuli but not in inverted walkers whereas inversion preserves configural features such as opponent movements of the feet) and their vision activates differentially the STS region (Grossman and Blake, 2001).

Second, we assessed the sensitivity of the smooth pursuit system to the proximity of the stimuli to the walker. In this respect, we correlated results from the behavioral experiment and from a psychophysics experiment. In the latter, the proximity to the walker was defined as the amount of information about the direction contained in the scrambled stimulus and extracted from local motion cue of biological motion. This proximity was assessed by determining how accurately subjects could indicate the walking direction of the different scrambled walkers. The strong correlation between the output measures of the behavioral and psychophysics experiments suggests that attentional factors cannot explain the difference in behaviors elicited by the different stimuli.

Finally, given that smooth pursuit eye movements were faster for the biological motion stimuli, compared to the control stimuli, we investigated whether the point-light walker facilitated or the control stimuli deteriorated smooth pursuit eye movements. In this respect, we compared smooth pursuit eye movements elicited either by those

stimuli or by a single dot moving at a comparable speed. We found that biological motion perception facilitated smooth pursuit eye movements. Therefore, we concluded that, similarly to motion perception, biological motion perception influences smooth pursuit eye movements. This suggests that the biological motion network functions as an input to the smooth pursuit system and demonstrates that biological motion can affect both perception and action.

Materials and methods

Thirteen human subjects (9 males) participated in the experiments after informed consent. They were between 20 and 42 years old. Six of them had never participated in oculomotor experiments. All procedures were approved by the Université catholique de Louvain Ethics Committee and were in agreement with the Declaration of Helsinki.

Stimuli

Our experiments involved a biological motion stimulus (point-light walker) and some control stimuli. Movies of those stimuli are available in the supplementary material. The motion of the 11 dots of the point-light walker was computed using Cutting's algorithm (Fig. III.1; Cutting, 1978).

Therefore, the trajectory of each point can be described as a pair of functions:

$$\left(x_i^{BM}(t), y_i^{BM}(t)\right) \quad where\ y_i^{BM}(t) = y_i^{local}(t) + \bar{y}_i \qquad \text{Eq. III.1}$$

Here, y_i^{local} represents the local vertical motion of the point around its mean vertical position $(\bar{y}_i)$. The scrambled walker was obtained by shuffling the mean vertical position $(\bar{y}_i)$ of the dots (except the hip dot) to disrupt the global form, while keeping the same local motion (y_i^{local}). Therefore, the trajectories of the dots for the scrambled walker were defined as follows:

$$x_i^{SCR}(t) = x_i^{BM}(t) \quad for\ all\ i \qquad \text{Eq. III.2}$$

$$\left(x_i^{SCR}(t), y_i^{SCR}(t)\right) \quad where\ y_i^{SCR}(t) = y_i^{BM}(t) \quad if\ i = hip \qquad \text{Eq. III.3}$$

$$y_i^{SCR}(t) = y_i^{local}(t) + \bar{y}_k \quad if\ i \neq hip \qquad \text{Eq. III.4}$$

The association between *'k'* and *'i'* was determined by random permutation of *'i'* and differed for each scrambled stimulus. The inverted stimulus was obtained by flipping the original point-light walker upside-down:

$$x_i^{INV}(t) = x_i^{BM}(t) \quad for\ all\ i \qquad \text{Eq. III.5}$$

$$y_i^{INV}(t) = -y_i^{BM}(t) \quad for\ all\ i \qquad \text{Eq. III.6}$$

Whatever the stimulus type, the hip dot (highlighted in green) followed an identical trajectory and subjects were asked to track this particular dot. The different stimulus speeds were obtained by varying the step size of the walker.

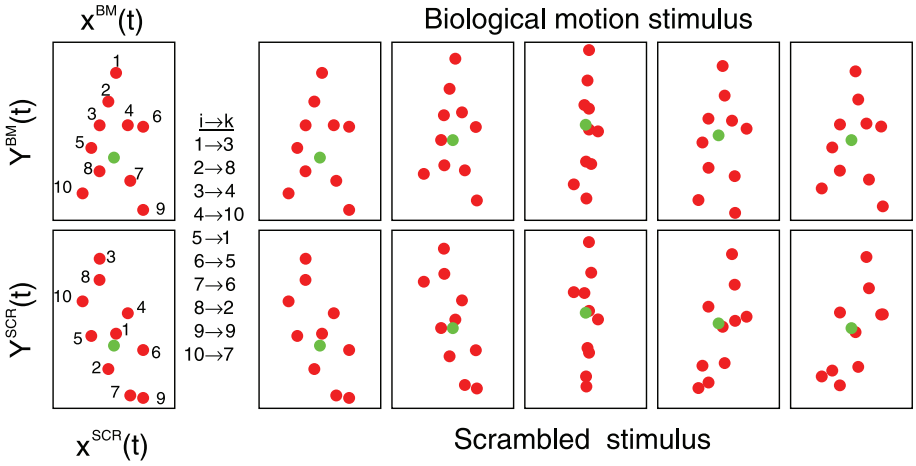

Figure III.1: Representative pictures of the biological and scrambled walkers used in this study. On the left, we describe the algorithm used to produce scrambled stimuli and provide the correspondence table between the two stimuli as explained in Materials and methods. On the right, the upper panels represent five pictures of the biological motion stimulus, whereas the lower panels depict five pictures of an example of a scrambled stimulus (picture interval: 150 ms). The hip point that the subjects were asked to pursue is represented in green.

Procedure

We conducted one psychophysics and two behavioral experiments. In the psychophysics experiment, ten subjects were required to indicate the heading direction (i.e. the direction of walking) of an animated, but stationary (as if on a treadmill), point-light stimulus presented on the screen (7.2 degrees in height). For each trial, the stimulus was chosen randomly among a set of 14 scrambled stimuli plus the point-light walker, and the heading direction of the associated walker was randomized. Because each scrambled stimulus was obtained from a biological motion stimulus (see above), we considered the heading direction of the scrambled stimulus as the heading direction of its original point-light walker stimulus. The animation of the dots around the hip dot was similar to when the walker was moving at a speed of 10 deg/s (see behavioral experiments below) but the hip dot remained stationary.

In the first behavioral experiment, after a period of fixation, eight subjects from the psychophysics experiment were asked to pursue the hip dot of either a moving point-light walker or one of its scrambled versions. The stimulus moved either to the left or to the right at a velocity of 5, 10 or 15 deg/s for 800 ms (measured as the average velocity of the hip dot, see below). The type of stimulus, its direction, and its velocity were selected at random for each trial. The facing direction of the stimulus was always congruent with its direction of motion. For each block, the scrambled walker stimulus was chosen randomly from a set of possible stimuli consisting of nine stimuli selected from the psychophysics experiment (see Results).

The second behavioral experiment was very similar to the first, except that the scrambled control stimuli were replaced by an upside-

down point-light walker. Ten subjects participated in this experiment, five of whom had already performed the first experiment. During the same session, seven out of the ten subjects performed a few more trials during which the hip dot only was presented (DOT stimulus). For those trials, the motion of the hip dot corresponded to a stimulus moving at 15 deg/s. On average, we obtained 360 valid trials per subject for the point-light walker stimulus, 300 for the scrambled stimuli, 65 for the inverted stimulus and 63 for the DOT stimulus.

Data collection and analysis

Subjects sat in a dark room in front of a large screen that spanned 50 deg of their visual field and was 1.5 m away. Their head was restrained by a chin-rest. Stimuli were projected onto the screen with a cine8 Barco projector (Refresh rate: 100 Hz; Barco NV, Belgium) that was controlled by a VSG graphic card, in real time (Cambridge Research System Ltd, UK). Eye movements were recorded at 200 Hz using a Chronos Eye Tracker (Skalar Medical BV, The Netherlands) and with an Eyelink 1000 (SR Research Ltd., Ottawa, Ontario, Canada) at 1000 Hz for three subjects. Eye movements were low-pass filtered at 45 Hz using a zero-phase digital filter (auto-regressive forward-backward filter), and velocity and acceleration signals were derived from position signals using a central difference algorithm with a ±10 ms interval. Saccades, which were detected using a 500 deg/s² threshold on the vectorial acceleration, were removed from the smooth eye velocity trace (see details in de Brouwer et al., 2002). Since the vertical component of eye velocity remained below 3 deg/s, the rest of the analyses focused

on the horizontal component of eye velocity or saccade amplitudes. Pursuit onset was determined by fitting a piece-wise linear function on the eye velocity trace measured during an interval of 250 ms starting at stimulus onset:

$$f(t) = \begin{cases} A & if\ t < T \\ B\,(t - T) & if\ t \geq T \end{cases} \qquad \text{Eq. III.7}$$

where *t* was the time (s), *T* is the time of pursuit onset (s), *A* the level of eye velocity before pursuit onset (deg/s) and *B* the mean acceleration during pursuit initiation (deg/s²). The constants *A*, *B* and *T* were the free parameters of the function. The average values of *A* and *B* were 0.03 deg/s and 65 deg/s². Trials were visually inspected, and trials with blink, saccades before pursuit onset, etc. were discarded.

In the psychophysics experiment, we analyzed the response time and the percentage of correct answer. In the behavioral experiments, we analyzed smooth eye velocity, pursuit latency and catch-up saccade latency, accuracy (horizontal position error at the end of the saccade) and amplitude. For the purposes of statistical analyses, we calculated intra-subject means for selected measures. Similarly, the average profiles shown on Fig. III.3 were obtained by averaging, across subjects, their intra-subject means for the highest stimulus velocity. We used repeated measures ANOVA on the intra-subjects means of those measures with stimulus type and velocity as within-subject factors. Tukey's Post Hoc test was used to evaluate one-to-one differences. Statistical analyses were performed with Statistica (Statsoft, Tulsa, OK).

Results

Scrambling disrupts biological motion perception

Scrambling the dots of the point-light walker impaired the biological relevance of the stimulus, but this impairment might depend on the scrambling method. Therefore, we investigated the proximity to the walker stimulus of our 14 scrambled stimuli in a motion direction discrimination task; subjects had to indicate the heading direction of the displayed stimulus by pressing a button that recorded both their responses and their response times. We found a strong relationship between those two measures (Fig. III.2A). The parabola ($R^2 = 0.96$) that fit those points indicated that the maximum response time was close to the maximum uncertainty about motion direction (maximum of uncertainty: 50% correct responses; maximum of the parabola at x = 46.3). In some instances, the more stimulus direction was ambiguous, the more uncertain subjects were about the specific direction and the more time it took them to indicate the direction in which the stimulus was heading. On the other hand, some stimuli were less ambiguous and the response time was shorter. In these cases, uncertainty was reduced, even if the directions reported were wrong (uttermost left point on Fig. III.2A). Nonetheless, the uncertainty about stimulus direction was much larger for any scrambled stimulus than for the point-light walker, as indicated by the longer reaction time for scrambled stimuli (>1088 ms), compared to the response time for the biological motion stimulus (inter-subject

mean: 754 ms, inter-subject standard deviation SD: 106 ms). To avoid confounding results that may arise from differences in uncertainty about motion direction in our behavioral experiment, we focused on the nine stimuli with the maximum uncertainty (25–75% of correct answers).

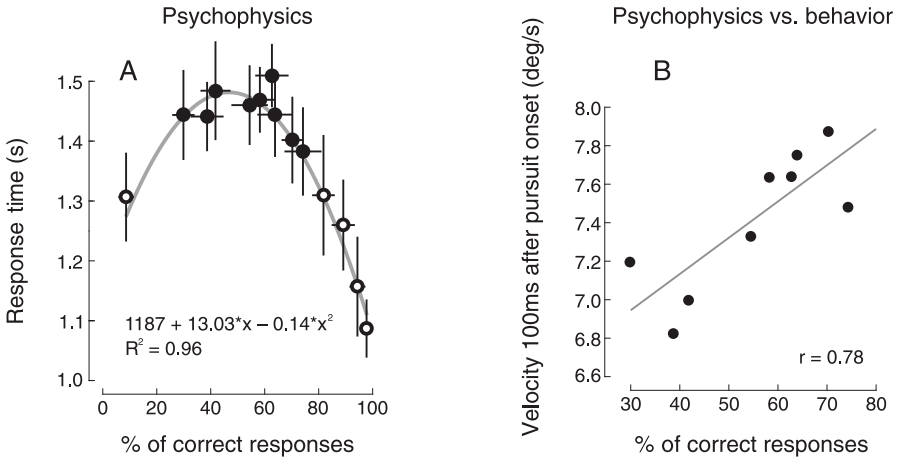

Figure III.2: A) Relationship between the average response time and the average percentage of correct responses across subjects measured during the psychophysics experiment. Each dot represents a different scrambled point-light walker. The line represents a parabola that was fit to the data, for which the equation was inserted in the panel. The filled dots were those considered for the subsequent analyses (panel B and Fig. III.3A). Error bars represent standard error of the mean. B) Correlation between the percentage of correct responses reported during the psychophysics experiment and the smooth eye velocity measured 100 ms after pursuit onset during the behavioral experiment. Each dot represents one scrambled stimulus and represents the average across subjects. Stimulus velocity was 15 deg/s.

The smooth pursuit response is influenced by the stimulus type

To test whether proximity to the walker affected the reactive smooth pursuit response in human subjects, we recorded the smooth pursuit response elicited by a biological point-light walker (BM) or by a control stimulus that was a scrambled version of the point-light walker (SCR; nine possible stimuli; black dots in Fig. III.2A). We predicted that the biological motion content of the stimulus might influence the latency of the motor response and/or its strength. We found that the latency of the smooth pursuit response was not influenced by the stimulus type (BM: 113 ms; SCR: 116 ms; ANOVA: $F(1, 7) = 3.57$, $p = 0.1$). In contrast, the stimulus type strongly influenced the velocity of smooth pursuit eye movements, as can be seen in Fig. III.3A and in Fig. III.4, which shows the inter-subject average of eye velocity as a function of time for the BM and SCR stimuli (time was synchronized with pursuit onset). The pursuit velocity observed in response to a BM stimulus is between 5 and 10% larger than the velocity measured in response to a SCR stimulus. A repeated measures ANOVA, with stimulus type (BM or SCR) and velocity as within-subject factors, indicated that, 150 ms after pursuit onset, there was a significant main effect of stimulus type on smooth eye velocity ($F(1, 7) = 14.78$, $p = 0.006$), whereas the interaction between stimulus type and speed was not ($F(2, 14) = 0.81$, $p = 0.46$).

Therefore, 150 ms after pursuit onset, smooth eye velocity evoked by biological motion was significantly higher than smooth eye velocity evoked by the scrambled stimuli for all stimulus velocities.

Fifty milliseconds earlier, there was already a trend for the influence of stimulus type on smooth eye velocity as early as 100 ms after pursuit onset (ANOVA: $F(1, 7) = 4.91$, $p = 0.06$). As shown in Fig. III.3A, the facilitating effect of biological motion lasted for several hundred milliseconds during visual pursuit, although the speed of the stimulus was the same. For instance, smooth eye velocity 400 ms after pursuit onset was higher for BM than for SCR stimuli ($F(1, 7) = 8.59$, $p = 0.022$).

Pursuit initiation is influenced by local biological motion perception

To test whether the differences in proximity to the walker among the scrambled stimuli were reflected in the behavioral responses, we tested the correlation between the psychophysics and behavioral responses. We found a strong correlation between the percentage of correct responses in the psychophysics experiment and the level of smooth eye velocity measured 100 ms after pursuit onset in the first behavioral experiment (Fig. III.2B, fastest target velocity, Spearman correlation: $R = 0.78$, $p = 0.01$). This correlation was still present 50 ms later (Spearman correlation: $R = 0.68$, $p = 0.042$) but disappeared afterwards. In addition, for those trials, the average acceleration during pursuit initiation (see Materials and methods) did correlate with the percentage of correct response (Spearman correlation: $R = 0.7$, $p = 0.036$), a finding that emphasizes

the differential influence of perceptual mechanisms on pursuit initiation and maintenance (Wilmer and Nakayama, 2007)

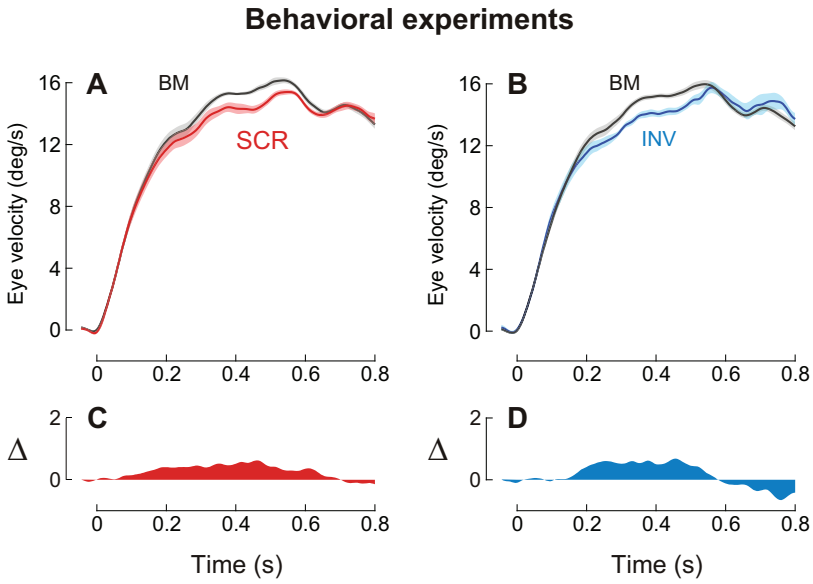

Figure III.3: Pursuit velocity profiles. A) Average smooth eye velocity profiles (thin lines) evoked either by the biological motion stimuli (BM, black) or by the control stimuli (SCR, scrambled point-light walker, in red) for all subjects pooled together. Areas surrounding the traces represent confidence intervals. B) Average smooth eye velocity profiles (thin lines) evoked either by the biological motion stimuli (BM, black) or by the control stimuli (INV, inverted point-light walker in blue) for all subjects pooled together. C) and D) Average difference between the two average profiles presented in the upper panel (e.g. panel C: average BM profile minus average SCR profile). Trials were aligned at smooth pursuit onset (time 0), prior to averaging. Stimulus velocity was 15 deg/s.

Saccades cannot account for the differences in behavior

In addition, we investigated whether the saccades might be responsible for the observed difference in smooth eye velocity evoked by the point-light walker or the scrambled stimuli. We found no significant difference in saccade latency, with respect to the stimulus motion onset (BM vs. SCR, ANOVA: $F(1, 7) = 2.66$, $p = 0.15$) or to pursuit onset ($F(1, 7) = 0.27$, $p = 0.87$). On average, saccade latency was 113 ms after pursuit onset. Catch-up saccade accuracy was not influenced by the stimulus type ($F(1, 7) = 0.001$, $p = 0.97$) even though stimulus type tended to influence the amplitude of catch-up saccades ($F(1, 7) = 3.66$, $p = 0.09$). The amplitude of the saccades in response to the scrambled stimuli (mean = 2.03 deg, SD = 0.90) was slightly larger than with the biological motion stimulus (mean = 1.94 deg, SD = 0.87 deg). As the saccadic amplitudes evoked by the scrambled stimuli tended to be larger than for the BM stimuli, any hypothetical bias of saccades on the measure of smooth pursuit velocity would reduce the observed difference in smooth eye velocity between BM and SCR.

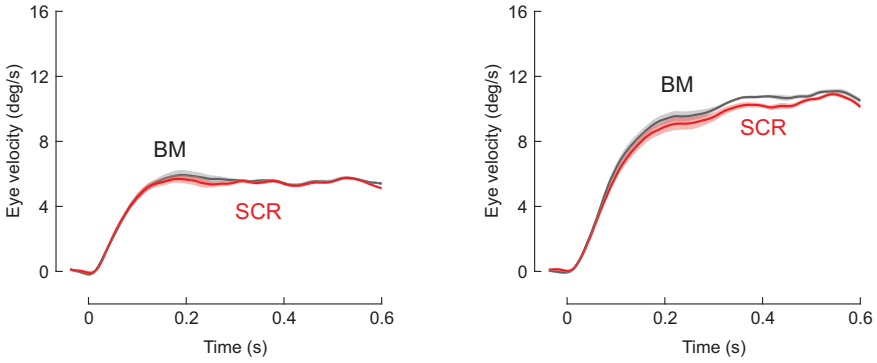

Figure III.4: Pursuit velocity profiles. Average smooth eye velocity profiles (thin lines) evoked either by the biological motion stimuli (BM, black) or by the control stimuli (SCR, scrambled point-light walker, in red) for all subjects pooled together. Areas surrounding the traces represent confidence intervals. Trials were aligned at smooth pursuit onset (time 0), prior to averaging. Stimulus velocity was 5 deg/s (left panel) or 10 deg/s (right panel).

Inversion of the point-light walker influences smooth pursuit

We also performed a third experiment, where the scrambled stimuli were replaced by an inverted point-light walker. In this experiment, we were able to reproduce the results obtained with the scrambled stimuli. We found no difference in pursuit onset in the smooth pursuit response elicited by the point-light walker and inverted point-light walker stimuli (BM vs. INV, $F(1, 9) = 0.17$, $p = 0.69$). In contrast, 200 ms after pursuit onset, the smooth pursuit response elicited by the upright point-light walker was higher than the response

elicited by the upside-down walker (Fig. III.3B and Fig. III.5, ANOVA: $F(1, 9) = 16.06$, $p = 0.003$). This difference lasted a few hundreds of milliseconds. Indeed, at 400 ms, the smooth eye velocity was different between the two stimuli ($F(1, 9) = 34.5$, $p = 0.0002$). Again, catch-up saccade latency, amplitude or accuracy was not different between the two conditions (ANOVAs, latency: $F(1, 9) = 0.051$, $p = 0.83$; amplitude: $F(1, 9) = 0.019$, $p = 0.89$; accuracy: $F(1, 9) = 0.03$, $p = 0.86$).

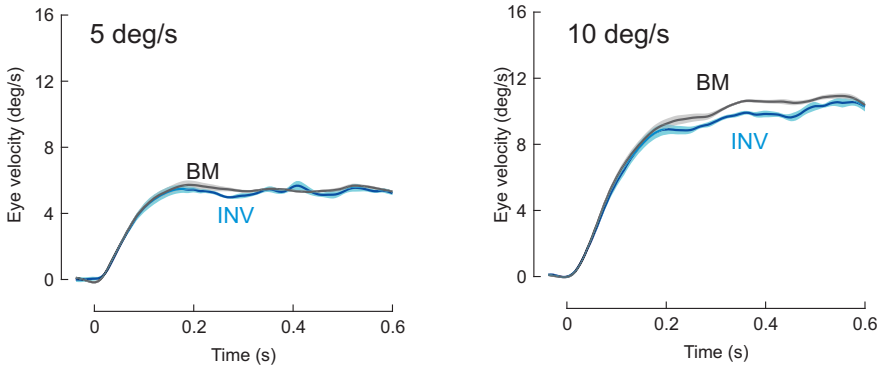

Figure III.5: Pursuit velocity profiles. Average smooth eye velocity profiles (thin lines) evoked either by the biological motion stimuli (BM, black) or by the control stimuli (INV, inverted point-light walker in blue) for all subjects pooled together. Trials were aligned at smooth pursuit onset (time 0), prior to averaging. Stimulus velocity was 5 deg/s (left panel) or 10 deg/s (right panel).

Biological motion facilitates smooth pursuit

Finally, to test whether normal biological motion facilitated pursuit or scrambled biological motion impaired pursuit, we analyzed the trials during which only the hip dot was presented on the screen. Indeed, it has been reported that adding coherently moving dots facilitates smooth pursuit eye movements (Heinen and Watamaniuk, 1998; Watamaniuk and Heinen, 1999). Therefore, we compared the smooth pursuit response to the BM, INV and DOT stimuli. Interestingly and consistently with those studies, we found that pursuit velocity was higher for the BM and INV stimuli than for the DOT stimuli during the very early part of the pursuit response. Indeed, at 50 and 100 ms, smooth eye velocity was larger for the BM and INV than for the DOT stimulus (Tukey Post-Hoc test: BM vs. DOT: $p = 0.013$ and INV vs. DOT: $p = 0.003$). In contrast, 200 ms after pursuit onset, when we observed a difference between the smooth eye velocity elicited by the BM and INV stimulus, the response to the DOT stimulus was smaller than to the BM stimulus (Tukey Post-Hoc: $p = 0.03$) but not different from the INV stimulus (Tukey Post-Hoc: $p = 0.4$). This last result shows that biological motion did facilitate smooth pursuit eye movements.

Discussion

In the present study, we reported an effect of the proximity of the stimuli to the walker on the smooth eye velocity during a visual tracking task. In line with the differential effects of perception during pursuit initiation and maintenance (Wilmer and Nakayama, 2007; Rasche and Gegenfurtner, 2009), we found that, during pursuit initiation, smooth eye velocity was modulated by the proximity of the scrambled stimuli to the walker measured during our psychophysics experiment. In addition, during pursuit maintenance, smooth eye velocity was higher for a point-light walker than for a scrambled stimulus or inverted point-light walker. As in many other studies (Ikeda et al., 2005; Lange et al., 2006; Hiris, 2007; Pavlova et al., 2007; Billino et al., 2008a; Hunt and Halper, 2008; Saygin et al., 2008), we used Cutting's algorithm to simulate the point-light walker stimulus. We considered the use of this algorithm to create our stimuli as a worst-case scenario, since it has been argued that it could be suboptimal, compared with biological motion stimuli from human motion recordings. Therefore, the difference between the biological and non-biological conditions could have been even bigger, if we had used a point-light walker based on data from actual human actions; even though, to our knowledge, the difference between those techniques has never been clearly demonstrated.

Rather than the proximity to the walker, could the differences in smooth pursuit response be due to attentional effects? Indeed, it has been shown that divided attention decreases smooth eye velocity during pursuit (Souto and Kerzel, 2008). We could also interpret the dots of the scrambled walkers as distractors, which would reduce the ability of underlying motion detectors to extract target motion

information. If motion processing was impaired by the scrambling of the dots, we would predict that the accuracy of the first catch-up saccades would be deteriorated as catch-up saccade amplitudes are influenced by target motion information (de Brouwer et al., 2001, 2002; Orban de Xivry et al., 2006, 2008; Schreiber et al., 2006). Indeed, Newsome, Wurtz, Dursteler, and Mikami (1985) showed that temporary lesion of the monkey area MT, which is essential for motion perception (Born and Bradley, 2005), impairs both the smooth pursuit performance and the accuracy of catch-up saccades. Similarly, if attention was divided by the scrambled process because subjects had to pay attention to several points, we would predict that the catch-up saccades should be delayed by the divided attention (Souto and Kerzel, 2008). In our data, we did observe neither a difference in catch-up saccades accuracy nor a difference in catch-up saccade latency. In sum, neither attentional factors nor increased noise due to the scrambling process is likely to explain the difference in behavior elicited by the BM and SCR stimuli.

The same reasoning can be applied to interpret the difference in smooth pursuit elicited by BM and INV stimuli. Since the inversion of the walker is less susceptible to increase the level of noise as the shape of the walker is still perceptible after the inversion (Sumi, 1984) and since the accuracy of catch-up saccades was not different between the point-light walker and its upside-down version, we do not believe that an increased level of noise due to the inversion was responsible for the differences in smooth pursuit velocity.

Of course, this does not mean that attention does not play a role in biological motion processing. However, it shows that the attentional load is similar in both conditions as it is required to process biological motion stimuli (Cavanagh et al., 2001; Thornton et

al., 2002; Thornton and Vuong, 2004) or to filter out irrelevant motion signals (Khurana and Kowler, 1987; Spering et al., 2006; Spering and Gegenfurtner, 2007). In addition, the correlation we found between the results from the psychophysics and behavioral experiments suggests that local motion cues, which are not impaired by the scrambling process and which are processed by the bottom-up pathway, influence the smooth pursuit initiation. Their influence was only detectable during the pursuit initiation (first 150 ms of the response). This is reminiscent of the early influence of the low-level motion processing pathway on pursuit initiation (Wilmer and Nakayama, 2007). Importantly, dividing attention has little effect on the low-level, bottom-up pathway (Thornton et al., 2002) and therefore, attentional factors would not account for this observation. Finally, we believe that attentional factors might not account for our results, as the smooth pursuit to the INV stimuli does not appear deteriorated when compared to a single dot stimulus. Therefore, biological motion facilitates smooth pursuit.

The effect of biological motion on oculomotor response might result from the activation of a specific neuronal pathway for biological motion processing (Grossman et al., 2000, 2005; Saygin et al., 2004; Saygin, 2007). Evidence from single neuron recordings suggests that the region of the superior temporal sulcus (STS) of the macaque monkey is specifically involved in the perception of biological motion. The network dedicated to biological motion perception is partially independent of the low-level motion perception network (first- and second-order motion). Indeed, in humans, disruption of the motion-sensitive, middle temporal area (MT) did not affect the perception of biological motion (Vaina et al., 1990; Saygin, 2007; Billino et al., 2009), whereas a lesion in MT reduced low-level motion perception

(Komatsu and Wurtz, 1989) and impaired smooth pursuit eye movements in monkeys (Newsome et al., 1985; Dursteler and Wurtz, 1988). Similarly, psychophysics testing of the low-level motion perception network (speed discrimination, coherent motion detection, etc.) showed that processing of motion degraded with age (Sekuler et al., 1980; Warren et al., 1989; Gilmore et al., 1992; Norman et al., 2003), whereas the perception of biological motion did not (Norman et al., 2004; Billino et al., 2008b). In contrast, the third-order motion processing system, which is strongly influenced by attention (Lu and Sperling, 2001), was necessary for perceiving biological motion (Garcia and Grossman, 2008). For instance, patient studies demonstrated that lesions in the parietal lobe degraded third-order and biological motion perception, while low-level motion perception remained intact (Battelli et al., 2003; Billino et al., 2009). In sum, there are at least two different motion processing pathways: the classical one, which involves area V5/MT (Born and Bradley, 2005) and a second, which might rely on the STS area (Perrett et al., 1985; Barraclough et al., 2006) and be subservient to biological motion perception. The relative independence of the biological motion and low-level motion perception networks, together with our results, suggests that the biological motion perception pathway might directly influence the smooth pursuit network (Ilg and Thier, 2008).

It might also be possible that the biological motion network changes the activity in areas MT/MST, which in turn affect smooth pursuit. Indeed, the fact that the latency did not differ between the conditions and that pursuit velocity differed significantly only from 150 ms after pursuit onset would be compatible with this hypothesis. This possibility is supported by anatomical studies, which showed the existence of direct and indirect projections from STPa (anterior

superior temporal polysensory) to the MT complex (Boussaoud et al., 1990) and studies about implied biological motion, which are in favor of this hypothesis (Kourtzi and Kanwisher, 2000; Jellema and Perrett, 2003a; Kourtzi et al., 2008). Therefore, it might be that the enhanced smooth pursuit response to BM resulted from a top-down projection from STPa to the MT complex, which is the main input of the smooth pursuit system. These feedback projections might also explain why people are better at discriminating biological motion than translational motion (Neri et al., 1998).

To disambiguate between those two hypotheses (direct input to the smooth pursuit network or feedback projections to the MT complex), one would need to study patients with lesions covering the MT complex but not the STS. In this case, smooth pursuit eye movements would be heavily affected (Newsome et al., 1985; Dursteler and Wurtz, 1988) but biological motion perception would be preserved (Vaina et al., 1990; Saygin, 2007; Billino et al., 2009). For those patients, the direct input hypothesis would predict that their smooth pursuit response would be impaired to a lesser extent for biological motion stimuli. In contrast, the feedback projection hypothesis would predict that the impairment of the smooth pursuit response would be similar for both biological and non-biological stimuli.

Our study highlights the necessity to integrate perception and retinal slip as one input to the smooth pursuit system (Krauzlis and Stone, 1999), independently of the network that subserves motion perception. In this respect, because sensitivity for biological is higher than for translational motion (Neri et al., 1998), we would expect that our smooth eye velocity will also be more sensitive for biological motion than for translational motion.

In our psychophysics experiment, we interpret the percentage of correct responses as the proximity of the stimulus to the walker and the response time as the uncertainty about its direction. We are not aware of any other studies reporting a gradual effect of scrambling on biological motion. Here, we showed that biological motion perception is not an ON–OFF mechanism (as shown during pursuit initiation), but that local motion cues are sufficient to infer a certain degree of biological motion (for example if the movement of the feet is still present, Chang and Troje, 2009). Similar local motions, however, can yield different degrees of biological motion, which could be explained by the importance of particular points from the display (Casile and Giese, 2005; Troje and Westhoff, 2006). However, even if local motion produced a good perception of the heading direction for some stimuli, the shortest response times recorded during our psychophysics experiment were still much longer than response times for biological motion (on average, larger than 1100 ms for SCR and around 750 ms for BM).

In conclusion, we demonstrated that smooth pursuit eye movements are sensitive to the degree of proximity to the walker of the tracked target. These results suggest that the biological motion perception network is an important input to the smooth pursuit system and can modulate transformation of visual signals into eye movement commands. Therefore, biological motion is relevant to both perception and action.

Chapter IV

Biological motion influences the visuomotor transformation for smooth pursuit eye movements

Abstract

Humans are very sensitive to the presence of other living persons or animals in their surrounding. Human actions can readily be perceived, even in a noisy environment. We recently demonstrated that biological motion, which schematically represents human motion, influences smooth pursuit eye movements during the initiation period (Orban de Xivry et al., 2010). This smooth pursuit response is driven both by a visuomotor pathway, which transforms retinal inputs into motor commands, and by a memory pathway, which is directly related to the predictive properties of smooth pursuit. To date, it is unknown which of these pathways is influenced by biological motion. In the present study, we first use a theoretical model to demonstrate that an influence of biological motion on the visuomotor and memory pathways might both explain its influence on

smooth pursuit initiation. In light of this model, we made theoretical predictions of the possible influence of biological motion on smooth pursuit during and after the transient blanking of the stimulus. These qualitative predictions were then compared with recordings of eye movements acquired before, during and after the transient blanking of the stimulus. The absence of difference in smooth pursuit eye movements during blanking of the stimuli and the stronger visually guided smooth pursuit reacceleration after reappearance of the biological motion stimuli in comparison with control stimuli suggests that biological motion influences the visuomotor pathway but not the memory pathway.

*This chapter has been published : "**Coppe S, Orban de Xivry J-J, Missal M, Lefèvre P**. Biological motion influences the visuomotor transformation for smooth pursuit eye movements. Vision Research 50: 2721-2728, 2010."*

Introduction

Perception and action have been hypothesized to be subserved by the independent ventral and dorsal streams (Goodale and Milner, 1992). However, data on smooth pursuit eye movements demonstrated that those two streams are not completely independent as perception can influence smooth pursuit eye movements (i.e. action). For instance, a sinusoidally-moving line-figure diamond perceived through two vertical apertures evokes different eye movements depending on whether the apertures are visible or not (Krauzlis and Stone, 1999; Stone et al., 2000) even though the

physical motion is completely identical in both cases. Similarly, a tilted line moving horizontally will first evoke oblique eye movements before the vertical component disappears within 200 ms (Pack and Born, 2001; Masson and Stone, 2002). This temporal dynamics reflects neuronal dynamics at the level of the middle temporal area (MT; Pack and Born, 2001; Born and Bradley, 2005), which is the primary input to the smooth pursuit system (Thier and Ilg, 2005; Orban de Xivry and Lefèvre, 2007; Lisberger, 2010).

In the framework of modeling the smooth pursuit system, this interaction between perception and action occurs at the level of the visuomotor transformation stage, which consists in the transformation of retinal signals into motor commands (Buneo et al., 2002; Blohm and Crawford, 2007; Blohm et al., 2009). To account for pursuit maintenance during blanking periods or occlusions (Mitrani and Dimitrov, 1978; Pola and Wyatt, 1997), smooth pursuit models also incorporate a predictive component, which consists in a memory that stores a dynamic representation of target motion (Bennett and Barnes, 2003; Orban de Xivry et al., 2008). This predictive pathway allows maintaining non-zero eye velocity when the moving stimulus disappears from the screen for several hundreds of milliseconds, although the gain of the response is reduced (Mitrani and Dimitrov, 1978; Becker and Fuchs, 1985; Bennett and Barnes, 2003; Orban de Xivry et al., 2006, 2008; Bennett et al., 2010).

We recently showed evidence for a specific interaction between perception and action by demonstrating that a point-light walker stimulus (Johansson, 1973) evoked a stronger smooth pursuit response than a control stimulus devoid of biological relevance (Orban de Xivry et al., 2010). However, it is unclear which part of the smooth pursuit system is influenced by the percept of biological

motion. Indeed, biological motion could influence either the visuomotor transformation stage or the output of the memory pathway.

The influence of biological motion on the visuomotor transformation would parallel the studies on the aperture problem where misleading retinal signals result in a bias during the initiation of the smooth pursuit response (Beutter and Stone, 2000; Stone et al., 2000; Pack and Born, 2001; Masson and Stone, 2002). The changes in smooth pursuit initiation observed in the aperture problem framework and with the biological motion stimulus could result from a similar influence on the visuomotor transformation stage. In contrast, an influence of biological motion on the predictive component of the smooth pursuit system would be compatible with different situations in which a trajectory with natural kinematics leads to better prediction of a moving object than a trajectory with non-natural kinematics. For instance, human subjects predict more accurately the endpoint of a given trajectory if this trajectory follows the natural dynamics of a human arm movement than if the trajectory is not natural (Pozzo et al., 2006; Saunier et al., 2008). Similarly, the kinematics of the hand and racket appear to be of particular importance to predict the ball trajectory from the opponent in tennis (Huys et al., 2008, 2009; Mark Williams et al., 2009). Note that point-light displays are sufficient to make such accurate predictions (Munzert et al., 2010). Thus biological motion appears to enhance the ability to predict.

Given that the percept of biological motion could potentially influence either the visuomotor transformation or the memory pathway, the goal of the present study is to investigate which part of the smooth pursuit system is actually influenced by biological motion. Using a simplified model of the smooth pursuit system, we will first

demonstrate that an influence of the biological motion percept on the visuomotor transformation or on the memory pathway could theoretically reproduce the results of our previous study (Orban de Xivry et al., 2010). Namely biological motion stimuli evoke a faster smooth eye velocity during pursuit initiation than control stimuli. We will then compare the predictions made by those two hypotheses during and after the transient blanking of the moving stimuli. These predictions will be confronted with the results of a behavioral study during which the stimulus (biological motion or control stimulus) was blanked temporarily for 800 ms.

Methods

Participants

Thirteen human subjects (four females) participated in the experiments after informed consent. They were between 22 and 42 years old (mean age of 26.2 years). Eight of them were completely naïve of oculomotor experiments. Eight subjects participated in the first experiment. Seven subjects (including two subjects from the first group) participated in the second one. All procedures were approved by the Université catholique de Louvain Ethics Committee and were in agreement with the Declaration of Helsinki.

Stimuli

All trials started with an initial fixation during which a green dot was visible. Then, we presented either a moving point-light walker or one of its scrambled versions (see Fig. III.1). The stimulus appeared and immediately started to move in a randomized heading direction for 800 ms, before gradually disappearing behind an invisible occluder for 800 ms. After the blanking period, the stimulus gradually reappeared and moved for an additional 800 ms period. The temporary blanking mimicked the disappearance of a human walker behind a large object, i.e. it would not disappear and reappear at once. The type of stimulus (biological motion (BM) or control), its direction (leftward or rightward), and its velocity (5, 10 or 15 deg/s) were selected at random for each trial. Typically, subjects performed three sessions of this experiment and each session contained 13 blocks of 30 trials. In the first experiment, the control stimulus consisted of a scrambled walker (SCR) that was chosen randomly from a set of nine stimuli for each block. In the second experiment, the control stimulus was the inverted walker (INV), which is known for being devoid of biological relevance.

The point-light walker was created using Cutting's algorithm (Cutting, 1978) and consisted of a green hip dot and 10 red dots representing other body joints (7.2 degrees in height). Subjects were asked to pursue the green hip dot. The scrambled control stimulus was obtained by shuffling the mean vertical position of the 10 red dots (all dots except the hip dot) to disrupt the global form while keeping the same local motion for the 10 red dots (see Eq. III.1 to Eq. III.6 for details). Subjects were asked to pursue the hip dot that was

highlighted in green and had identical motion whatever the stimulus type (see Fig. III.1).

Apparatus and data analysis

Subjects were seated in a dark room with their head restrained by a chin-rest and faced a 1.5 m distant tangent screen that spanned 40 degrees of their visual field. Stimuli were projected onto the screen with a cine8 Barco projector (Refresh rate: 100 Hz; Barco NV, Belgium). Eye movements were recorded at 200 Hz using a Chronos Eye Tracker (Skalar Medical BV, The Netherlands) and with an Eyelink 1000 (SR Research Ltd., Ottawa, Ontario, Canada) at 1000 Hz for the three last subjects.

Eye movements were low-pass filtered at 45 Hz and velocity and acceleration signals were derived from position signals using a central difference algorithm on a ±10 ms interval. Saccades were detected using a 500 deg/s² acceleration threshold. Those saccades were removed from the smooth eye velocity trace (see details in de de Brouwer et al., 2002). Given that the vertical component of eye velocity was very small (below 3 deg/s), the analyses focus on the horizontal component of eye velocity. The analyses were aligned on stimulus onset. Trials were selected manually (no blink during the trial, no come back of the eye to the fixation point during blanking,…).

Model

The motivation for this chapter is to show the efficiency of a simple model to assess different hypotheses. In order to test if the advantage of the BM stimulus is coming either from the visuomotor processing or from the memory, we designed the simplest pursuit model composed of these two different parts. This model, based on previous models (see below for details), is therefore much simpler than the one presented in Chapter II. The model used here is deterministic and simply sums the two signals coming from the visuomotor transformation and from the memory loop. Therefore, this model is not able to reproduce several simulations shown in Chapter II, as for instance the anticipatory pursuit during a gap period or the sinusoidal pursuit.

Our model incorporated two main elements: a visuomotor transformation process and a memory pathway (Fig. IV.1A). In our model, the retinal slip is computed from the subtraction of the eye velocity from the target velocity. This signal is delayed by 100 ms and sent to the visuomotor transformation box as in Krauzlis and Miles (1996b). This box is composed of two parallel pathways. In the image acceleration pathway, the retinal slip signal is first differentiated (i.e. acceleration error) and then transformed into motor commands by the following equation:

$$y = a \ \ \mathrm{sgn}(x) \ \ e^{-\frac{(|x|-b)^2}{2c^2}} \qquad \text{Eq. IV.1}$$

where *y* is the resulting motor command and *x* the acceleration error signal.

The constants *a*, *b* and *c* are set to 90, 200 and 62, respectively (same values as in (Krauzlis and Miles, 1996b). The image velocity pathway transforms the retinal slip signal into motor commands through a linear scaling with gain α. The outputs of the two pathways are then summed together. The motor command resulting from the visuomotor transformation is then summed up with the output of the memory pathway before being sent to the eye plant (modeled as a low-pass filter with a time constant of 150 ms). To simulate the effect of biological motion on the visuomotor transformation, we set the gain α to 11 for control stimuli and 13 for the biological motion stimuli. Krauzlis and Miles (1996b) set α to 12.

The memory pathway works as a short-term memory. It contains an integrator that sums the motor commands within the local feedback loop until the output of the memory pathway matches the current motor commands (Bennett and Barnes, 2003). This output of the memory pathway is then multiplied by a memory gain β before being summed with the signal coming from the visuomotor transformation. The memory gain β is modulated by the blanking of the target and reinstated to its initial value to account for predictive velocity recovery before the end of the blanking period (Bennett and Barnes, 2003). To simulate the effect of biological motion on the memory pathway, we made β reach its maximum value faster (for biological motion pursuit initiation and pursuit recovery after blanking). The value of the different parameters was not fit to our data but was inferred from existing models. Our model is only a tool to make qualitative predictions for both hypotheses.

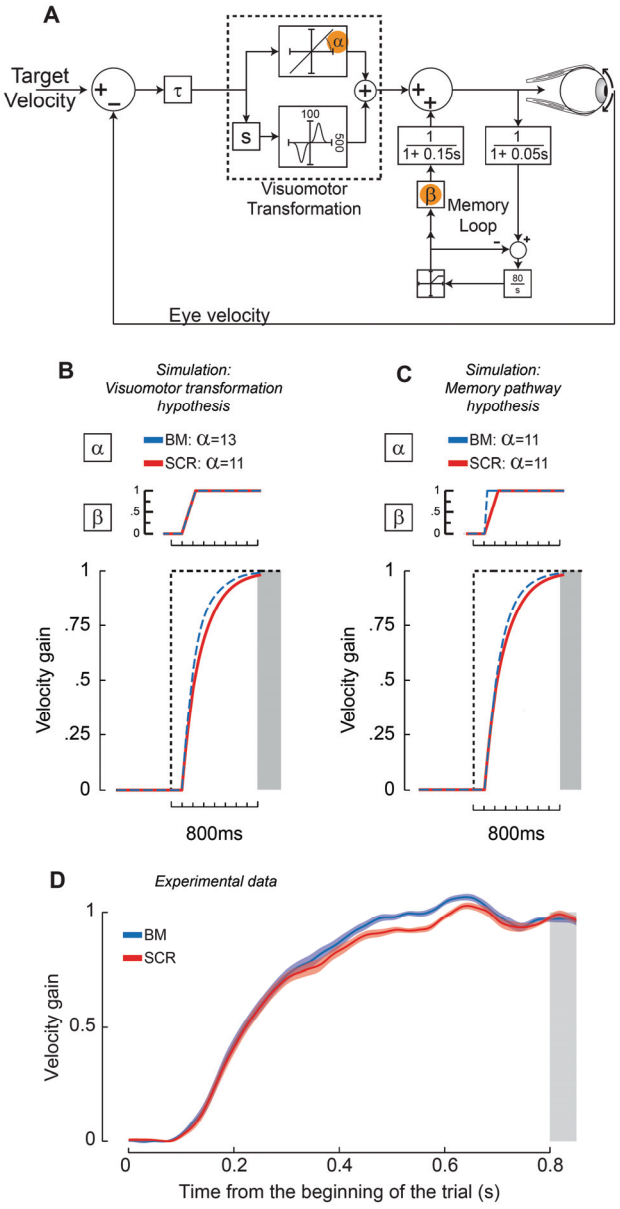

Figure IV.1: (A) Smooth pursuit model of the ocular pursuit. The visuomotor transformation is adapted from Krauzlis and Miles (1996b). The memory pathway is adapted from Bennett and Barnes

(2003). The parameter α represents the gain of the visuomotor pathway and plays an important role in the transformation of the retinal slip into motor command. The parameter β is in the memory pathway, and represents the expectation to perceive an upcoming target. s corresponds to Laplace operator for derivative. Visual feedback delay τ = 0.1 s. B and C) Simulations of the pursuit gains for pursuit initiation by two different models corresponding to the two hypotheses. (B) Prediction when the visuomotor pathway gain is modulated by BM (α=13 for BM and α=11 for SCR). (C) Prediction when the gain of the memory pathway is modulated by BM. Top insets: gains of the memory pathway (β) evoked either by the biological motion stimuli (BM, blue) or by the control stimuli (SCR, red). Bottom graphs: Velocity smooth pursuit gains. Blue traces are BM-related and red are SCR-related. Black corresponds to a unitary velocity gain. Grey area represents the blanking of the stimuli. X-axis is time whereas Y-axis is the gain of the pursuit. (D) Average gain of the smooth pursuit from experimental data, evoked either by BM or by SCR during pursuit initiation. Areas surrounding the traces represent confidence intervals.

Results

Pursuit initiation

In our model, increasing either the gain of the visuomotor transformation (α) or the gain of the memory pathway (β) could

qualitatively reproduce the increase in smooth eye velocity observed in our previous experiment during pursuit initiation. Namely, biological motion stimuli evoke a transiently larger smooth eye velocity than control stimuli. In the case of the visuomotor transformation hypothesis, we increased the gain of the transformation of retinal slip into motor command (α, see Fig. IV.1A) by 20% when the stimulus was biologically relevant, which produced a larger eye velocity during pursuit initiation (Fig. IV.1B). In the case of the memory pathway hypothesis, the memory gain (β, see Fig. IV.1A) more rapidly reached its maximum (Fig. IV.1C, top insets). Therefore, this faster increase of the memory gain also produced a larger smooth eye velocity during pursuit initiation (Fig. IV.1C). In our dataset (see Methods), we did observe a significant advantage to pursue biological motion (BM) instead of a scrambled stimulus from 150 ms to 500 ms after pursuit onset (Fig. IV.1D). For instance, a repeated measure ANOVA, with stimulus type (BM or SCR) and stimulus velocity as within subject factors indicated a main effect of stimulus type on smooth pursuit velocity 300 ms after stimulus onset ($F(1, 7) = 22.3$, $p = 0.002$) but no interaction between stimulus type and stimulus velocity ($F(2, 14) = 0.26$, $p = 0.77$).

Although both hypotheses might explain the difference in the smooth pursuit initiation observed in experimental data, these two hypotheses made very different predictions during and around the time of target blanking. These differences will be explained in the following paragraphs and tested against experimental results recorded during and after the temporary blanking of the moving stimuli.

Blanking period and predictive recovery

During the transient blanking of the pursued target, the smooth pursuit response is solely driven by the memory pathway given that there are no visual inputs. Therefore, any difference in the visuomotor transformation will not produce differences in behavior during blanking periods. In contrast, differences in memory gain will result in differences in behavior during blanking. For instance, if the biological motion influenced the plateau value of the memory gain β, it would influence the minimum of speed velocity during the blanking. The β parameter used in this model plays the same role as the G_{int} gain used in Chapter II.

To account for predictive recovery of smooth eye velocity during blanking of the target, several authors have hypothesized that the memory gain is reinstated to its maximal value before the end of the occlusion. Under the memory loop hypothesis, the reinstatement of β would be faster during the blanking as it was during the initiation. Therefore, the memory loop hypothesis predicts a higher predictive velocity recovery for the biological motion stimuli than for the control ones (Fig. IV.2B). Again, no difference is expected from the visuomotor transformation hypothesis (Fig. IV.2A).

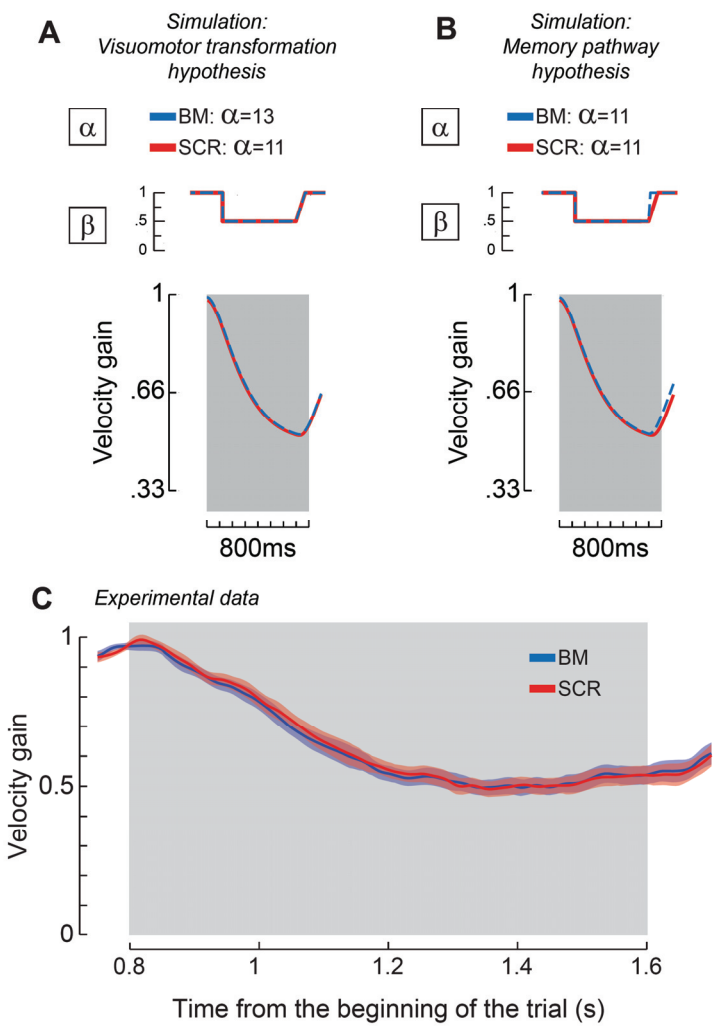

Figure IV.2: Comparison between simulations and experimental data for the blanking period. Top insets (A and B): gains of the visuomotor pathway (α) and the memory pathway (β) for the biological motion stimuli (BM, blue) or the control stimuli (SCR, red). Bottom: prediction when the visuomotor pathway gain α is modulated by BM (A) or when the gain β of the memory pathway is modulated by BM (B). Blue traces are BM-related and red are SCR-related. Grey area

represents the blanking of the stimuli. X-axis is time whereas Y-axis is the gain of the pursuit. (C) Average gain of the smooth pursuit from experimental data, evoked either by BM or by SCR. Areas surrounding the traces represent confidence intervals.

The analysis of smooth pursuit velocity of human subjects during the blanking period did not reveal any significant difference (no effect of stimulus type on velocity measured each 50 ms from the beginning to the end of the blanking; all $p > 0.3$) between the two types of stimuli (Fig. IV.2C). For instance, 200 ms before reappearance of the stimuli, a repeated measure ANOVA, with stimulus type (BM or SCR) and stimulus velocity as within subject factors indicated no main effect of stimulus type on smooth pursuit velocity ($F(1, 7) = 0.085$, $p = 0.78$), whereas there was a main effect for stimulus velocity ($F(2, 14) = 72.6$, $p < 0.001$).

The comparison of eye velocity evoked by BM and control stimuli around the time of target reappearance (before visual feedback can influence the smooth pursuit response) did not reveal any significant difference in predictive recovery. We measured the predictive recovery by subtracting eye velocity measured 200 ms before the end of blanking from eye velocity measured 50 ms after target reappearance (before any influence of visual feedback). The change in smooth pursuit gain during the predictive recovery ranged from 0.13 to 0.2 for the different conditions and was significantly larger than zero in all six conditions (two stimulus types and three stimulus velocities; paired t-test, all $p < 0.002$; Bonferroni correction requires all $p < 0.008$). A repeated measure ANOVA on smooth pursuit gain with time (200 ms before and 50 ms after target reappearance), stimulus type (BM or SCR) and stimulus velocity as within subject factors demonstrated the significance of the predictive

recovery (main effect of time, $F(1, 7) = 22.9$, $p = 0.002$). This measure significantly varied with stimulus velocity (interaction between time and stimulus velocity, $F(1, 7) = 7.15$, $p = 0.007$) as it was larger for smaller stimulus velocities. However, this analysis did not reveal any significant effect of stimulus type on the predictive recovery (main effect, $F(1, 7) = 0.61$, $p = 0.46$; interaction between time and stimulus type, $F(1, 7) = 0.001$, $p = 0.97$; between velocity and stimulus type, $F(2, 14) = 0.006$, $p = 0.99$; three way interaction, $F(2, 14) = 0.05$, $p = 0.95$).

In sum, our behavioral data appear to reject any influence of the percept of biological motion when this stimulus is not present on the screen. Thus biological motion does not influence the predictive component of the smooth pursuit response. This conclusion seems incompatible with the memory pathway hypothesis.

Visually-guided reacceleration

When motor commands are again partially driven by visual feedback (>100 ms after target reappearance), the visuomotor transformation hypothesis predicts some differences between the smooth eye velocity evoked by biological motion stimuli and by control stimuli. Indeed, given the residual retinal slip present after target reappearance, the visuomotor transformation hypothesis predicts a stronger reacceleration in the case of biological motion stimuli than in the case of control stimuli (Fig. IV.3A). In contrast, the differences observed following the memory hypothesis arise from the differences predicted during the occlusion (Fig. IV.3B).

Our analysis revealed that the behavior was consistent with the visuomotor transformation hypothesis. Indeed, ANOVA on smooth eye acceleration between 100 and 250 ms after stimuli reappearance exhibited a significant main effect of stimulus type ($F(1, 7) = 19.11$, $p = 0.003$) and of target speed ($F(1, 7) = 22.17$, $p < 0.001$). Independently of target speed ($F(2, 14) = 2.51$, $p = 0.11$), the visually guided acceleration evoked by biological motion between 100 and 250 ms after stimulus reappearance was significantly larger than the one evoked by the scrambled stimuli (Fig. IV.3C). This higher acceleration for BM than SCR resulted in a higher velocity from 150 ms to 350 ms after reappearance (main effect on stimulus type on pursuit velocity 150 ms after stimulus reappearance: $F(1, 7) = 3.2$, $p = 0.031$).

Our results are independent of the type of control stimuli as we reproduced the same results in a second experiment where the scrambled walker was replaced by the inverted walker (Fig. IV.4A).

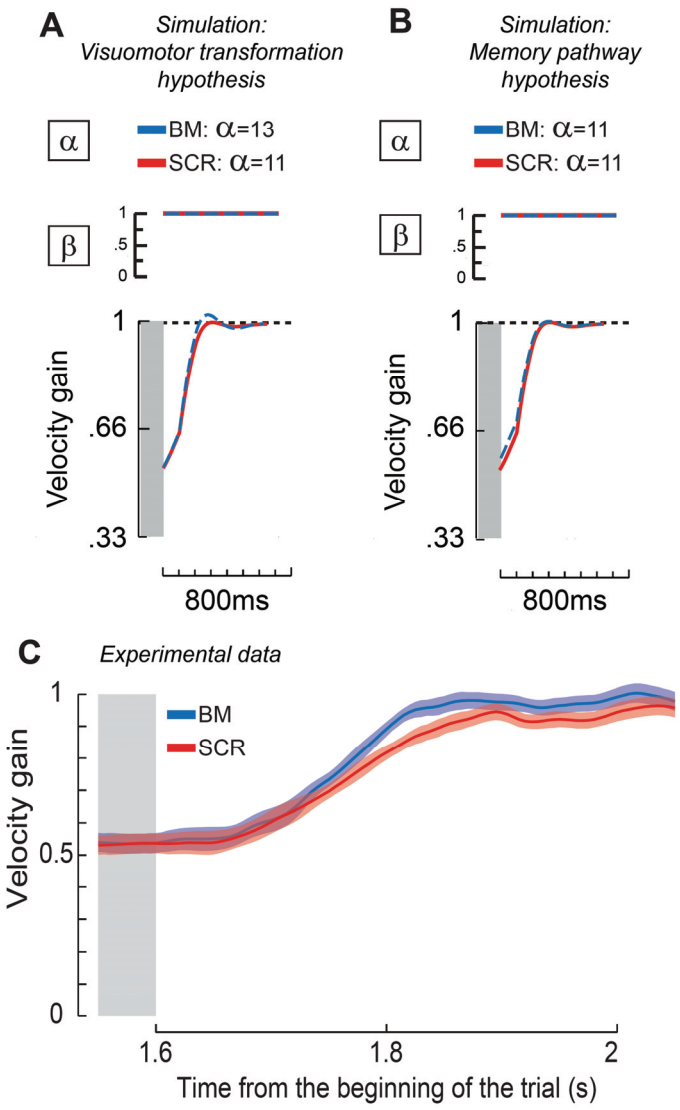

Figure IV.3: Comparison between simulations and experimental data for the reappearance of the stimulus. Top insets (A and B): gains of the visuomotor pathway (α) and the memory pathway (β) for the biological motion stimuli (BM, blue) or the control stimuli (SCR, red). Bottom: prediction when the visual feedback gain α is modulated by

BM (A) or when the gain β of the memory pathway is modulated by BM (B). Blue traces are BM-related and red are SCR-related. Black corresponds to a unitary velocity gain. Grey area represents the occlusion (blanking of the stimuli). X-axis is time whereas Y-axis shows the gain of the pursuit. (C) Average gain of the smooth pursuit from experimental data, evoked either by the BM or by SCR. Areas surrounding the traces represent confidence intervals.

As summarized on Fig. IV.4A and B (green trace), the biological motion stimuli evoked a larger smooth eye velocity gain than the inverted walker both during pursuit initiation (main effect of stimulus type on eye velocity gain 300 ms after target onset: $F(1, 6) = 21.7$, $p = 0.009$) and during the reacceleration after the transient blanking of the target (main effect of stimulus type on eye acceleration computed between 100 and 250 ms after stimulus reappearance: $F(1, 6) = 48.4$, $p < 0.001$). The influence of the type of stimulus on the smooth pursuit response occurred earlier at reappearance (around 150 ms after target reappearance) than during pursuit initiation (around 260 ms after stimulus onset).

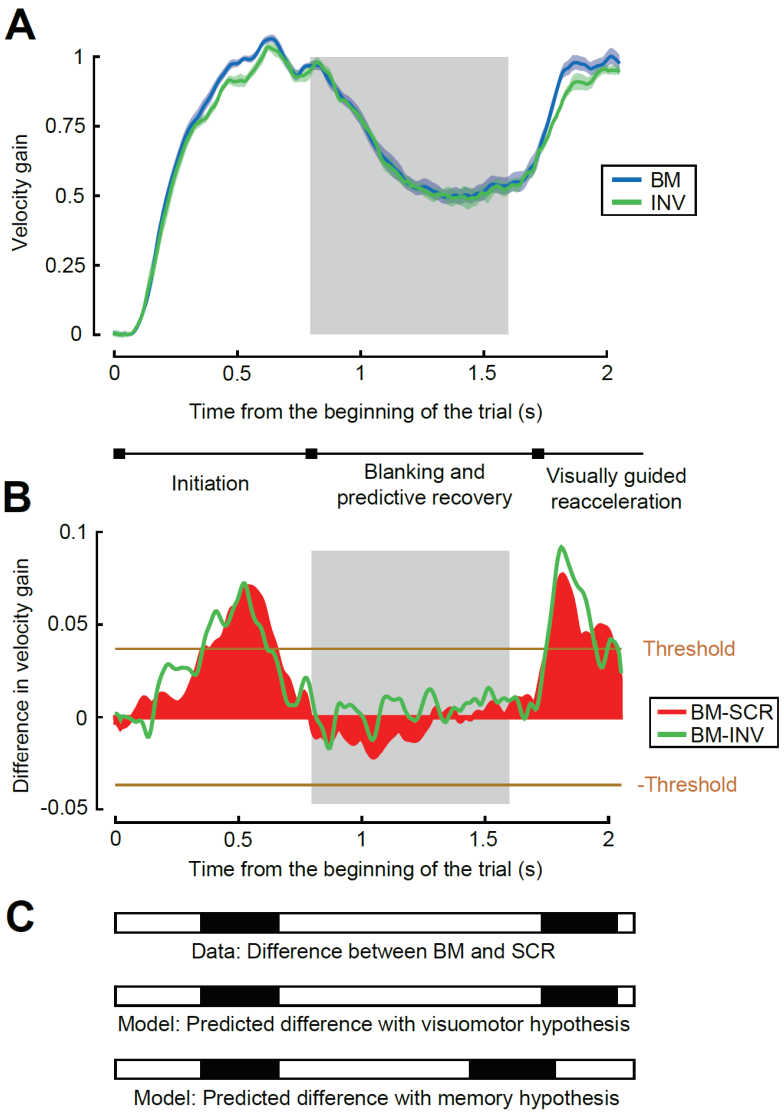

Figure IV.4: (A) Average gain of the smooth pursuit from experimental data, evoked either by the BM (blue) or by the INV (green). Areas surrounding the traces represent confidence intervals. Grey area represents the occlusion (blanking of the stimuli). X-axis is time whereas Y-axis shows the gain of the pursuit. (B) Average difference

between the pursuit gains evoked by BM and by SCR (red trace) and between the pursuit gains evoked by BM and by INV (green trace) versus time. C) The upper horizontal bar shows the periods where the difference between the pursuit responses evoked by BM and SCR (red) is larger than a given threshold. This threshold corresponds to the average 99% confidence interval of the difference between pursuit gains evoked either by BM and SCR during all the trial. The two lower bars represent the periods during which there is a theoretical difference between pursuit induced by BM or a control stimulus (SCR).

Independently of the control stimulus, there is an important difference in gain during smooth pursuit initiation (Orban de Xivry et al., 2010) and after reappearance of the target (Fig. IV.4B). This last result reflects a larger visually-guided pursuit reacceleration evoked by biological motion. The upper bar in Fig. IV.4C shows the significant difference between the pursuit response evoked by BM and SCR. We used a threshold (difference of velocity gains of 0.037) based on the average 99% confidence interval of these differences during the trial. The two lower bars show the qualitative difference between the theoretical predictions for BM and SCR, for both hypotheses. This schema summarizes our results and shows that the influence of biological motion on the smooth pursuit response observed in the experimental data is likely due to changes in the visuomotor transformation pathway.

Discussion

In this paper, we investigated the influence of the biological motion percept on the smooth pursuit system. We hypothesized that biological motion could either influence the transformation of motion perception into motor commands or increase the reliance of the system on its predictive pathway. Although we found that both hypotheses could account for the observed difference during pursuit initiation, the absence of difference in predictive smooth pursuit during the transient blanking of the stimulus appeared to rule out the influence of the biological motion stimulus on the predictive pathway. In contrast, the observation that reacceleration after the blanking period was again facilitated by the biological motion stimuli with respect to control stimuli appeared to support an influence of biological motion on the visuomotor transformation process.

The influence of perception on smooth pursuit initiation has also been studied in the framework of the aperture problem (Pack and Born, 2001) where a tilted stimulus that is moving horizontally is initially perceived moving in an oblique direction (Marr and Ullman, 1981). Similarly to our study, this percept of an oblique moving direction influences smooth pursuit eye movements, i.e. this percept initially biases smooth pursuit eye movements towards the oblique direction. The influence of the aperture problem and of biological motion on the visuomotor transformation clearly differs. Indeed, unlike our study, the reacceleration phase after a short blanking period of a tilted diamond stimulus that is moving horizontally does not exhibit the same vertical deviation as during pursuit initiation (Masson and Stone, 2002).

Two possible explanations might account for this difference. On one hand, the blanking period used by Masson and Stone (2002) might have been too short (90 ms) to cause a sufficiently large reduction in eye velocity. A higher reduction in eye velocity during the blanking period would have required a higher involvement of the visuomotor transformation process during the reacceleration phase. Consequently, oblique eye movements might have been evoked again during the reacceleration phase. On the other hand, the biological motion perception and the tilted line perception are thought to be mediated by different neuronal substrates and might therefore impact different stages of the visuomotor transformation. Indeed, object motion is processed by MT (Pack and Born, 2001; Born and Bradley, 2005) whereas biological motion is processed by the posterior part of superior temporal sulcus (STS) and the anterior portion of the intraparietal sulcus (IPS) among others (Oram and Perrett, 1994; Decety and Grezes, 1999; Grezes et al., 2001; Billino et al., 2009). In addition, MT lesion does not abolish biological motion perception (Vaina et al., 1990; McLeod et al., 1996). Therefore, the difference in the reacceleration phase could also be due to differences in neural substrates.

It was possible for Lisberger and Movshon (1999) to reconstruct image velocity (input of the visuomotor transformation) with a distributed response recorded in MT in monkeys. MT is essential for both motion perception (Born and Bradley, 2005) and smooth pursuit eye movements (Newsome et al., 1985). The biological motion network could act directly (in parallel to MT) or indirectly (via MT/MST) on the visuomotor transformation process. Projections from STS to MT/MST have been demonstrated anatomically in monkeys (Boussaoud et al., 1990) and hypothesized

to be responsible for the activation of these areas in the case of implied human motion (Jellema and Perrett, 2003a).

In other contexts, perception of human action has been shown to influence action production, hence the visuomotor transformation stage (see Blake and Shiffrar (2007) for review). Observing actions performed by a human actor, not a robot, can influence the production of other actions (Kilner et al., 2003). In one study, visual presentation of a finger movement slows down the reaction time to initiate another finger movement (Brass et al., 2001) and this finding has been reproduced in another study with grasping movements (Craighero et al., 2002). These results illustrate that perception of human action can influence the visuomotor transformation process (for arm or hand movements but also for pursuit eye movements).

In addition, action can also influence perception (Grezes et al., 2001; Hamilton et al., 2004; Casile and Giese, 2005; Schütz-Bosbach and Prinz, 2007). For instance, Jacobs and Shiffrar (2005) showed that discriminating point-light walker speed is disrupted by concurrent walking of the observer. In sum, an observer's own activity influences his/her perception of the activity of other people. Therefore, the link between perception and action is then present in both ways (Blake and Shiffrar, 2007).

Finally, the absence of influence of the biological motion on the predictive pursuit response during the temporary blanking of the target was unexpected for several reasons. First, observation of biological motion leads to better prediction than when this component of motion is absent (Huys et al., 2008, 2009; Mark Williams et al., 2009). Second, some neurons in STS that are selectively responsive to biological motion (Oram and Perrett, 1994; Puce and Perrett, 2003) continue to respond when the initially visible moving walker

disappears behind an occluder (Baker et al., 2001; Jellema and Perrett, 2003b). These cells showed their highest levels of activity when the walker was totally hidden from view. Although it did not influence the predictive smooth pursuit response, the maintenance of BM-related activity during occlusion might result in a priming effect for biological motion and be responsible for the earlier effect observed at target reappearance. On the basis of those two observations, biological motion could have yielded a better prediction based on an improved internal representation of the biological relevant stimulus.

In conclusion, the present study shed some light on how biological motion acts on the smooth pursuit system. Although biological motion does not influence the response of the smooth pursuit system during blanking periods, it does during initiation phase of the response and during the reacceleration phase after the blanking period. Importantly, during those periods, the smooth pursuit response was primarily driven by retinal inputs. Therefore, we conclude that biological motion influences the visuomotor transformation for smooth pursuit eye movements.

Chapter V
Dramatic impairment of prediction due to frontal lobe degeneration

Abstract

Prediction is essential for motor function in everyday life. For instance, predictive mechanisms improve the perception of a moving target by increasing eye speed anticipatively, thus reducing motion blur on the retina. Subregions of the frontal lobes play a key role in eye movements in general and in smooth pursuit in particular but their precise function is currently not firmly established. Here, the role of frontal lobes in the timing of predictive action is demonstrated by studying predictive smooth pursuit during transient blanking of a moving target in mild frontotemporal lobar degeneration (FTLD) and Alzheimer's disease (AD) patients. While control subjects and AD patients predictively reaccelerated their eyes before the predicted time of target reappearance, FTLD patients did not. The difference

was so dramatic (classification accuracy > 90%) that it could even lead to the definition of a new biomarker. In contrast, anticipatory eye movements triggered by the disappearance of the fixation point were still present before target motion onset in FTLD patients and visually-guided pursuit was normal in both patient groups compared to controls. Therefore, FTLD patients were only impaired when the predicted timing of an external event was required to elicit an action. These results argue in favor of a role of the frontal lobes in predictive movement timing.

*This chapter has been published: "**Coppe S, Orban de Xivry J-J, Yüksel D, Ivanoiu A, Lefèvre P**. Dramatic impairment of prediction due to frontal lobe degeneration. Journal of Neurophysiology (in press), 2012."*

Introduction

Prediction is a corner stone of human motor function. It is used to improve the perception of a moving object (Orban de Xivry and Lefèvre, 2007; Barnes, 2008), to avoid the slippage of a handheld object during its transport (Flanagan and Wing, 1997) or to anticipate the consequences of one's own actions (Blakemore et al., 2000). In the present study, we focus on predictive mechanisms active during smooth pursuit eye movements that are normally used to overcome sensorimotor delays (Carl and Gellman, 1987).

Predictive smooth pursuit eye movements are especially highlighted when the fixation cue disappears for a few hundred

milliseconds before target motion onset (Kowler and Steinman, 1979a, 1979b, 1981; Barnes et al., 1987; Boman and Hotson, 1988, 1989; Barnes and Asselman, 1991, 1992; Kowler, 2011) or when the target transiently disappears from the visual environment (Mitrani and Dimitrov, 1978; Becker and Fuchs, 1985; Barnes, 2008). In this case, smooth pursuit eye movements are maintained in the absence of visual feedback through predictive mechanisms.

During this blanking period, smooth pursuit eye velocity decreases to a plateau value (Becker and Fuchs, 1985; Orban de Xivry et al., 2006, 2008) and is compensated for by saccades (Bennett and Barnes, 2003; Orban de Xivry et al., 2009). Moreover, if the duration of the blanking period is predictable, a predictive eye reacceleration takes place before target reappearance (Bennett and Barnes, 2003, 2004; Churchland et al., 2003; Orban de Xivry et al., 2006). This predictive reacceleration is scaled to upcoming target velocity (Bennett and Barnes, 2004; Orban de Xivry et al., 2006). It is present in experiments where target velocity at reappearance changes from trial-to-trial but can be anticipated from the pre-blanking period (Bennett et al., 2007). When the same target motion is used in consecutive trials, it takes three trials to build up an appropriate predictive reacceleration (Bennett et al., 2010). In contrast, such a predictive reacceleration is absent when the duration of the blanking period is unknown (Orban de Xivry et al., 2008).

Three lines of evidence highlight the implication of the frontal lobes in predictive smooth pursuit in humans (Sharpe, 2008). First, fMRI studies found changes in activation during predictive smooth pursuit in the frontal eye fields (FEF), the supplementary motor area (SMA), including supplementary eye fields (SEF), and the dorsolateral prefrontal cortex (DLPFC) (Schmid et al., 2001; Lencer

et al., 2004; Nagel et al., 2006, 2007). Second, anticipatory and visually-guided smooth pursuit eye movements are impaired in stroke patients when frontal areas are damaged (Morrow and Sharpe, 1995; Heide et al., 1996; Lekwuwa and Barnes, 1996). Third, disrupting FEF activity by transcranial magnetic stimulation impairs predictive pursuit whereas disrupting the SEF affects the phase around the time of target direction reversal (Gagnon et al., 2006; Nyffeler et al., 2008). However, the functional significance of these findings remains unclear.

In monkeys, the role of the FEF and SEF subregions of the frontal lobes in smooth pursuit is still much debated and three hypotheses have been presented. Based on recordings of FEF neurons during target blanking, Ferrera and colleagues suggested that the FEFs contain an internal motion representation (Barborica and Ferrera, 2003, 2004; Xiao et al., 2007). Based on smooth pursuit perturbation, Tanaka and Lisberger identified FEF neuron responses consistent with a gain controller for visually-guided pursuit (Tanaka and Lisberger, 2001, 2002). Finally, the behavior of FEF neurons during visually-guided and anticipatory smooth pursuit might also be consistent with a role of FEF in timing representation (de Hemptinne et al., 2008; Schoppik et al., 2008; Li and Lisberger, 2011). One goal of this study was therefore to investigate which function of the pursuit system will be impaired by the degeneration of the frontal lobes of human brain.

To do so, we compare the predictive abilities of frontotemporal lobar degeneration (FTLD) patients to those of age-matched control subjects and Alzheimer's disease patients (AD). Previous studies have shown that a subset of FTLD patients performed significantly worse during an anti-saccade task (Meyniel et al., 2005; Boxer et al.,

2006; Garbutt et al., 2008) and exhibited a lower eye velocity during the steady state pursuit (Boxer et al., 2006; Garbutt et al., 2008). Some FTLD patients could also present larger saccade latencies and smaller visually guided saccade velocity and gain (Boxer et al., 2012; Burrell et al., 2012). Frontotemporal lobar degeneration (FTLD) is a neurodegenerative disorder that is associated with degeneration of the frontal and/or anterior temporal lobes with relative sparing of more posterior cortical regions. The frontal eye fields (FEF) and the supplementary motor area (SMA) are among the first areas impaired by this neurodegenerative process (Broe et al., 2003). Neurologically, it distinguishes from AD because at its early stage, the frontal lobes are relatively spared (Nelson et al., 2009; Aries et al., 2010; Vemuri et al., 2011).

Therefore, the comparison of the predictive tracking behavior of FTLD and AD patients will highlight the importance of the integrity of the frontal lobes in the control of predictive smooth pursuit.

Materials and Methods

Participants

Eye movements of 14 patients (three females) with mild FTLD were recorded. They were between 49 and 82 years old (mean age of 62.9 years, std of 5.9 years). FTLD patients were diagnosed according to their presentation as behavioral and dysexecutive frontotemporal dementia (FTD), semantic dementia (SD) and progressive non-fluent aphasia (PA). All subjects met criteria of Neary

(Neary et al., 1998) for FTD (8), SD (2) or PA (4). Two FTD patients also showed signs of motor neuron disease (MND), a well-known association (Bak and Hodges, 2001; Lomen-Hoerth et al., 2002; Lillo and Hodges, 2009). Diagnosis was supported by clinical assessment, neuropsychological evaluation, magnetic resonance imaging, functional imagery (F-18 FDG PET scanner, Tc-99m HMPAO or ECD brain scintigraphy) and, in six patients, by cerebrospinal fluid (CSF) biomarkers assay. One FTD patient carried a mutation in progranulin (GRN) gene (Chen-Plotkin et al., 2011), another FTD patient associated with motor neuron disease has a familial history (genetic assessment ongoing).

Twelve AD patients (three females) participated in the same experiment. They were between 58 and 85 years old (mean age of 67.3 years, std of 7.3 years). Diagnosis of AD followed the NINCDS-ADRDA criteria (McKhann et al., 1984). All AD patients underwent neuropsychological assessment, structural and functional brain imaging. In ten AD patients the diagnosis was corroborated by specific biomarkers assessment: either a CSF analysis showing pathological levels of tau protein and/or amyloid beta42 or a 18F-flutemetamol amyloid imaging PET scanner displaying senile plaques in the brain (Vandenberghe et al., 2010). The positivity of CSF and/or imaging biomarkers in the AD patients supported the diagnosis in mild cases when the MMSE was above the classical threshold of 24/30 (Jack et al., 2011).

All patients were followed-up by the same neurologist that made the diagnosis initially (author AI) and were re-examined six months after the eye recording in order to validate the diagnosis. The morphological and functional imaging deficits were recorded by the

same neurologist (AI) who was unaware of the oculomotor performances of the patients.

Sixteen age-matched control subjects (four females) participated in the same experiment as control (CTRL) subjects. They were between 55 and 83 years old (mean age of 64.3 years, std of 4.3 years).

Data of one FTLD patient (from FTD subgroup), one AD patient and one CTRL subject were excluded based on their abnormal visually-guided pursuit performance (see “data analysis” part of the methods). We analyzed the data from thirteen FTLD patients, eleven AD patients and fifteen CTRL subjects. The patient demographics as well as their disease related characteristics are summed up in Table V.1. Magnetic resonance imaging and functional imagery (F-18 FDG PET scan) of two typical patients (patients #FTLD5 and #AD9) are shown in Fig. V.1.

All procedures were approved by the Université catholique de Louvain Ethics Committee and were in agreement with the Declaration of Helsinki. All participants gave their informed consent prior to participating in the experiment.

Table V.1: Patient demographics and disease characteristics

Patients	**Age**	**Educ**	**Gender**	**Type**	**D Dur**	**Morphological impairment**	**Functional impairment**
FTLD 1	59	9	M	SD	50	temporal pole L, frontal L	Temporal, fronto-lateral and parietal L
FTLD 2	63	18	M	FTD$	19	temporo-polar R	frontal medial, orbital & temporal poles R
FTLD 3	59	20	M	PA	25	Normal	fronto-lateral, inferior & SMA L
FTLD 4	60	18	M	FTD	30	fronto-insular R	bifrontal; temporo-polar R
FTLD 5	58	12	M	FTD	24	Bifrontal	bifrontal; temporo-parietal R
FTLD 6	69	18	M	SD	24	bitemporo-polar L	temporal L
FTLD 7	73	12	F	PA	40	diffuse atrophy	bifrontal; premotor, temporal & parietal R
FTLD 8	66	18	F	FTD	42	bifrontal (basal) & subcortical	bifrontal
FTLD 9	82	20	M	PA	60	diffuse atrophy	frontal lateral premotor L
FTLD 10	55	18	M	FTD$	12	diffuse atrophy	frontal L
FTLD 11	49	10	F	PA	16	temporal L	temporal L
FTLD 12	63	12	M	FTD	50	vertex & para hippo L	frontal L
FTLD 13	62	18	M	FTD	48	frontal dorso-lateral & inferior L	bitemporal
MEAN	**62.9**	**15.6**	**10/3**		**34**		
AD 1	58	9	M	/	48	quite normal	superior parietal L

AD 2	60	20	F	/	30	slight diffuse & medial temporal	parietal L
AD 3	63	15	M	/	20	slight diffuse & medial temporal	parietal & lateral temporal R
AD 4	68	15	M	/	18	slight diffuse & medial temporal L	bilateral superior parietal
AD 5	59	18	M	/	62	slight bi-temporal atrophy	parietal & posterior temporal R
AD 6	79	14	M	/	66	diffuse & medial temporal atrophy	posterior temporal R
AD 7	63	20	F	/	50	medial temporal atrophy	parietal & posterior temporal R
AD 8	74	15	M	/	39	slight bi-temporal atrophy	posterior temporal R
AD 9	85	15	M	/	72	medial temporal atrophy	medial temporal & anterior and posterior cingulate cortex
AD 10	71	16	F	/	60	slight diffuse & medial temporal	posterior temporal L
AD 11	61	18	M	/	42	slight diffuse & medial temporal	parietal & posterior temporal L
MEAN	**67.3**	**15.9**	**8/3**		**46**		

Table V.1 “Demographics and imagery characteristics of the patients”

Educ = Education (in years), Type = syndrome for FTLD patients; FTD = frontotemporal behavioral subtype, SD = semantic dementia subtype and PA = progressive aphasia subtype. $ = FTD patients with motor neuron disease, D Dur = Disease duration (in months) from the first symptoms observed by the patient (or his/her family) until the moment of the eye assessment. Morphological and functional imaging deficits are based on the visual appreciation of the

neurologist who was unaware of the oculomotor performances of the patients. For impairments; L = Left and R = Right.

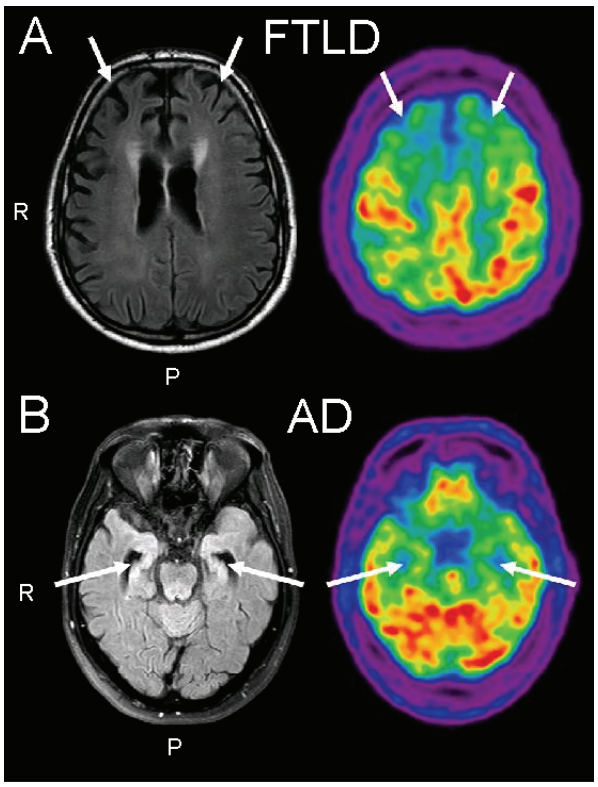

Figure V.1: Typical brain imaging of FTLD and AD patients. Magnetic resonance imaging and functional imagery (F-18 FDG PET scan) of one typical FTLD patient, with frontal lobes impairment (panel A, patient FTLD5), and of one typical AD patient, with medial temporal lobe impairment (panel B, patient AD9).

Neuropsychological testing

Patients performed a standard neuropsychological battery of tests that measures several domains of cognition. This includes verbal tests (e.g. word fluencies) but also tests of executive function: the Luria series test (non verbal visuo-spatial test) and the TMT test (no verbal production) (Table V.2). General cognitive performance was evaluated using the Mini-Mental State Examination (MMSE) (Folstein et al., 1975). Language was assessed using the LEXIS Graded Naming Test as well as a Semantic Fluency (animals in 2 min) and Phonemic Fluency (P-words in 2 min) tests (de Partz et al., 2001). Visuo-spatial processing assessment included the Clock Drawing Test (Rouleau et al., 1992) and the “Praxis” part of the CERAD battery (Morris et al., 1988), which consisted in drawing 4 simple shapes. Executive functions were assessed using verbal fluency tests (see above, de Partz et al., 2001), a variant of “Luria's graphical or alternating sequences test” which consisted in copying iteratively some series of geometric forms (local battery, unpublished) and using the “Trail Making Test”. Long term memory assessment was completed by using the “Doors test” of the “Doors and people Test” (Baddeley et al., 1994) and the French adaptation of the RL/RI 16 items Test (Grober and Buschke, 1987; Van der Linden et al., 2004).

Table V.2: Scores of neuropsychological tests

Patients	MMSE	DaMM	DaNP	Den (%)	SeFl	PhFl	Clock /8	CER /11	LUR /32	TMT Ti B-A	TMT Er B-A	Doors /24	Sum /48	Recall /16
FTLD 1	27	5	5	0.47	11	8	6	10	30	45	0	21	15	5
FTLD 2	28	0	0	0.68	19	7	7	11	26	50	0	17	17	6
FTLD 3	24	2	2	0.85	7	6	7	10	27	87	0	15	25	12
FTLD 4	28	1	1	0.93	31	12	3	9	20.5	58	0	18	23	10
FTLD 5	29	0	0	0.82	29	15	7	9	23	108	3	16	30	14
FTLD 6	21	3	3	0.13	10	3	7	11	31	41	0	17	9	2
FTLD 7	27	0	11	0.86	15	5	6	10	/	/	/	/	/	/
FTLD 8	22	0	7	0.84	19	20	5	9	20	344	6	16	26	10
FTLD 9	27	2	2	0.66	8	4	3	9	19	90	1	8	16	6
FTLD 10	28	5	5	0.79	21	5	7	10	27	204	4	12	24	12
FTLD 11	24	0	0	0.34	8	4	1	7	6	285	6	13	20	7
FTLD 12	24	4	4	0.84	28	14	7	8	25	59	0	5	8	2
FTLD 13	30	3	3	0.9	27	14	8	10	29	51	0	21	22	5

AD 1	27	4	4	0.91	20	21	6	10	31	56	1	12	10	6
AD 2	24	2	2	0.92	25	19	8	11	30.5	37	0	12	5	3
AD 3	26	3	15	0.89	21	22	8	10	31	62	0	12	6	2
AD 4	22	6	6	0.92	25	13	5	10	28.5	88	1	13	3	1
AD 5	28	2	30	0.85	18	20	7	6	19.5	95	1	11	6	3
AD 6	28	0	20	0.81	14	7	8	10	22.5	261	5	12	9	2
AD 7	23	5	5	0.88	28	17	5	9	15	402	7	9	3	0
AD 8	27	9	9	0.78	22	9	7	9	21.5	42	1	7	13	5
AD 9	27	1	12	0.84	29	12	8	11	16.5	69	2	16	10	5
AD 10	25	0	16	0.94	36	17	7	9	27.5	85	0	14	13	2
AD 11	24	4	4	0.80	24	21	5	8	20.5	209	0	17	8	2
MEAN FTLD	**25.9**	**1.9**	**3.3**	**0.70**	**17.7**	**9.5**	**5.7**	**9.4**	**23.7**	**118**	**1.7**	**14.9**	**18.8**	**7.6**
MEAN AD	**25.5**	**3.3**	**11**	**0.87**	**24.4**	**16.2**	**6.7**	**9.4**	**25.7**	**125**	**1.6**	**12.3**	**7.8**	**2.7**

Table V.2 “Neuropsychological results for all patients”

MMSE = Mini Mental State Examination (/30), Da MM = number of months between the MMSE and the eye recording, Da NP = number of months between the neuropsychological examination and the eye recording, Den = Denomination task (two variants of the task: / 64 for individuals older than 60 years and /80 for younger individuals. Performance is reported as the percentage of correct response), Se Fl = Semantic Fluency (number of animals in 2 minutes), Ph Fl = Phonemic Fluency (number of P-words in 2 minutes), Clock = Clock

Test (/8), CER = Praxis part of the CERAD battery (drawing 4 simple shapes; /11), LUR = variant of “Luria's graphical or alternating sequences test” (/32), TMT Ti = Trail-Making Test Time (Time of Part B – Time of Part A), TMT Er = Trail-Making Test Errors (number of errors in Part B – number of errors in Part A), Doors = Sum of the two sets of 12 doors (/24), Sum and Recall (last two columns) are coming from the RL/RI16 test, a French adaptation of the Grober and Buschke (1987) task with 3 learning trials of 16 items including a support at the encoding phase by semantic category cueing. Among the different scores available we considered the sum of the free recall 1-3 (/48) and the free recall after 20 minutes (last column, /16). Underlined results are considered to be pathological (results inferior to two standard deviations away from the healthy controls mean, which is weighted by the age and education of each patient). The numbers in parenthesis represent the maximum possible score for each test when relevant. Patient FTLD7 did not conclude all tests. The two last lines show the mean results for the FTLD group and for the AD group. Bold values indicate a significant difference between the two groups (ANOVA with Tukey post hoc, $p<0.05$).

Stimuli

All trials started with an initial fixation during which a yellow dot (diameter of 0.8 deg) was visible on one side of horizontal meridian of the screen (between 25 and 15 deg of eccentricity) for 1000 ms (Fig. V.2). The stimulus disappeared for 300 ms (gap period) and then immediately started to move toward the center at constant velocity for 2000 ms. After 600 ms, the target transiently disappeared

for 800 ms and then reappeared for an additional 600 ms period (test trials). The direction (leftward or rightward) and the velocity of the target (10, 15 or 20 deg/s) were kept constant within a block but changed randomly across blocks. The duration of the block (between 20 and 25 trials) was adjusted for each subject to reduce fatigue effects. In order to minimize sequence effects, the order in which the blocks were received was randomized across subjects. The subjects were instructed to follow the dot even when it was blanked. Each subject or patient performed between 8 and 12 blocks. So, there were at least 30 test trials per subject per target velocity. There was a 2 minute break between two consecutive blocks in order to keep the subjects alert and concentrated.

During the first two trials as well as 3 other trials of each block, the target was continuously visible (control trials) in order to reinforce the continuous movement of the target. The visually guided smooth pursuit gain was measured in these trials. Except the first two, the control trials were randomly inserted in the block but were always followed by at least three test trials.

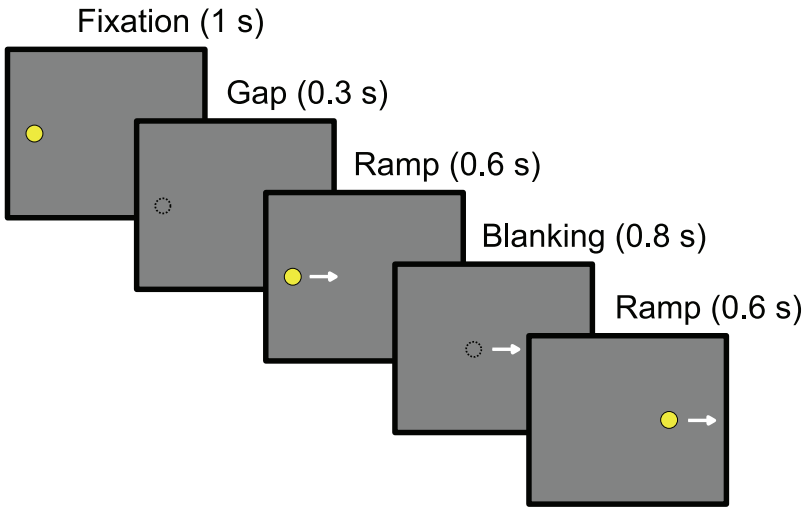

Figure V.2: Test trials used in the experiments. A yellow target was projected on a black screen. After one second, a 300 ms gap period preceded target motion onset. Then, target moved at a constant velocity for 2 seconds. Target was visible the first 600 ms, and then was blanked for 800 ms (test trials). Target was visible again the last 600 ms of the trial. Target velocity (10, 15 or 20 deg/s) and direction (from left to right, as illustrated, or from right to left) were randomly chosen in the beginning of a block, and were kept constant into the block.

Apparatus and data analysis

Subjects were seated in a dimly lit room with their head restrained by a chin-rest and a forehead-rest. They faced a 1.5 m distant tangent screen that spanned 40 degrees of their visual field. Stimuli were projected onto the screen with a cine8 Barco projector (Refresh rate: 100 Hz; Barco NV, Belgium). Eye movements were

recorded at 1000 Hz using an Eyelink 1000 (SR Research Ltd., Ottawa, Ontario, Canada). A calibration was performed at the beginning of each block.

Eye movements were low-pass filtered at 45 Hz. Velocity and acceleration signals were obtained from position signals using a central difference algorithm on a ±10 ms interval. Saccade onset and offset were detected using a 500 deg/s² acceleration threshold. Those saccades were removed from the smooth eye velocity trace (see details in de Brouwer et al., 2002). In such a block design, three trials are required before predictive behavior can be exhibited (Bennett et al., 2010). Therefore, the test trials were divided into early (first three test trials, also identified as P1) and late trials (remaining test trials). The late trials were further divided into three periods P2 (first five of them), P3 (next five ones) and P4 (remaining trials: between 5 and 10 trials).

In test trials, we measured the residual pursuit gain as the mean smooth pursuit velocity averaged over a 50 ms period centered at 500 ms after target disappearance, divided by target velocity. The same measure was extracted in control trials as a proxy of the visually-guided smooth pursuit gain. All patients and subjects had a visually-guided pursuit gain higher than 0.85, except three people (one FTLD patient, one AD patient and one CTRL subject) that had a pursuit gain lower than 0.6. These subjects were excluded from further analyses.

In test trials, the predictive smooth pursuit reacceleration was measured as the slope of the linear fit for the smooth velocity trace between 100 ms before target reappearance and 50 ms after this reappearance, i.e. before any influence of the visual feedback.

A “heat map” of saccade endpoints during blanking was computed for each participant in order to analyze the saccadic behavior. The saccade endpoint was estimated as the position of the eye when eye acceleration decreased below a 500 deg/s² threshold. To build the heat map, each saccade endpoint was represented by a 3D-Gaussian curve. The height of each Gaussian for one participant was equal to 1/x, with x equal the total number of saccades elicited by this participant during the blanking periods. The y-coordinate of the center of the Gaussian curve was the horizontal position of the saccade endpoint, and the x-coordinate of the center of the Gaussian curve was the time of saccade offset. The heat map for one participant was obtained by summing up all Gaussians together. The heat map for one population was constructed as the inter-subject average of the individual heat-maps. Saccades were tagged as predictive if they ended at least 200 ms after target blanking whereas earlier saccades were tagged as visually-guided because they were likely triggered before target blanking (Orban de Xivry et al., 2009).

An analysis of the interaction between saccades and pursuit was also performed. To do so, both the saccadic eye displacement (SAD, sum of predictive saccade amplitudes) and smooth eye displacement (SED, integral of smooth eye velocity during the blanking) were obtained and normalized by the target displacement during the blanking. The relationship between SAD and SED was quantified by the slope of the linear fit between the two variables (using the function “robustfit” in Matlab).

For the statistical analyses, data were collapsed across directions because none of the studied parameters was influenced by the direction of target motion. ANOVA was performed on intra-subject mean of the different parameters with group as between-subject

factor and velocity as within-subject factors. Tukey's Post Hoc test was used to evaluate one-to-one differences. Statistical analyses were performed with Statistica (Statsoft, Tulsa, OK).

Results

Visually-guided and predictive smooth pursuit

In control trials (target continuously visible), the performance of the smooth pursuit response was comparable across groups (Fig. V.3A, dashed traces). This indicates that visually-guided pursuit was normal in FTLD and AD patients in early course of the disease when compared to age-matched control subjects (ANOVA main effect of group on smooth pursuit gain: $F(2,36)=0.81$, $p=0.57$). In test trials, when the target was blanked, subjects continued to track the target with the same eye velocity for another 100 ms before it decreased exponentially towards a plateau level. During the first three test trials of each block (early test trials), eye velocity continued to decay slowly until 100 ms after target reappearance, i.e. when visual feedback of target motion became available and elicited a visually-guided reacceleration (Fig. V.3A, solid traces). In these trials, subjects from all groups exhibited a similar behavior.

In the late test trials (all test trials except the first three, i.e. periods P2 to P4), the decay in eye velocity was similar to the one observed during the early trials for all groups. However, 200 ms

before target reappearance, subjects from the CTRL and AD groups increased their eye velocity and exhibited a positive predictive reacceleration (Fig. V.3B, blue and green traces, respectively). In contrast, FTLD patients failed to reaccelerate predictively (Fig. V.3B, red trace). Rather, eye reacceleration was prompted by the visual feedback of the target after its reappearance, similarly to what happened in the early trials (around 100 ms after target reappearance).

Oculomotor performance was quantified by the measure of pursuit gain 500 ms into the blanking period in order to assess the decay in eye velocity and by the eye acceleration at the end of the blanking period in order to assess the predictive reacceleration. The between-group differences were analyzed over the course of the block (periods P1 to P4, see Methods) and for the late trials only (P2 to P4 merged together).

As illustrated in Fig. V.3, pursuit gain 500 ms into the blanking period was very similar across groups (Fig. V.4A; ANOVA main effect of group: $F(2,144)=1.27$ $p=0.38$) and did not evolve over the course of the blocks (ANOVA main effect of period: $F(3,144)=0.29$ $p=0.83$). Moreover, there was no between-group difference in residual velocity when it was measured from 400 ms to 600 ms. Comparison of the individual data from all subjects (Fig. V.4B) revealed that the residual pursuit gain was quite variable across subjects but had a similar range for all three groups (Fig. V.4B: CTRL: [0.31, 0.87]; FTLD: [0.33, 0.87]; AD: [0.26, 0.86]; ANOVA main effect of group: $F(2,36)=0.17$ $p=0.85$).

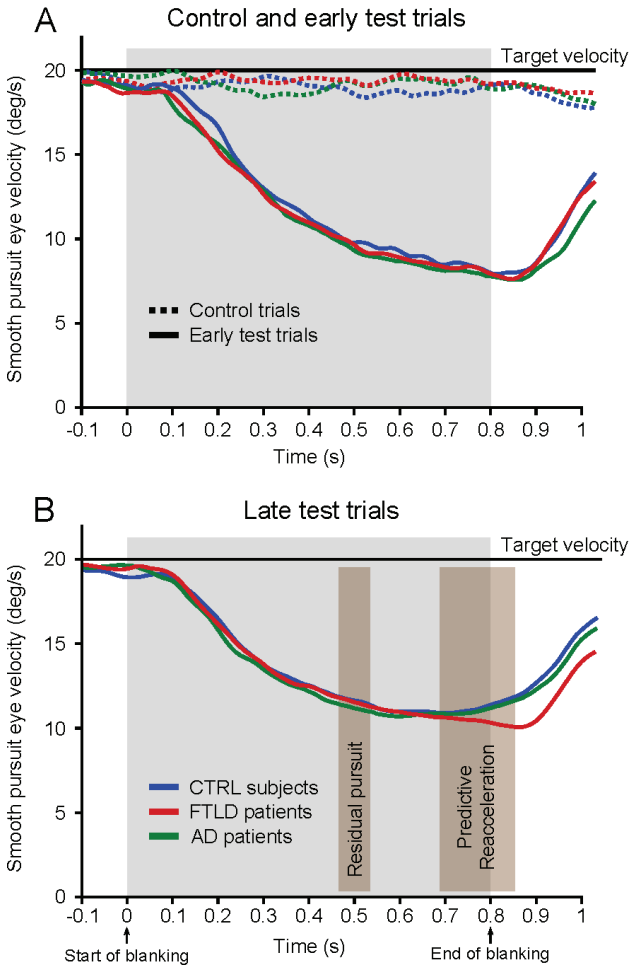

Figure V.3: Average smooth pursuit velocity of FTLD patients (red traces), of AD patients (green traces) and of CTRL subjects (blue traces). (A) Eye velocity profiles for the control (dashed traces) and early test trials (solid traces; first three trials of each block). (B) Eye velocity profile for the late test trials, i.e. all test trials except the first three. The grey area represents the blanking period for the test trials. The darker areas represent the periods where the residual pursuit gain and the predictive reacceleration were measured for the test trials. Target was moving rightward at 20 deg/s (black traces).

In contrast, the evolution of the predictive reacceleration from P1 to P4 differed across the populations (Fig. V.4C, ANOVA, groups by periods interaction: $F(6,144)=4.6$ $p=0.00027$). This interaction was observed for the three different target velocities separately (ANOVA, groups by periods interaction: 10 deg/s: $F(6,144) = 3.6$, $p = 0.0021$; 15 deg/s: $F(6,144) = 6.2$, $p < 0.00001$; 20 deg/s: $F(6,144) = 4.5$, $p = 0.0003$). Initially, as noted in Fig. V.3A, the acceleration around the time of target reappearance was negative (no evidence of predictive reacceleration for P1) and similar across groups (ANOVA $F(2,36) = 0.97$, $p = 0.39$). However, this acceleration became positive from P1 to P2 for the CTRL and AD groups (P1 vs. P2 Tukey Post Hoc: CTRL: $p=0.000018$ AD: $p=0.000023$) but not for the FTLD group ($p=0.99$).

For the controls and AD patients, this predictive reacceleration did not improve further and was maintained until the end of the block. For the FTLD group, the acceleration around the time of target reappearance never became positive, even at the end of the blocks. Therefore, during late trials, predictive reacceleration was significantly higher in CTRL and AD groups than in the FTLD group (ANOVA, $t(26)=23.7$, $p<0.00001$ and $t(22)=10.8$, $p=0.003$). This effect is significant for each target velocity separately (10 deg/s: $p<0.00001$ and $p=0.005$; 15 deg/s: $p<0.00001$ and $p<0.00001$; 20 deg/s: $p<0.00001$ and $p=0.00003$).

Inter-individual variability of reacceleration during all late trials was very low within groups (Fig. V.4D). All subjects from the control group (N=15) exhibited a positive reacceleration around the time of target reappearance. Only one from the AD group (N=11) did not (patient AD2). Moreover, the excluded control subject and AD patient also showed a predictive reacceleration. In contrast, only two of the

FTLD patients (N=13) showed signs of predictive reacceleration (patients FTLD6 and FTLD2). The excluded FTLD patient did neither reaccelerate predictively. There was no difference in predictive reacceleration between the three FTLD subgroups. Yet, the size of each subgroup prevents any strong conclusion.

Given the very small overlap in predictive reacceleration across groups, the absence of predictive reacceleration could be considered as a potential biomarker for FTLD. This biomarker has a sensitivity of 85% (=11/13). Its specificity between CTRL and FTLD is 100% (=15/15) and between AD and FTLD is about 91% (10/11). Sensitivity and specificity measures are improved if the subjects that were excluded because of low visually-guided pursuit gain are included in the analysis. Sensitivity becomes 86% (12/14). Specificity between CTRL and FTLD remains at 100%. Specificity between AD and FTLD increases to 92% (11/12).

In contrast, the neuropsychological data did not separate FTLD patients from AD patients as accurately as the predictive reacceleration (Table V.2). As expected, AD patients were in general more amnesic but less impaired at language tests than FTLD patients. However, the variability across patients was quite high. In addition, the executive tests were comparable across the two groups of patients.

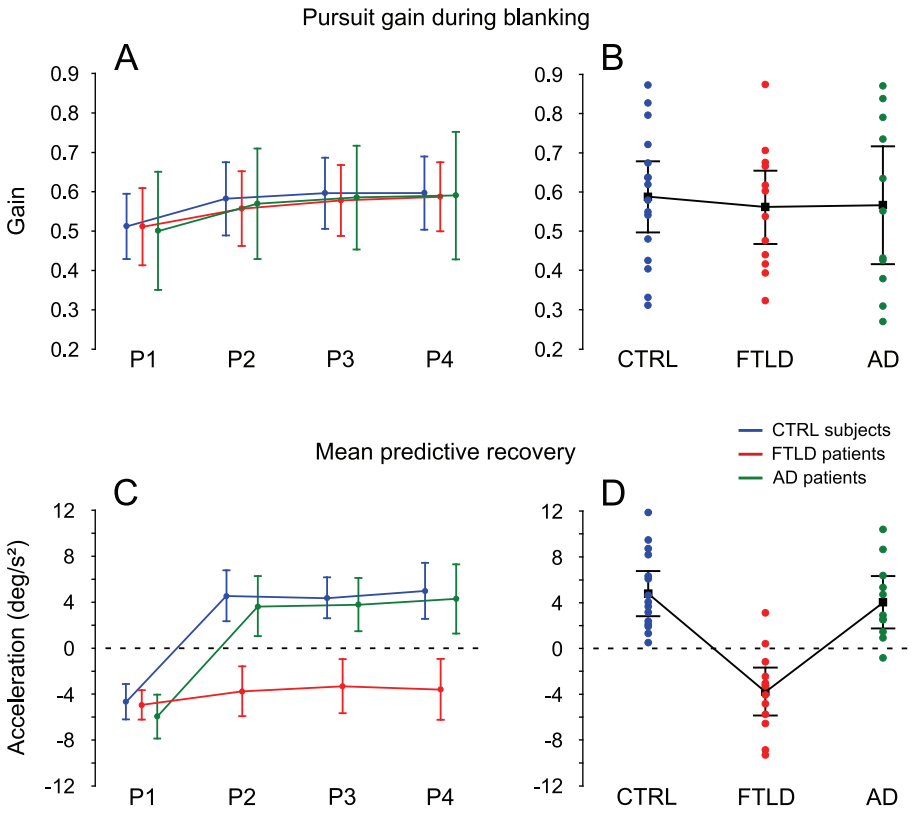

Figure V.4: Predictive behavior analysis (A) Evolution of the residual pursuit gain during blanking through trials for FTLD patients (red traces), CTRL subjects (blue traces) and AD patients (green traces) within the blocks (P1 to P4) (B) Residual pursuit gain during blanking for the "late trials" (P2 to P4). All patients and subjects are represented separately with a dot. (C) Evolution of the predictive reacceleration within the blocks for the three groups. (D) Predictive reacceleration for the three groups and individual subjects. Data from all conditions. Spreads represent the 95% confidence intervals.

Predictive smooth pursuit before target motion onset

The absence of predictive reacceleration in the FTLD group could be due either to the inability to elicit any predictive action or to the inability to know when the target will reappear. Indeed, in absence of timing information, no predictive reacceleration is observed (Orban de Xivry et al., 2008). In the present experiment, predictive mechanisms could also be observed during the 300 ms gap period that took place immediately before target motion onset (Barnes and Asselman, 1991). In this case, the extinction of the fixation cue elicited anticipatory smooth eye movements in the absence of visual motion signals. On average, smooth eye velocity reached 21% of target velocity by the time of target motion onset. This percentage did not differ across the groups (ANOVA, $F(2,36) = 0.15$, $p = 0.86$).

Predictive saccades

The absence of predictive reacceleration for FTLD patients could be explained by a difference in strategy. Indeed, rather than tracking the target during the blanking period, FTLD patients could focus on the position of the target at its reappearance. Following this assumption, saccade endpoints should differ across the groups, by being closer to the position of the target at its reappearance for the FTLD group. However, a difference in saccade endpoint was not observed (Fig. V.5). In this figure, eye positions at the end of the

saccades are represented in function of time with the red color corresponding to places where saccade endpoints were often observed and the blue colored areas representing places where very few saccades landed. Most predictive saccades landed ahead of the target (red colored areas are located above the white line). Importantly, this feature was present for all three groups and the distribution of predictive saccades did not differ across the groups (Fig. V.5). For instance, position error was similar across the three groups at the end of the first and second predictive saccades (ANOVA, first: $F(2,36) = 0.82$, $p = 0.49$; second: $F(2,36) = 1.03$, $p = 0.59$). Therefore, the strategy appeared comparable across groups.

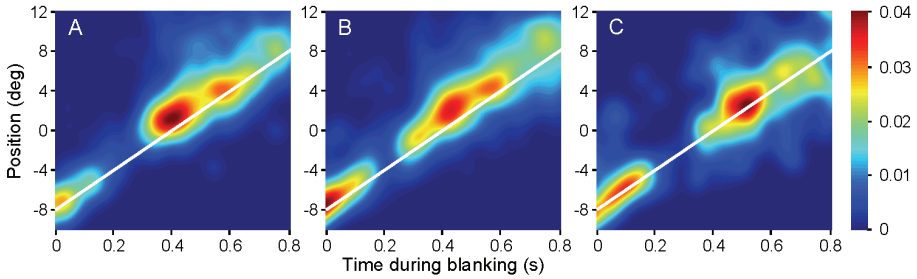

Figure V.5: “Heat map” of the position of the saccade endpoints versus time during the blanking of the target (0 ms corresponds to target blanking onset). (A) CTRL subjects, (B) FTLD patients, (C) AD patients. White lines represent target position. Color scales represent the probability that a saccade triggered during the blanking period lands on a point. Target velocity was 20 deg/s.

Interaction between saccades and pursuit

During blanking of the target, the amplitude of the saccades is adjusted to the level of the eye velocity decay on a trial-to-trial basis (e.g. Fig. V.6.A). A difference in modulation of the saccadic amplitude by the smooth pursuit performance across populations would highlight a deficit in internal representation of target motion as this modulation depends on where and when the target will reappear. This modulation is revealed by the strong correlation between the smooth eye displacement (SED; how much smooth pursuit moved the eyes) and the saccadic displacement (SAD; how much the saccades moved the eyes) during the blanking period (see Methods).

The SED is predominantly determined by the eye velocity decay and not by the predictive reacceleration, which happened too late to largely influence the smooth eye displacement. The correlation between SED and SAD is illustrated for a typical FTLD patient in Fig. V.6A. This plot shows that the inter-trial variability of the smooth eye displacement during the blanking was quite high (variability along the x-axis) but that the saccades largely compensated for this variability. Indeed, in trials during which the smooth eye displacement was small, saccadic displacement was large (Fig. V.6A point #1).

In contrast, when the smooth eye displacement was large, the saccadic displacement was reduced (Fig. V.6A point #2). In both cases, the synergy between saccades and pursuit allowed the eyes to be close to the target at its reappearance (target position corresponds to the dashed trace).

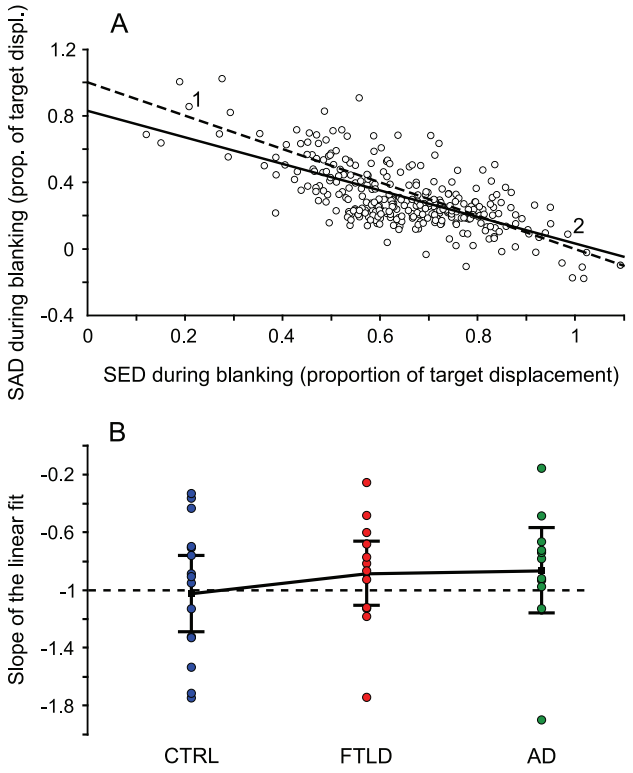

Figure V.6: Saccade-pursuit interactions (A) Saccadic eye displacement (SAD) during blanking versus smooth pursuit eye displacement (SED) during blanking, for a typical FTLD patient (patient #FTLD5). These displacements were normalized by the target displacement during blanking. Each dot represents one trial. All trials are displayed, merging all velocities and directions together. The continuous line represents the linear fit and has a slope of -0.89. The dashed line represents the optimal compensation, with slope equal to -1. (B) Mean slope of the linear fits, all patients or subjects averaged by group. Spreads represent the 95% confidence intervals.

To quantify the synergy between saccades and pursuit, the slope of the linear fit performed on the SED-SAD relationship (solid trace) was used. Perfect synergy would correspond to a slope of -1. In the experiment, the synergy between saccades and pursuit did not differ across groups (Fig. V.6B; ANOVA, $F(2,36) = 0.56$, $p = 0.57$) and did not differ from the ideal slope for each group separately (T-tests, CTRL: $p=0.84$; FTLD: $p=0.23$; AD: $p=0.4$).

Discussion

In the present study, the smooth pursuit response of mild FTLD patients during a visually-guided and a predictive tracking task was compared to the performance of control subjects and mild Alzheimer's disease patients. All groups had normal visually-guided pursuit responses. During the blanking, eye velocity dropped in all groups to a "plateau level". After some practice, eye velocity increased before target reappearance in control subjects and AD patients but failed to recover predictively in FTLD patients. All other measures of oculomotor performance during the blanking period were similar across the groups. These results suggest that subtle and specific oculomotor deficiencies are present in the early course of FTLD. This impairment in predictive reacceleration is a potential biomarker of early stage of FTLD, which can help the clinician in the early differential diagnosis between neurodegenerative disorders. This also highlights the role of the frontal lobes in prediction.

What FTLD tells us about the smooth pursuit system

Primate studies have suggested that the FEF could play a critical role in the maintenance of the internal representation of target motion during a blanking period (Barborica and Ferrera, 2003, 2004; Xiao et al., 2007), in the gain control mechanisms of visually-guided pursuit (Tanaka and Lisberger, 2001, 2002) and in the timing representation during smooth pursuit (Schoppik et al., 2008; Li and Lisberger, 2011).

The present results suggest that mild degeneration of the frontal lobes affects the timing function first. Indeed, while FTLD patients had an impaired predictive reacceleration, their dynamic internal representation of target motion was not impaired, as assessed either by the endpoint of predictive saccades or by the synergy between saccades and pursuit during the blanking periods. Neither was there an impairment of the gain control mechanism as assessed by the gain of visually-guided pursuit. Another hypothesis would be to have an impairment of the “working memory” for these FTLD patients. One way to assess this hypothesis would be to test a sequence of memory-guided saccades, as it has been done previously with patients suffering of schizophrenia.

However, the ability of eliciting anticipatory eye movements was still present in FTLD patients as they were able to elicit them before target motion onset (i.e., during the initial gap period). In this case, the disappearance of the fixation point could act as a “go signal” for all subjects, which could help them to anticipate target

motion onset. In contrast, the long blanking period with the absence of go cue prevented them to reaccelerate predictively. The duration of the blanking period (800 ms) is also close to the well-known inferior limit of 1 s for the “long time scales”. Results would then probably have been different with a gap duration of around a second (much larger than the 300 ms used in this study).

Interestingly enough, this impairment is not present in mild AD patients, which reflects the particular involvement of the frontal lobes in predictive reacceleration. Indeed, frontal lobes are deteriorated early in the degeneration process in FTLD patients but are relatively spared during the early stages of the Alzheimer’s disease (Nelson et al., 2009; Aries et al., 2010; Vemuri et al., 2011). To the best of our knowledge, the importance of the frontal lobes for the timing of predictive behavior has not been demonstrated previously, neither in human nor in animal studies.

The FEF and SEF might have a predominant role in eliciting predictive reacceleration at the appropriate time for the four following reasons. First, they are involved in timing representation during smooth pursuit eye movements (Schoppik et al., 2008). Second, neural learning emerges in the FEF during an oculomotor task that involves learning the timing of a change in target direction (Li and Lisberger, 2011). Third, the timing of anticipatory pursuit is reflected in SEF neurons (de Hemptinne et al., 2008). Finally, the observed deficit in predictive reacceleration in mild FTLD can be associated with the early impairment of both FEF and SEF in FTLD (Broe et al., 2003).

Alternatively, the absence of predictive reacceleration might also reflect a network disruption rather than damage to a specific brain area. Changes in connectivity among brain areas occur early in

neurodegenerative disorders (Seeley et al., 2009; Pievani et al., 2011). In FTLD, this connectivity change is especially marked in the frontal lobes (Zhou et al., 2010). Predictive smooth pursuit relies on the connectivity between frontal areas more heavily during target blanking than during visually-guided tracking (Ding et al., 2009). Therefore, this reliance on brain connectivity might explain why FTLD results in a subtle deficit, different from those seen in focal lesions (Morrow and Sharpe, 1995; Heide et al., 1996; Lekwuwa and Barnes, 1996). However, it is surprising that the interaction between the saccadic and pursuit systems was not strongly affected given that it probably also relies on the interaction between several areas (Krauzlis, 2004, 2005; Orban de Xivry et al., 2006; Orban de Xivry and Lefèvre, 2007).

The observed deficit might be linked to general time estimation impairment in frontal lobe patients. Indeed, the frontal lobes have been involved in several timing tasks (Lewis and Miall, 2003a; Buhusi and Meck, 2005; Koch et al., 2009). For instance, patients with frontal lesions are impaired in time estimation (Harrington et al., 1998; Mimura et al., 2000; Koch et al., 2002). However, this deficit is predominant for tasks in the range of seconds but not at the milliseconds time scale (Mangels et al., 1998; Jones et al., 2004). Likewise, a timing deficit has been reported in one FTLD patient with time interval in the range of seconds (Wiener and Coslett, 2008). Moreover, AD patients also exhibit some deficits in time estimation tasks (Caselli et al., 2009; Rueda and Schmitter-Edgecombe, 2009), even at the milliseconds time scale. The existence of different timing mechanisms for automatic and cognitively controlled tasks (Lewis and Miall, 2003b) might explain

why AD patients are impaired in cognitively controlled estimation tasks but not in automatically controlled tasks (our task).

What predictive smooth pursuit tells us about FTLD

FTLD patients are difficult to differentiate from AD patients in the early stages of the disease (Shaw et al., 2007; Hampel et al., 2010; Hu et al., 2011). The diagnosis criteria of FTLD should be supported by brain imaging (Piguet et al., 2011), which is the case for every FTLD and AD patients included in the present study. Indeed, classical executive tests used in clinic are not always able to distinguish the groups at an early stage. In the present study, even the executive tests used (Luria and TMT, see methods) do not show differences between the groups. Indeed, the aphasic subgroup of FTLD (6 patients) is not supposed to be impaired for this kind of test and not all behavioral FTD patients show deficits on formal executive tests at an early stage. In some cases, the executive impairment is purely behavioral, especially when the lesions are localized in the inferior and medial part of the frontal lobes (Gregory et al., 1999). Conversely, some mild AD patients may show deficits on tests such as Luria and TMT for different reasons, including incipient visuo-spatial deficits and forgetting the wording. In contrast, our task was very sensitive to subtle deficits present in early stage FTLD patients.

Based on predictive smooth pursuit measurements, we differentiated FTLD patients from AD patients and controls. All of the

15 controls and 10 out of 11 of the mild AD patients exhibited a predictive reacceleration before target reappearance while only 2 out of the 13 FTLD patients were able to do so. This dramatic impairment of mild FTLD patients on a very particular aspect of a smooth pursuit task when compared to healthy controls and mild AD patients highlights the potential of this oculomotor task in order to isolate a cheap and efficient biomarker for FTLD.

Finally, it is important to highlight that the deficit of predictive acceleration is present in a very early phase of the FTLD when the usual measures of smooth pursuit are still normal. This contrasts with earlier studies (Boxer et al., 2006; Garbutt et al., 2008) with later stage FTLD patients (disease duration of 60 months vs. 30 months in this study) who already had impaired visually-guided smooth pursuit and with patients with focal lesions in the frontal lobes (Morrow and Sharpe, 1995; Heide et al., 1996; Lekwuwa and Barnes, 1996). Longitudinal follow-up will need to evaluate whether the gain of the visually-guided smooth pursuit or any other characteristics of the oculomotor performance could be used to assess the stage of FTLD.

Chapter VI
Conclusion and perspectives

Discussion and major contributions

This thesis shows the importance of combining experimental and theoretical approaches to investigate the oculomotor system. In particular, this thesis focus on pursuit eye movements. Many experimental studies have shown that pursuit eye movements are driven by retinal and extra-retinal signals. Depending on the context, the pursuit system relies more or less on retinal signals. For instance, smooth pursuit is only driven by extra-retinal signals during the transient disappearance of the target. In a laboratory, such transient target blanking provides a simple way to cancel retinal inputs, and therefore to explore the predictive mechanisms that help the oculomotor system to track the invisible target.

A new pursuit model was designed to simulate the main experimental results in the smooth pursuit litterature, taking into account both sensory (retinal) and internal (extra-retinal) inputs. The brain has to handle noisy signals, from the sensors on the retina to

the neurons firing to encode oculomotor commands. However, most of the previous models used deterministic input signals to simulate eye movement responses. This is clearly not realistic. If you are playing tennis and facing Roger Federer's serve, it is evident that the time required to estimate the ball motion after he has hit the ball (its direction, velocity, the spin of the ball) is not equal to zero. In other words, the visual motion processing takes time to enhance the estimation of target motion. It is exactly the way our model works, with Kalman filtering applied to noisy input signals to continuously improve the current estimation of the sensory inputs based on the last evidences (i.e., the last measures coming from the retina). The internal target velocity signal is also estimated by a Kalman filter applied to past information about target velocity, and is finally combined with the estimation of the current eye velocity (i.e. coming from an efference copy) to give an estimation of the internal retinal slip.

The basic idea of the Kalman filtering in our model is that the pursuit system relies less on the signal (i.e. either sensory or internal) that has the larger uncertainty. For instance, the sensory signal will be favored if the internal signal is absent or inaccurate. To our knowledge, our smooth pursuit model is the first one to combine retinal and extra-retinal estimations by weighting them according to their uncertainty. This theoretical hypothesis implies that the brain has a continuous estimation of the reliability of these inputs. In our pursuit model, this estimation is also estimated by the Kalman filter. Previous models that combined retinal and extra-retinal inputs used a kind of "on-off" mechanism (Bennett and Barnes, 2003, 2006b). Moreover, we know that the weighting used in our model is optimal if the

uncertainty present in the system is correctly estimated by the brain (Ernst and Banks, 2002; Beck et al., 2012).

Last but not least, our model is the first to include a dynamic memory, constructed from past information through the Kalman filter. This model is therefore able to learn about the past target movement in order to improve the estimation of the future target motion. We have shown that this is crucial when anticipating a moving target already tracked before (i.e. the predictability increases with each presentation of the same target motion), or when following a sinusoidal moving target.

Simulations of the model reproduce realistic pursuit responses with very different target conditions. Comparison with experimental data was achieved for pursuit initiation and for the influence of the retinal slip on pursuit acceleration, and our model gives similar results.

The model can also reproduce experimental results obtained in the other studies of this thesis. The predictive recovery observed in normal control subjects depends on a high level mechanism. This predictive mechanism includes a time estimator that can predictively increase the gain of the system before target reappearance (Chapter V). Different simulations of the predictive reacceleration are shown on Fig. II.9. We can observe the inter-trial variability observed experimentally, even with control subjects. Typically, patients with frontotemporal lobar degeneration (i.e. FTLD patients) did not initiate any pursuit reacceleration before the visual feedback was available (i.e., around 100 ms after target reappearance). This was simulated by resetting the gain of the pursuit system to one once the sensory input was available again after target reappearance. In contrast, the model can simulate the predictive recovery observed for AD patients

and CTRL subjects by smoothly increasing the gain of the pursuit system before target reappearance (Fig. II.9).

The model also proposes a hypothesis to explain the advantage of tracking biological motion stimuli (Chapter III). The noise level initially perceived is smaller when looking at a moving biological motion stimulus (BM) than when following a scrambled control stimulus (SCR). In our model, we model this by changing the variance of the uncertainty present in the system. This is achieved for instance by reducing the standard deviation of θ_k (Eq. II.2) by a factor of 2 (i.e., the value of Q is changed from 1 to 0.25) when simulating a response elicited by a BM stimulus. It is worth noting that by doing so, we do not change the variance of the sensory noise present in the system (the local motion of the dots composing the control stimulus and the biological motion walker was identical). Instead, we change the brain perception of the uncertainty by the brain, which in our model will influence the Kalman filtering of the sensory retinal slip. Indeed, for BM simulations, Kalman filtering gives more confidence in new observations (i.e. measures of the retinal slip on the retina), leading to a faster updating of the new target velocity. Therefore, the pursuit acceleration will be larger when tracking BM instead of SCR. Interestingly, the difference in pursuit acceleration is not the largest at the beginning of pursuit initiation. Indeed, since the retinal slip is large, new noisy observations are taken into account because the brain considers them to be relevant. But when the retinal slip becomes smaller, the fact that the brain assumes the noise to be smaller when tracking BM stimulus implies that the brain gives more confidence to new noisy observations, and then updates faster the retinal slip, leading to a larger acceleration. In contrast, the noisy observations of SCR stimulus could be seen as “too noisy” by the

brain, and as a consequence, the brain has to wait a bit to get more observations (i.e., to be more confident in the input and produce the same acceleration).

Fig. VI.1 shows the experimental results already shown before (Fig. III.3A) and the theoretical results generated by our pursuit model. Both behavioral and simulated data seem to be comparable. As explained before, the BM response was simulated by reducing the value of Q since the pursuit response elicited by a SCR stimulus was similar to the one elicited by a single dot stimulus (Chapter III). It is worth noting that these simulations look like the ones from Fig. II.13, where parameters D and R from Eq. II.3 have been modified instead of parameter Q on Fig. VI.1.

There are probably other ways to explain or simulate the difference in pursuit velocity observed when tracking a BM stimulus. However, if the noise value level change and if this change is correctly perceived by the brain (same ratio of change in the Kalman parameters D and R from Eq. II.3 as in the noise parameters $Sens_{add}$ and $Sens_{mult}$ from Eq. II.1), the pursuit acceleration will be different from the beginning of the pursuit initiation (Fig. VI.2). Therefore, the difference between the two simulations is not really similar to the one coming from behavioral data in response to SCR or BM stimuli (Fig. VI.1). A difference in noise level is thus not probably responsible for the observed difference between BM and SCR stimuli, if this change in noise is well perceived by the brain.

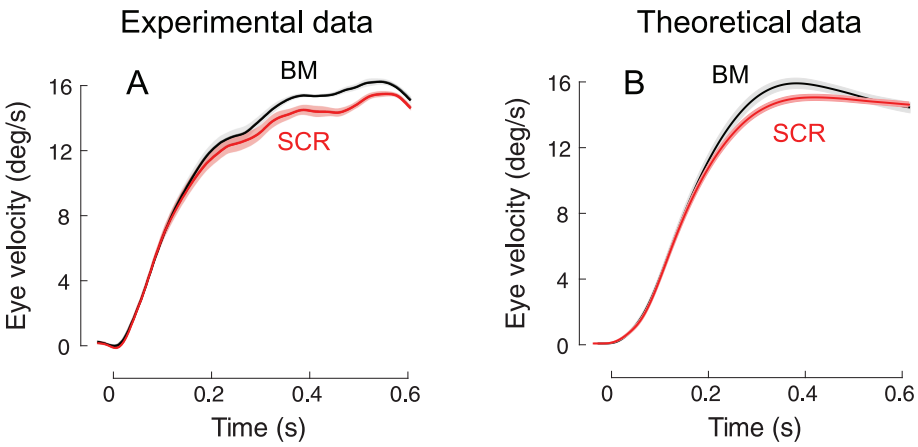

Figure VI.1: Behavioral and simulated data in response to SCR or BM stimuli. (A) Same panel than shown previously in Fig. III.A. (B) Simulation results of the pursuit model. Black thin line represents the average response (over 100 simulations) to a BM stimulus ($Q = 0.25$) whereas red thin trace shows the average response (also over 100 simulations) to a SCR stimulus ($Q = 1$). Translucent areas indicate confidence intervals.

This thesis also answers several important questions about the pursuit system. Biological motion stimulus is well-known to influence the perception, probably because it is processed differently by the visual system. Moreover, perception and smooth pursuit eye movements have been shown to share some mechanisms (Krauzlis and Stone, 1999; Masson and Stone, 2002; Rasche and Gegenfurtner, 2009). Here, we presented results that demonstrate the influence of biological motion stimulus on the motor action, i.e. the pursuit eye movement (Chapter III).

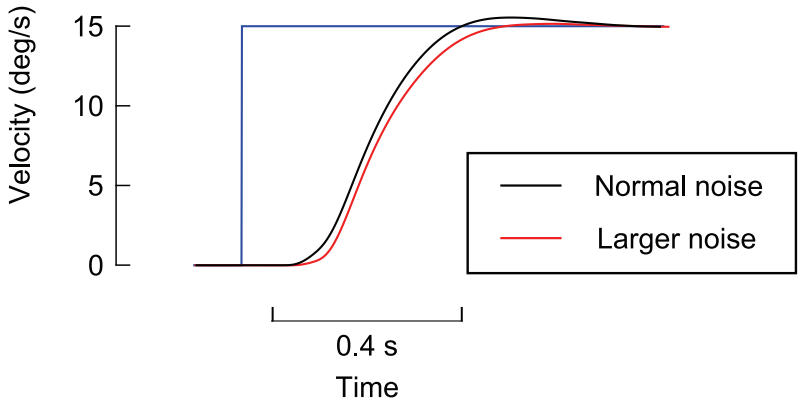

Figure VI.2: Simulation results of the pursuit model for different levels of noise. Black line represents the average response (over 100 simulations) to a stimulus with normal noise level whereas red trace shows the average response (also over 100 simulations) to a stimulus with higher noise value (parameters D, R, $Sens_{add}$ and $Sens_{mult}$ from Eq. II.1 and Eq. II.3 are 4 times larger than in the normal noise condition).

Indeed, pursuit velocity during pursuit initiation was larger in response to the BM stimulus than in response to a SCR stimulus. Moreover, we showed that this difference in favor of BM stimulus is the same if we compare it to an inverted walker or even to a single dot stimulus. In addition, we classified the SCR stimuli with respect to their biological relevance in a motion direction discrimination task and showed that the smooth pursuit response evoked by those stimuli was modulated by their proximity to the walker.

In a second study on biological motion (Chapter IV), we did not find any advantage to follow a BM stimulus during the transient blanking of the stimulus. Using a simple pursuit model, we proposed

two different theoretical hypotheses to explain this result and concluded that biological motion influence the visuomotor pathway, but not the memory pathway.

The last experimental study achieved in this thesis focuses on the frontal lobes and their role for predictive pursuit eye movements. Because we believed that the frontal areas of the brain are important for pursuit, we analyzed the oculomotor behavior of patients with frontotemporal lobar degeneration. These FTLD patients were in the first stages of the disease and had small atrophies in the frontal parts of the brain. We also recorded the eye movements of control subjects and patients in the early phase of Alzheimer's Disease (AD patients). The oculomotor behavior of FTLD patients was similar to the one of controls and AD patients, except for the predictive reacceleration observed before the target reappearance. This difference was so important that it could even lead to the definition of a new biomarker. The fact that FTLD patients were only impaired when the predicted timing of an external event was required to elicit an action suggests that the frontal lobes may have an important role in predictive movement timing. Even if FTLD patients seem to have normal internal representation of the target and predictive pursuit eye movements during the blanking period, their lack of predictive recovery could be due to a working memory impairment. This hypothesis could be investigated by studying some sequences of memory-guided saccades.

Further work on the model

Several extensions of the proposed pursuit model can be considered, as the generalization to oblique eye movements (i.e. in 2D) for instance or by the addition of a position input. Indeed, position error influences smooth pursuit eye movements (Blohm et al., 2005; Orban de Xivry and Lefèvre, 2007). However, this influence is not large, and can even be smaller during fixation (Morris and Lisberger, 1987). The idea suggested by Blohm et al. (2005) is that the omnipause neurons (OPN) could gate the smooth pursuit response during fixation. Missal and Keller (2002) also reported that the neuronal activity of the OPN is decreased during smooth pursuit, as it is the case during saccadic eye movements when the OPN are paused. This would explain why the superior colliculus, which encodes position error signals, influences pursuit movements only during pursuit and not during fixation (Krauzlis, 2004). Moreover, the inhibitory mechanism driven by the OPN is most likely required to avoid reflexive eye movements toward targets that are not really selected. Adding the influence of the OPN could improve our pursuit model, especially during fixation, since our current model sometimes shows some pursuit initiations or oscillations in response to the noisy signal of the fixed target. Another improvement for the pursuit model would be to simulate different pursuit responses for a change in target position/velocity in the same direction as the ongoing pursuit or in the opposite direction. Basically, pursuit latencies are larger and pursuit accelerations are smaller for a step in target velocity in the same direction than the ongoing pursuit. An additional development for the model would reside in having time-dependent parameters. If the external environment changes during the simulation, it can be

interesting to change some parameters as well. However, this question is not simple. Indeed, one could use different sets of parameters, but the best would be to let some parameters (coming from the Kalman filter) evolve naturally.

Another improvement of the model is the ability to generate saccadic eye movements, and to combine it with pursuit eye movements. A schematic representation of this model simulating the saccade-pursuit interactions is presented in Fig. VI.3. In this model, we have two Kalman filters in the visual processing step (i.e. one for the estimation of the position error and one for the estimation of the retinal slip). Typically, the noise associated with position inputs is smaller than the one associated with velocity inputs. Therefore, the uncertainty linked to the estimation of the position error (PE) is smaller than the one linked to retinal slip. Two Kalman predictions are also used in the model for the internal representation of the target, to predict the future target position and the future target velocity.

These signals are all taken into account by the trigger mechanism, which takes the decision to trigger a saccadic eye movement. The amplitude of this saccade is then computed by the saccadic system, which also takes these signals into account. The pursuit system is the same than the one presented in Chapter II (and could be slightly improved by adding position input). Both the saccadic and pursuit commands are added and sent to the common premotor system and finally to the eye plant.

The trigger mechanism can be viewed as an optimal decision strategy that can be described quantitatively as a rise to threshold process. The benefit to trigger a saccade (i.e. better vision after the saccade) is weighted by the inconvenience (i.e. the potential

inaccuracy of the saccade and the loss of clear vision during the saccade).

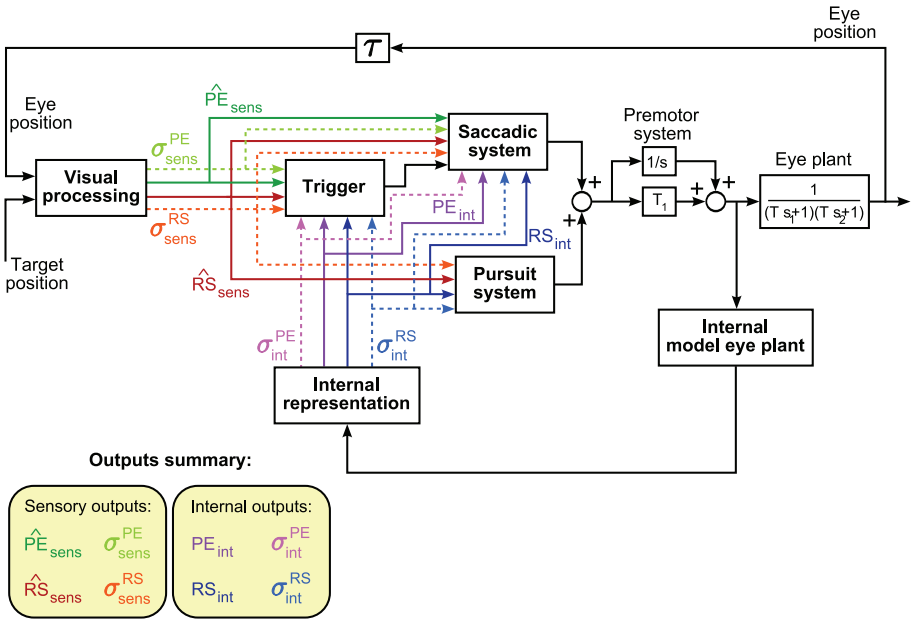

Figure VI.3: Schematic diagram of the saccade-pursuit interactions. The visual processing step computes the position and velocity inputs (i.e. with the two sensory Kalman filters) to give the estimations of RS and PE and their variance. The internal representation box outputs the internal predictions of RS and PE and their uncertainty. Both RS and PE coming from the visual processing and the internal representation are used by the trigger mechanism, which takes the decision to trigger a saccade and then by the saccadic system to compute the desired amplitude for the saccade. The addition of the saccadic and pursuit command is transmitted to the premotor system and finally to the eye plant. A summary of the different outputs with the color code is shown in the inset.

This non-deterministic approach (for both the inputs and the trigger mechanism) accounts for the variability of catch-up saccade latency or accuracy. For instance, a catch-up saccade with a larger latency is more accurate (because of the better estimation of the retinal slip). Moreover, the continuous update of the desired eye position during the planning or execution of saccades (due to the continuous update of the estimations of RS and PE which are generated by the sensory Kalman filters) can lead to the online adjustment of saccade trajectories. This online adjustment can be executed if a threshold of the potential saccadic error at its endpoint (e.g. 15% of saccade amplitude) is reached, and produces a double-peaked saccade, similar to those observed experimentally (e.g. Schreiber et al., 2006).

Further work on the patient study

The patient study described in Chapter V highlights the importance of the frontal lobes on the predictive timing mechanism. In contrast, anticipatory eye movements generated by the disappearance of the fixation point were still present before target motion onset in FTLD patients and visually-guided pursuit was normal compared to control subjects. This means that mild degeneration of the frontal lobes does not impair heavily visually-guided eye movements or the dynamic internal representation of target motion, but first affects the timing function needed to initiate a predictive reacceleration.

In our study, the recorded FTLD patients were all in the early stages of the neurodegenerative disease. Therefore, one could wonder how their oculomotor behavior will evolve with time. For that reason, we asked our FTLD patients to repeat the experiment every six months, in addition to their classical neurological examination. With the evolution of the disease, some of them did not want to see the neurologist or to repeat the experiment. However, 7 FTLD patients completed 2 more sessions, and 3 of them competed at least 5 more sessions. The results will illustrate the evolution of the oculomotor impairments of these patients. The evolution of their oculomotor behavior will be compared with the neurological degeneration of their frontal lobes. This longitudinal study will be discussed in a future paper (in preparation).

Abbreviations

AD	Alzheimer's Disease
BM	Biological Motion stimulus (i.e. a human walker)
CB	Cerebellum
CTRL	control (used for stimulus in Ch. III - Ch. IV or for patient in Ch. V)
DLPFC	Dorsolateral Prefrontal Cortex
DOT	Single dot stimulus (same motion than the hip dot of the BM)
FEF	Frontal Eye Field
fMRI	Functional Magnetic Resonance Imaging
FTD	Frontotemporal Dementia
FTLD	Frontotemporal lobar degeneration
INV	Inverted BM stimulus (i.e. upside down walker)
IPS	Intraparietal Sulcus
LIP	Lateral Intraparietal cortex
MMSE	Mini Mental State Examination
MN	Motor Neurons
MND	Motor Neuron Disease
MST	Medial Superior Temporal cortex
MT	Medial Temporal cortex

OKN	Optokinetic reflex
OPN	Omni-Pause Neurons
PA	Progressive non-fluent Aphasia
PE	Position Error
PPC	Posterior Parietal Cortex
RI	Resettable Integrator
RS	Retinal Slip
SAD	Saccadic Eye Displacement
SC	Superior Colliculus
SCR	Scrambled control stimulus (same local motion than the BM)
SD	Semantic Dementia
SED	Smooth (pursuit) Eye Displacement
SEF	Supplementary Eye Field
SMA	Supplementary Motor Area
STPa	Anterior Superior Temporal Polysensory
STS	Superior Temporal Sulcus
TMS	Transcranial Magnetic Stimulation
TV	Target Velocity
V1	Primary visual cortex
VOR	Vestibolo-Ocular Reflex
VPF	Ventral Paraflocculus (cerebellum)

References

Andersen RA, Bracewell RM, Barash S, Gnadt JW, Fogassi L. Eye position effects on visual, memory, and saccade-related activity in areas LIP and 7a of macaque. *J Neurosci* 10: 1176-96, 1990.

Angelaki DE, Shaikh AG, Green AM, Dickman JD. Neurons compute internal models of the physical laws of motion. *Nature* 430: 560-4, 2004.

Anstis SM. Letter: A chart demonstrating variations in acuity with retinal position. *Vision Res* 14: 589-92, 1974.

Aries MJH, Le Bastard N, Debruyne H, Van Buggenhout M, Nagels G, De Deyn PP, Engelborghs S. Relation between frontal lobe symptoms and dementia severity within and across diagnostic dementia categories. *Intern J Geriatr Psychiatry* 25: 1186-95, 2010.

Baddeley A, Emslie H, Nimmo-Smith I. *Doors and People test. Bury St Edmunds: Thames Valley Test Company.* 1994.

Badler JB, Heinen SJ. Anticipatory movement timing using prediction and external cues. *J Neurosci* 26: 4519-25, 2006.

Badler JB, Lefèvre P, Missal M. Causality attribution biases oculomotor responses. *J Neurosci* 30: 10517-25, 2010.

Bahill AT, Clark MR, Stark L. The main sequence, a tool for studying human eye movements. *Mathematical Biosciences* 24: 191-204, 1975.

Bahill AT, McDonald JD. Smooth pursuit eye movements in response to predictable target motions. *Vision Res* 23: 1573-83, 1983a.

Bahill AT, McDonald JD. Model emulates human smooth pursuit system producing zero-latency target tracking. *Biological cybernetics* 48: 213-22, 1983b.

Bak TH, Hodges JR. Motor neurone disease, dementia and aphasia: coincidence, co-occurrence or continuum? *J Neurol* 248: 260-70, 2001.

Baker CI, Keysers C, Jellema T, Wicker B, Perrett DI. Neuronal representation of disappearing and hidden objects in temporal cortex of the macaque. *Exp Brain Res* 140: 375-381, 2001.

Barborica A, Ferrera VP. Estimating invisible target speed from neuronal activity in monkey frontal eye field. *Nat Neurosci* 6: 66-74, 2003.

Barborica A, Ferrera VP. Modification of saccades evoked by stimulation of frontal eye field during invisible target tracking. *J Neurosci* 24: 3260-7, 2004.

Barnes GR, Asselman PT. The mechanism of prediction in human smooth pursuit eye movements. *J Physiol* 439: 439-61, 1991.

Barnes GR, Asselman PT. Pursuit of intermittently illuminated moving targets in the human. *J Physiol* 445: 617-37, 1992.

Barnes GR, Barnes DM, Chakraborti SR. Ocular pursuit responses to repeated, single-cycle sinusoids reveal behavior compatible with predictive pursuit. *J Neurophysiol* 84: 2340-55, 2000.

Barnes GR, Collins CJS. Evidence for a link between the extra-retinal component of random-onset pursuit and the anticipatory pursuit of predictable object motion. *J Neurophysiol* 100: 1135-46, 2008a.

Barnes GR, Collins CJS. The influence of briefly presented randomized target motion on the extraretinal component of ocular pursuit. *J Neurophysiol* 99: 831-42, 2008b.

Barnes GR, Donelan SF. The remembered pursuit task: evidence for segregation of timing and velocity storage in predictive oculomotor control. *Exp Brain Res* 129: 57-67, 1999.

Barnes GR, Donnelly SF, Eason RD. Predictive velocity estimation in the pursuit reflex response to pseudo-random and step displacement stimuli in man. *J Physiol* 389: 111-36, 1987.

Barnes GR, Goodbody S, Collins CJS. Volitional control of anticipatory ocular pursuit responses under stabilised image conditions in humans. *Exp Brain Res* 106: 301-17, 1995.

Barnes GR, Grealy MA, Collins CJS. Volitional control of anticipatory ocular smooth pursuit after viewing, but not pursuing, a moving target: evidence for a re-afferent velocity store. *Exp Brain Res* 116: 445-55, 1997.

Barnes GR, Ruddock CJ. Factors affecting the predictability of pseudo-random motion stimuli in the pursuit reflex of man. *J Physiol* 408: 137-65, 1989.

Barnes GR, Schmid AM. Sequence learning in human ocular smooth pursuit. *Exp Brain Res* 144: 322-35, 2002.

Barnes GR, Smith R. The effects of visual discrimination of image movement across the stationary retina. *Aviat Space Environ Med* 52: 466-72, 1981.

Barnes GR, Wells SG. Modelling prediction in ocular pursuit: the importance of short-term storage. In: *Current Oculomotor Research: Physiological and Psychological Aspects*, edited by Becker W, Deubel H, Mergner T. New-York: Plenum, 1999, p. 97-107.

Barnes GR. Visual-vestibular interaction in the control of head and eye movement: the role of visual feedback and predictive mechanisms. *Prog Neurobiol* 41: 435-72, 1993.

Barnes GR. Cognitive processes involved in smooth pursuit eye movements. *Brain Cogn* 68: 309–326, 2008.

Barraclough NE, Xiao D, Oram MW, Perrett DI. The sensitivity of primate STS neurons to walking sequences and to the degree of articulation in static images. *Prog Brain Res* 154: 135-48, 2006.

Battelli L, Cavanagh P, Thornton IM. Perception of biological motion in parietal patients. *Neuropsychologia* 41: 1808-1816, 2003.

Beck JM, Ma WJ, Pitkow X, Latham PE, Pouget A. Not Noisy, Just Wrong: The Role of Suboptimal Inference in Behavioral Variability. *Neuron* 74: 30-39, 2012.

Becker W, Fuchs AF. Prediction in the oculomotor system: smooth pursuit during transient disappearance of a visual target. *Exp Brain Res* 57: 562-75, 1985.

Becker W. Saccades. In: *Eye movements*, edited by Carpenter RHS. MacMillan Press, Houndmills, UK, 1991, p. 95-137.

Beintema JA, Lappe M. Perception of biological motion without local image motion. *Proc Natl Acad Sci U S A* 99: 5661-3, 2002.

Bennett SJ, Barnes GR. Human ocular pursuit during the transient disappearance of a visual target. *J Neurophysiol* 90: 2504-20, 2003.

Bennett SJ, Barnes GR. Predictive smooth ocular pursuit during the transient disappearance of a visual target. *J Neurophysiol* 92: 578-90, 2004.

Bennett SJ, Barnes GR. Combined smooth and saccadic ocular pursuit during the transient occlusion of a moving visual object. *Exp Brain Res* 168: 313-21, 2006a.

Bennett SJ, Barnes GR. Smooth ocular pursuit during the transient disappearance of an accelerating visual target: the role of reflexive and voluntary control. *Exp Brain Res* 175: 1-10, 2006b.

Bennett SJ, Orban de Xivry J-J, Barnes GR, Lefèvre P. Target acceleration can be extracted and represented within the predictive drive to ocular pursuit. *J Neurophysiol* 98: 1405, 2007.

Bennett SJ, Orban de Xivry J-J, Lefèvre P, Barnes GR. Oculomotor prediction of accelerative target motion during occlusion: long-term and short-term effects. *Exp Brain Res* 204: 493-504, 2010.

Bertenthal B, Pinto J. Global Processing of Biological Motions. *Psychol Sci* 5: 221-224, 1994.

Beutter BR, Stone LS. Human motion perception and smooth eye movements show similar directional biases for elongated apertures. *Vision Res* 38: 1273-86, 1998.

Beutter BR, Stone LS. Motion coherence affects human perception and pursuit similarly. *Vis Neurosci* 17: 139-53, 2000.

Billino J, Braun DI, Böhm K-D, Bremmer F, Gegenfurtner KR. Cortical networks for motion processing: effects of focal brain lesions on perception of different motion types. *Neuropsychologia* 47: 2133-44, 2009.

Billino J, Bremmer F, Gegenfurtner KR. Motion processing at low light levels: Differential effects on the perception of specific motion types. *J Vis* 8: 14.1-10, 2008a.

Billino J, Bremmer F, Gegenfurtner KR. Differential aging of motion processing mechanisms: evidence against general perceptual decline. *Vision Res* 48: 1254-61, 2008b.

Blake R, Shiffrar M. Perception of human motion. *Annu Rev Psychol* 58: 47-73, 2007.

Blakemore SJ, Wolpert DM, Frith C. Why can't you tickle yourself? *Neuroreport* 11: R11-6, 2000.

Blohm G, Crawford JD. Computations for geometrically accurate visually guided reaching in 3-D space. *J Vis* 7: 4.1-22, 2007.

Blohm G, Keith GP, Crawford JD. Decoding the cortical transformations for visually guided reaching in 3D space. *Cereb Cortex* 19: 1372-93, 2009.

Blohm G, Missal M, Lefèvre P. Direct evidence for a position input to the smooth pursuit system. *J Neurophysiol* 94: 712-21, 2005.

Boman DK, Hotson JR. Stimulus conditions that enhance anticipatory slow eye movements. *Vision Res* 28: 1157-65, 1988.

Boman DK, Hotson JR. Motion perception prominence alters anticipatory slow eye movements. *Exp Brain Res* 74: 555-62, 1989.

Boman DK, Hotson JR. Predictive smooth pursuit eye movements near abrupt changes in motion direction. *Vision Res* 32: 675-689, 1992.

Born RT, Bradley DC. Structure and function of visual area MT. *Annu Rev Neurosci* 28: 157-89, 2005.

Born RT, Pack CC, Ponce CR, Yi S. Temporal evolution of 2-dimensional direction signals used to guide eye movements. *J Neurophysiol* 95: 284-300, 2006.

Boussaoud D, Ungerleider LG, Desimone R. Pathways for motion analysis: cortical connections of the medial superior temporal and fundus of the superior temporal visual areas in the macaque. *J Comp Neurol* 296: 462-95, 1990.

Boxer AL, Garbutt S, Rankin KP, Hellmuth J, Neuhaus J, Miller BL, Lisberger SG. Medial versus lateral frontal lobe contributions to voluntary saccade control as revealed by the study of patients with frontal lobe degeneration. *J Neurosci* 26: 6354-63, 2006.

Boxer AL, Garbutt S, Seeley WW, Jafari A, Heuer HW, Mirsky J, Hellmuth J, Trojanowski JQ, Huang E, Dearmond S, Neuhaus J, Miller BL. Saccade abnormalities in autopsy-confirmed frontotemporal lobar degeneration and Alzheimer disease. *Arch Neurol* 69: 509-17, 2012.

Brass M, Bekkering H, Prinz W. Movement observation affects movement execution in a simple response task. *Acta Psychologica* 106: 3-22, 2001.

Bremmer F, Distler C, Hoffmann K-P. Eye position effects in monkey cortex. II. Pursuit- and fixation-related activity in posterior parietal areas LIP and 7A. *J Neurophysiol* 77: 962-77, 1997.

Bridgeman B, Hendry D, Stark L. Failure to detect displacement of the visual world during saccadic eye movements. *Vision Res* 15: 719-22, 1975.

Broe M, Hodges JR, Schofield E, Shepherd CE, Kril JJ, Halliday GM. Staging disease severity in pathologically confirmed cases of frontotemporal dementia. *Neurology* 60: 1005-11, 2003.

Buhusi CV, Meck WH. What makes us tick? Functional and neural mechanisms of interval timing. *Nat Rev Neurosci* 6: 755–765, 2005.

Buneo CA, Jarvis MR, Batista AP, Andersen RA. Direct visuomotor transformations for reaching. *Nature* 416: 632-6, 2002.

Burrell JR, Hornberger M, Carpenter RHS, Kiernan MC, Hodges JR. Saccadic abnormalities in frontotemporal dementia. *Neurology*, 78: 1816-1823, 2012.

Carl JR, Gellman RS. Human smooth pursuit: stimulus-dependent responses. *J Neurophysiol* 57: 1446-63, 1987.

Carpenter RHS, Williams ML. Neural computation of log likelihood in control of saccadic eye movements. *Nature* 377: 59-62, 1995.

Caselli L, Iaboli L, Nichelli P. Time estimation in mild Alzheimer's disease patients. *Behav Brain Funct* 5: 32, 2009.

Casile A, Giese MA. Critical features for the recognition of biological motion. *J Vis* 5: 6, 2005.

Cavanagh P, Labianca AT, Thornton IM. Attention-based visual routines: sprites. *Cognition* 80: 47-60, 2001.

Cerminara NL, Apps R, and Marple-Horvat DE. An internal model of a moving visual target in the lateral cerebellum. *J Physiol* 587.2: 429– 442, 2009.

Chang DHF, Troje NF. Acceleration carries the local inversion effect in biological motion perception. *J Vis* 9: 19.1-17, 2009.

Chen-Plotkin AS, Martinez-Lage M, Sleiman PMA, Hu WT, Greene R, et al. Genetic and clinical features of progranulin-associated frontotemporal lobar degeneration. *Arch Neurol* 68: 488-97, 2011.

Churchland MM, Chou I-H, Lisberger SG. Evidence for object permanence in the smooth-pursuit eye movements of monkeys. *J Neurophysiol* 90: 2205-18, 2003.

Churchland MM, Lisberger SG. Experimental and computational analysis of monkey smooth pursuit eye movements. *J Neurophysiol* 86: 741-59, 2001a.

Churchland MM, Lisberger SG. Shifts in the population response in the middle temporal visual area parallel perceptual and motor illusions produced by apparent motion. *J Neurosci* 21: 9387-402, 2001b.

Coppe S, Orban de Xivry J-J, Missal M, Lefèvre P. Biological motion influences the visuomotor transformation for smooth pursuit eye movements. *Vision Res* 50: 2721-2728, 2010.

Coppe S, Orban de Xivry J-J, Yüksel D, Ivanoiu A, Lefèvre P. Dramatic impairment of prediction due to frontal lobe degeneration. *J Neurophysiol* (in press), 2012.

Craighero L, Bello A, Fadiga L, Rizzolatti G. Hand action preparation influences the responses to hand pictures. *Neuropsychologia* 40: 492-502, 2002.

Cutting JE. A program to generate synthetic walkers as dynamic point-light displays. *Behav Res Meth* 10: 91-94, 1978.

de Brouwer S, Missal M, Barnes GR, Lefèvre P. Quantitative analysis of catch-up saccades during sustained pursuit. *J Neurophysiol* 87: 1772-80, 2002.

de Brouwer S, Missal M, Lefèvre P. Role of retinal slip in the prediction of target motion during smooth and saccadic pursuit. *J Neurophysiol* 86: 550-8, 2001.

de Hemptinne C, Barnes GR, Missal M. Influence of previous target motion on anticipatory pursuit deceleration. *Exp Brain Res* 207: 173-84, 2010.

de Hemptinne C, Lefèvre P, Missal M. Influence of cognitive expectation on the initiation of anticipatory and visual pursuit eye movements in the rhesus monkey. *J Neurophysiol* 95: 3770-82, 2006.

de Hemptinne C, Lefèvre P, Missal M. Neuronal bases of directional expectation and anticipatory pursuit. *J Neurosci* 28: 4298-310, 2008.

de Hemptinne C, Nozaradan S, Duvivier Q, Lefèvre P, Missal M. How do primates anticipate uncertain future events? *J Neurosci* 27: 4334-41, 2007.

de Partz M, Bilocq V, De Wilde V, Seron X, Pillon A. *LEXIS: Tests pour l'évaluation des troubles lexicaux chez la personne aphasique*. Marseille, Solal, 2001.

Dallos P, Jones R. Learning behavior of the eye fixation control system. *IEEE Trans Automat Contr* 8: 218-227, 1963.

Decety J, Grezes J. Neural mechanisms subserving the perception of human actions. *Trends Cogn Sci* 3: 172-178, 1999.

Demer JL, Honrubia V, Baloh RW. Dynamic visual acuity: a test for oscillopsia and vestibulo-ocular reflex function. *Am J Otol* 15: 340-7, 1994.

Deno DC, Crandall WF, Sherman K, Keller EL. Characterization of prediction in the primate visual smooth pursuit system. *Bio Systems* 34: 107-28, 1995.

Denève S, Duhamel J-R, Pouget A. Optimal sensorimotor integration in recurrent cortical networks: a neural implementation of Kalman filters. *J Neurosci* 27: 5744-56, 2007.

Ding J, Powell DK, Jiang Y. Dissociable frontal controls during visible and memory-guided eye-tracking of moving targets. *Hum Brain Mapp* 30: 3541-52, 2009.

Drew AS, van Donkelaar P. The contribution of the human FEF and SEF to smooth pursuit initiation. *Cereb Cortex* 17: 2618-24, 2007.

Dursteler MR, Wurtz RH. Pursuit and optokinetic deficits following chemical lesions of cortical areas MT and MST. *J Neurophysiol* 60: 940-65, 1988.

Eggert T, Guan Y, Bayer O, Büttner U. Saccades to moving targets. *Ann N Y Acad Sci* 1039: 149-59, 2005.

Ernst MO, Banks MS. Humans integrate visual and haptic information in a statistically optimal fashion. *Nature* 415: 429-33, 2002.

Ferrera VP, Barborica A. Internally Generated Error Signals in Monkey Frontal Eye Field during an Inferred Motion Task. *J Neurosci* 30: 11612-11623, 2010.

Ferrera VP, Lisberger SG. Attention and target selection for smooth pursuit eye movements. *J Neurosci* 15: 7472-84, 1995.

Fetsch CR, Pouget A, DeAngelis GC, Angelaki DE. Neural correlates of reliability-based cue weighting during multisensory integration. *Nat Neurosci* 15: 146-54, 2012.

Filion CM, Washburn DA, Gulledge JP. Can monkeys (Macaca mulatta) represent invisible displacement? *Journal of Comparative Psychology* 110: 386-395, 1996.

Findlay JM. Active vision: visual activity in everyday life. *Curr Biol* 8: R640-2, 1998.

Fischer B, Boch R. Saccadic eye movements after extremely short reaction times in the monkey. *Brain Res* 260: 21-6, 1983.

Fischer B, Ramsperger E. Human express saccades: extremely short reaction times of goal directed eye movements. *Exp Brain Res* 57: 191-5, 1984.

Flanagan JR, Wing AM. The role of internal models in motion planning and control: evidence from grip force adjustments during movements of hand-held loads. *J Neurosci* 17: 1519-28, 1997.

Folstein MF, Folstein SE, McHugh PR. "Mini-mental state". A practical method for grading the cognitive state of patients for the clinician. *J Psychiatr Res* 12: 189-98, 1975.

Fukushima K, Yamanobe T, Shinmei Y, Fukushima J. Predictive responses of periarcuate pursuit neurons to visual target motion. *Exp Brain Res* 145: 104-20, 2002.

Gagnon D, Paus T, Grosbras M-H, Pike GB, O'Driscoll GA. Transcranial magnetic stimulation of frontal oculomotor regions during smooth pursuit. *J Neurosci* 26: 458-66, 2006.

Garbutt S, Matlin A, Hellmuth J, Schenk AK, Johnson JK, Rosen HJ, Dean D, Kramer JH, Neuhaus J, Miller BL, Lisberger SG, Boxer AL. Oculomotor function in frontotemporal lobar degeneration, related disorders and Alzheimer's disease. *Brain* 131: 1268-81, 2008.

Garcia JO, Grossman ED. Necessary but not sufficient: motion perception is required for perceiving biological motion. *Vision Res* 48: 1144-9, 2008.

Gaymard B, Pierrot-Deseilligny C, Rivaud S. Impairment of sequences of memory-guided saccades after supplementary motor area lesions. *Ann Neurol* 28: 622-6, 1990.

Gaymard B, Ploner CJ, Rivaud S, Vermersch AI, Pierrot-Deseilligny C. Cortical control of saccades. *Exp Brain Res* 123: 159-63, 1998.

Gaymard B, Rivaud S, Pierrot-Deseilligny C. Role of the left and right supplementary motor areas in memory-guided saccade sequences. *Ann Neurol* 34: 404-6, 1993.

Gellman RS, Carl JR. Motion processing for saccadic eye movements in humans. *Exp Brain Res* 84: 660-7, 1991.

Georgopoulos A, Schwartz A, Kettner R. Neuronal population coding of movement direction. *Science* 233: 1416-1419, 1986.

Giese MA, Poggio T. Neural mechanisms for the recognition of biological movements. *Nat Rev Neurosci* 4: 179-92, 2003.

Gilmore GC, Wenk HE, Naylor LA, Stuve TA. Motion perception and aging. *Psychol Aging* 7: 654-60, 1992.

Gold JI, Shadlen MN. The Influence of Behavioral Context on the Representation of a Perceptual Decision in Developing Oculomotor Commands. *Physiology* 23: 632-651, 2003.

Goodale MA, Milner AD. Separate visual pathways for perception and action. *Trends Neurosci* 15: 20-5, 1992.

Gregory CA, Serra-Mestres J, Hodges JR. Early diagnosis of the frontal variant of frontotemporal dementia: how sensitive are standard neuroimaging and neuropsychologic tests? *Neuropsychiatry Neuropsychol Behav Neurol* 12: 128-35, 1999.

Grezes J, Fonlupt P, Bertenthal B, Delon-Martin C, Segebarth C, Decety J. Does perception of biological motion rely on specific brain regions? *NeuroImage* 13: 775-85, 2001.

Grober E, Buschke H. Genuine memory deficits in dementia. *Dev Neuropsychol* 3: 13-36, 1987.

Groh JM, Sparks DL. Saccades to somatosensory targets. III. eye-position-dependent somatosensory activity in primate superior colliculus. *J Neurophysiol* 75: 439-53, 1996.

Grossman ED, Battelli L, Pascual-Leone A. Repetitive TMS over posterior STS disrupts perception of biological motion. *Vision Res* 45: 2847-53, 2005.

Grossman ED, Blake R. Brain activity evoked by inverted and imagined biological motion. *Vision Res* 41: 1475-82, 2001.

Grossman ED, Blake R. Brain Areas Active during Visual Perception of Biological Motion. *Neuron* 35: 1167-75, 2002.

Grossman ED, Donnelly M, Price R, Pickens D, Morgan V, Neighbor G, Blake R. Brain areas involved in perception of biological motion. *J Cogn Neurosci* 12: 711-20, 2000.

Hafed ZM, Krauzlis RJ. Interactions Between Perception and Smooth Pursuit Eye Movements. In: *Dynamics of Visual Motion Processing: Neuronal, Behavioral, and Computational Approaches*, edited by Ilg UJ, Masson GS. Boston, MA: Springer US, 2010, p. 189-211.

Hamilton A, Wolpert DM, Frith U. Your own action influences how you perceive another person's action. *Curr Biol* 14: 493-8, 2004.

Hampel H, Frank R, Broich K, Teipel SJ, Katz RG, Hardy J, Herholz K, Bokde ALW, Jessen F, Hoessler YC, Sanhai WR, Zetterberg H, Woodcock J, Blennow K. Biomarkers for Alzheimer's disease: academic, industry and regulatory perspectives. *Nat Rev Drug Discov* 9: 560-74, 2010.

Harrington DL, Haaland KY, Knight RT. Cortical networks underlying mechanisms of time perception. *J Neurosci* 18: 1085-95, 1998.

Haykin S, editor. Kalman Filtering and Neural Networks. *New York, USA: John Wiley & Sons*, Inc., 2001.

Heide W, Binkofski F, Seitz RJ, Posse S, Nitschke M, Freund HJ, Kömpf D. Activation of frontoparietal cortices during memorized triple-step sequences of saccadic eye movements: an fMRI study. *Eur J Neurosci* 13: 1177-89, 2001.

Heide W, Kurzidim K, Kömpf D. Deficits of smooth pursuit eye movements after frontal and parietal lesions. *Brain* 119: 1951-69, 1996.

Heinen SJ, Badler JB, Ting W. Timing and velocity randomization similarly affect anticipatory pursuit. *J Vis* 5: 493-503, 2005.

Heinen SJ, Liu M. Single-neuron activity in the dorsomedial frontal cortex during smooth-pursuit eye movements to predictable target motion. *Vis Neurosci* 14: 853-65, 1997.

Heinen SJ, Watamaniuk SNJ. Spatial integration in human smooth pursuit. *Vision Res* 38: 3785-94, 1998.

Heinen SJ. Single neuron activity in the dorsomedial frontal cortex during smooth pursuit eye movements. *Exp Brain Res* 104: 357-61, 1995.

Hiris E. Detection of biological and nonbiological motion. *J Vis* 7: 4.1-16, 2007.

Hu WT, Trojanowski JQ, Shaw LM. Biomarkers in frontotemporal lobar degenerations-progress and challenges. *Prog Neurobiol* 95: 636-48, 2011.

Hunt AR, Halper F. Disorganizing biological motion. *J Vis* 8: 12.1-5, 2008.

Huys R, Cañal-Bruland R, Hagemann N, Beek PJ, Smeeton NJ, Mark Williams A. Global information pickup underpins anticipation of tennis shot direction. *J Mot Behav* 41: 158-71, 2009.

Huys R, Smeeton NJ, Hodges NJ, Beek PJ, Williams AM. On the dynamic information underlying visual anticipation skill. *Percept Psychophys* 70: 1217-34, 2008.

Ikeda H, Blake R, Watanabe K. Eccentric perception of biological motion is unscalably poor. *Vision Res* 45: 1935-43, 2005.

Ilg UJ, Churan J. Motion perception without explicit activity in areas MT and MST. *J Neurophysiol* 92: 1512-23, 2004.

Ilg UJ, Schumann S, Thier P. Posterior parietal cortex neurons encode target motion in world-centered coordinates. *Neuron* 43: 145-151, 2004.

Ilg UJ, Thier P. Visual tracking neurons in primate area MST are activated by smooth-pursuit eye movements of an “imaginary” target. *J Neurophysiol* 90: 1489-502, 2003.

Ilg UJ, Thier P. The neural basis of smooth pursuit eye movements in the rhesus monkey brain. *Brain Cogn* 68: 229-40, 2008.

Ilg UJ. Visual-tracking neurons in area MST are activated during anticipatory pursuit eye movements. *Neuroreport* 14: 2219-23, 2003.

Ilg UJ. The role of areas MT and MST in coding of visual motion underlying the execution of smooth pursuit. *Vision Res* 48: 2062-9, 2008.

Indovina I, Maffei V, Bosco G, Zago M, Macaluso E, Lacquaniti F. Representation of visual gravitational motion in the human vestibular cortex. *Science* 308: 416-9, 2005.

Izawa J, Shadmehr R. On-line processing of uncertain information in visuomotor control. *J Neurosci* 28: 11360-8, 2008.

Jack CR, Albert MS, Knopman DS, McKhann GM, Sperling RA, Carrillo MC, Thies B, Phelps CH. Introduction to the recommendations from the National Institute on Aging-Alzheimer’s Association workgroups on diagnostic guidelines for Alzheimer's disease. *Alzheimers Dement* 7: 257-62, 2011.

Jacobs A, Shiffrar M. Walking perception by walking observers. *J Exp Psychol Hum Percept Perform* 31: 157-69, 2005.

Jarrett CB, Barnes GR. Volitional selection of direction in the generation of anticipatory ocular smooth pursuit in humans. *Neurosci Lett* 312: 25-8, 2001.

Jarrett CB, Barnes GR. Volitional scaling of anticipatory ocular pursuit velocity using precues. *Brain Res Cogn Brain Res* 14: 383-8, 2002.

Jay MF, Sparks DL. Auditory receptive fields in primate superior colliculus shift with changes in eye position. *Nature* 309: 345-347, 1984.

Jellema T, Maassen G, Perrett DI. Single cell integration of animate form, motion and location in the superior temporal cortex of the macaque monkey. *Cereb Cortex* 14: 781-90, 2004.

Jellema T, Perrett DI. Cells in monkey STS responsive to articulated body motions and consequent static posture: a case of implied motion? *Neuropsychologia* 41: 1728-1737, 2003a.

Jellema T, Perrett DI. Perceptual history influences neural responses to face and body postures. *J Cogn Neurosci* 15: 961-71, 2003b.

Johansson G. Visual perception of biological motion and a model for its analysis. *Percept Psychophys* 14: 201-211, 1973.

Jones CRG, Rosenkranz K, Rothwell JC, Jahanshahi M. The right dorsolateral prefrontal cortex is essential in time reproduction: an investigation with repetitive transcranial magnetic stimulation. *Exp Brain Res* 158: 366-72, 2004.

Kalman RE, Bucy RS. New results in linear filtering and prediction theory. *J Basic Eng* 83: 95-107, 1961.

Kalman RE. A New Approach to Linear Filtering and Prediction Problems. *J Basic Eng* 82: 35-45, 1960.

Kao GW, Morrow MJ. The relationship of anticipatory smooth eye movement to smooth pursuit initiation. *Vision Res* 34: 3027-36, 1994.

Kase M, Noda H, Suzuki DA, and Miller DC. Target velocity signals of visual tracking in vermal Purkinje cells of the monkey. *Science* 205: 717– 720, 1979.

Kawano K, Shidara M, Watanabe Y, Yamane S. Neural activity in cortical area MST of alert monkey during ocular following responses. *J Neurophysiol* 71: 2305-24, 1994.

Keating EG. Frontal eye field lesions impair predictive and visually-guided pursuit eye movements. *Exp Brain Res* : 311-323, 1991.

Keller EL, Johnsen SD. Velocity prediction in corrective saccades during smooth-pursuit eye movements in monkey. *Exp Brain Res* 80: 525-31, 1990.

Keller EL, Missal M. Shared brainstem pathways for saccades and smooth-pursuit eye movements. *Ann N Y Acad Sci* 1004: 29-39, 2003.

Kettner RE, Mahamud S, Leung HC, Sitkoff N, Houk JC, Peterson BW, Barto AG. Prediction of complex two-dimensional trajectories by a cerebellar model of smooth pursuit eye movement. *J Neurophysiol* 77: 2115-30, 1997.

Khurana B, Kowler E. Shared attentional control of smooth eye movement and perception. *Vision Res* 27: 1603-18, 1987.

Kilner JM, Paulignan Y, Blakemore SJ. An interference effect of observed biological movement on action. *Curr Biol* 13: 522-525, 2003.

Knox PC. The effect of the gap paradigm on the latency of human smooth pursuit of eye movement. *Neuroreport* 7: 3027-30, 1996.

Knox PC. Stimulus predictability and the gap effect on pre-saccadic smooth pursuit. *Neuroreport* 9: 809-12, 1998.

Koch G, Oliveri M, Caltagirone C. Neural networks engaged in milliseconds and seconds time processing: evidence from transcranial magnetic stimulation and patients with cortical or subcortical dysfunction. *Philos Trans R Soc Lond B Biol Sci* 364: 1907-18, 2009.

Koch G, Oliveri M, Carlesimo GA, Caltagirone C. Selective deficit of time perception in a patient with right prefrontal cortex lesion. *Neurology* 59: 1658-9, 2002.

Komatsu H, Wurtz RH. Relation of cortical areas MT and MST to pursuit eye movements. III. Interaction with full-field visual stimulation. *J Neurophysiol* 60: 621-44, 1988.

Komatsu H, Wurtz RH. Modulation of pursuit eye movements by stimulation of cortical areas MT and MST. *J Neurophysiol* 62: 31-47, 1989.

Körding KP, Wolpert DM. Bayesian integration in sensorimotor learning. *Nature* 427:244–247, 2004.

Kourtzi Z, Kanwisher N. Activation in human MT/MST by static images with implied motion. *J Cogn Neurosci* 12: 48-55, 2000.

Kourtzi Z, Krekelberg B, van Wezel RJA. Linking form and motion in the primate brain. *Trends Cogn Sci* 12: 230-6, 2008.

Kowler E, Martins A, Pavel M. The effect of expectations on slow oculomotor control—IV. Anticipatory smooth eye movements depend on prior target motions. *Vision Res* 24: 197-210, 1984.

Kowler E, McKee SP. Sensitivity of smooth eye movement to small differences in target velocity. *Vision Res* 27: 993-1015, 1987.

Kowler E, Steinman RM. The effect of expectations on slow oculomotor control. II. Single target displacements. *Vision Res* 19: 633-46, 1979a.

Kowler E, Steinman RM. The effect of expectations on slow oculomotor control–I. Periodic target steps. *Vision Res* 19: 633–646, 1979b.

Kowler E, Steinman RM. The effect of expectations on slow oculomotor control–III. Guessing. *Vision Res* 21: 191–203, 1981.

Kowler E. Cognitive expectations, not habits, control anticipatory smooth oculomotor pursuit. *Vision Res* 9: 1049-1057, 1989.

Kowler E. Eye movements: the past 25 years. *Vision Res* 51: 1457-83, 2011.

Kramer KA, Stubberud SC. Analysis and implementation of a neural extended Kalman filter for target tracking. *Int J Neural Syst* 16: 1-13, 2006.

Krauzlis RJ, Lisberger SG. A Control Systems Model of Smooth Pursuit Eye Movements with Realistic Emergent Properties. *Neural Comput* 1: 116-122, 1989.

Krauzlis RJ, Lisberger SG. A model of visually-guided smooth pursuit eye movements based on behavioral observations. *J Comput Neurosci* 1: 265–283, 1994.

Krauzlis RJ, Miles FA. Decreases in the latency of smooth pursuit and saccadic eye movements produced by the “gap paradigm” in the monkey. *Vision Res* 36: 1973-85, 1996a.

Krauzlis RJ, Miles FA. Transitions between pursuit eye movements and fixation in the monkey: dependence on context. *J Neurophysiol* 76: 1622-38, 1996b.

Krauzlis RJ and Miles FA. Role of the oculomotor vermis in generating pursuit and saccades: effects of microstimulation. *J Neurophysiol* 80: 2046–2062, 1998.

Krauzlis RJ, Stone LS. Tracking with the mind’s eye. *Trends Neurosci* 22: 544-550, 1999.

Krauzlis RJ. Recasting the smooth pursuit eye movement system. *J Neurophysiol* 91: 591-603, 2004.

Krauzlis RJ. The control of voluntary eye movements: new perspectives. *Neuroscientist* 11: 124-37, 2005.

Kveraga K, Fendrich R, Hughes H. Ocular pursuit of predicted motion trajectories. *Exp Brain Res* 138: 393-397, 2001.

Körding KP, Wolpert DM. Bayesian decision theory in sensorimotor control. *Trends Cogn Sci* 10: 319-26, 2006.

Lange J, Georg K, Lappe M. Visual perception of biological motion by form: a template-matching analysis. *J Vis* 6: 836-49, 2006.

Law C, Gold JI. Neural correlates of perceptual learning in a sensory-motor, but not a sensory, cortical area. *Nat Neurosci* 11: 505-513, 2008.

Leigh RJ, Zee DS. *The neurology of eye movements*. Fourth Edi. New York: Oxford University Press, 2006.

Lekwuwa GU, Barnes GR. Cerebral control of eye movements. II. Timing of anticipatory eye movements, predictive pursuit and phase errors in focal cerebral lesions. *Brain* 119: 491-505, 1996.

Lencer R, Nagel M, Sprenger A, Zapf S, Erdmann C, Heide W, Binkofski F. Cortical mechanisms of smooth pursuit eye movements with target blanking. An fMRI study. *Eur J Neurosci* 19: 1430-6, 2004.

Lencer R, Trillenberg P. Neurophysiology and neuroanatomy of smooth pursuit in humans. *Brain Cogn* 68: 219-28, 2008.

Leung H, Suh M and Kettner R. Cerebellar flocculus and paraflocculus Purkinje cell activity during circular pursuit in monkeys. *J Neurophysiol* 83(1): 13– 30, 2000.

Lewis PA, Miall RC. Brain activation patterns during measurement of sub- and supra-second intervals. *Neuropsychologia* 41: 1583-1592, 2003a.

Lewis PA, Miall RC. Distinct systems for automatic and cognitively controlled time measurement: evidence from neuroimaging. *Curr Opin Neurobiol* 13: 250-255, 2003b.

Li JX, Lisberger SG. Learned timing of motor behavior in the smooth eye movement region of the frontal eye fields. *Neuron* 69: 159-69, 2011.

Lillo P, Hodges JR. Frontotemporal dementia and motor neurone disease: overlapping clinic-pathological disorders. *J Clin Neurosci* 16: 1131-5, 2009.

Lisberger SG, Evinger C, Johanson GW, Fuchs AF. Relationship Between Eye Acceleration and Retinal Image Velocity During Foveal Smooth Pursuit in Man and Monkey. *J Neurophysiol* 46: 229-249, 1981.

Lisberger SG, Morris EJ, Tychsen L. Visual motion processing and sensory-motor integration for smooth pursuit eye movements. *Annu Rev Neurosci* 10: 97-129, 1987.

Lisberger SG, Movshon JA. Visual motion analysis for pursuit eye movements in area MT of macaque monkeys. *J Neurosci* 19: 2224-46, 1999.

Lisberger SG, Westbrook LE. Properties of Visual Inputs that Initiate Movements in Monkeys. *J Neurosci* 5: 1662-1673, 1985.

Lisberger SG. Visual guidance of smooth-pursuit eye movements: sensation, action, and what happens in between. *Neuron* 66: 477-491, 2010.

Lisberger S. Internal models of eye movement in the floccular complex of the monkey cerebellum. *Neurosci* 162(3): 763– 776, 2009.

Lomen-Hoerth C, Anderson T, Miller BL. The overlap of amyotrophic lateral sclerosis and frontotemporal dementia. *Neurology* 59: 1077-9, 2002.

Lu ZL, Sperling G. Three-systems theory of human visual motion perception: review and update. *J Opt Soc Am A Opt Image Sci Vis* 18: 2331-70, 2001.

MacAvoy MG, Gottlieb JP, Bruce CJ. Smooth-pursuit eye movement representation in the primate frontal eye field. *Cereb Cortex* 1: 95-102, 1991.

Madelain L, Krauzlis RJ. Effects of learning on smooth pursuit during transient disappearance of a visual target. *J Neurophysiol* 90: 972-82, 2003.

Majaj NJ, Carandini M, Movshon JA. Motion integration by neurons in macaque MT is local, not global. *J Neurosci* 27: 366-70, 2007.

Mangels JA, Ivry RB, Shimizu N. Dissociable contributions of the prefrontal and neocerebellar cortex to time perception. *Brain Res* 7: 15-39, 1998.

Mark Williams A, Huys R, Cañal-Bruland R, Hagemann N. The dynamical information underpinning anticipation skill. *Hum Mov Sci* 28: 362-70, 2009.

Marr D, Ullman S. Directional selectivity and its use in early visual processing. *Proc R Soc Lond B Biol Sci* 211: 151-80, 1981.

Masson GS, Castet E. Parallel motion processing for the initiation of short-latency ocular following in humans. *J Neurosci* 22: 5149, 2002.

Masson GS, Montagnini A, Ilg UJ. When the Brain Meets the Eye: Tracking Object Motion. In: *Dynamics of Visual Motion Processing: Neuronal, Behavioral, and Computational Approaches*, edited by Ilg UJ, Masson GS. Boston, MA: Springer US, 2010, p. 161-188.

Masson GS, Rybarczyk Y, Castet E, Mestre DR. Temporal dynamics of motion integration for the initiation of tracking eye movements at ultra-short latencies. *Vis Neurosci* 17: 753-67, 2000.

Masson GS, Stone LS. From following edges to pursuing objects. *J Neurophysiol* 88: 2869-73, 2002.

Masson GS. From 1D to 2D via 3D: dynamics of surface motion segmentation for ocular tracking in primates. *J Physiol* 98: 35-52, 2004.

Mather G, Radford K and West S. Low-level visual processing of biological motion. *Proc R Soc Lond B Biol Sci* 249(1325): 149-155, 1992.

McConkie GW, Zola D. Is visual information integrated across successive fixations in reading? *Percept Psychophys* 25: 221-4, 1979.

McKhann GM, Drachman D, Folstein MF, Katzman R, Price D, Stadlan EM. Clinical diagnosis of Alzheimer's disease: report of the NINCDS-ADRDA Work Group under the auspices of Department of Health and Human Services Task Force on Alzheimer's Disease. *Neurology* 34: 939-44, 1984.

McLeod P, Dittrich WH, Driver J, Perrett DI, Zihl J. Preserved and impaired detection of structure from motion by a "motion-blind" patient. *Vis cogn* 3: 363-392, 1996.

Meyer CH, Lasker AG, Robinson DA. The upper limit of human smooth pursuit velocity. *Vision Res* 25: 561-563, 1985.

Meyniel C, Rivaud-Pechoux S, Damier P, Gaymard B. Saccade impairments in patients with fronto-temporal dementia. *J Neurol Neurosurg Psychiatry* 76: 1581-4, 2005.

Mimura M, Kinsbourne M, O'Connor M. Time estimation by patients with frontal lesions and by Korsakoff amnesics. *J Int Neuropsychol Soc* 6: 517-28, 2000.

Missal M, Heinen SJ. Facilitation of smooth pursuit initiation by electrical stimulation in the supplementary eye fields. *J Neurophysiol* 86: 2413-25, 2001.

Missal M, Heinen SJ. Supplementary eye fields stimulation facilitates anticipatory pursuit. *J Neurophysiol* 92: 1257-62, 2004.

Missal M, Keller EL. Common inhibitory mechanism for saccades and smooth-pursuit eye movements. *J Neurophysiol* 88: 1880-92, 2002.

Mitrani L, Dimitrov G. Pursuit eye movements of a disappearing moving target. *Vision Res* 18: 537-9, 1978.

Montagnini A, Mamassian P, Perrinet LU, Castet E, Masson GS. Bayesian modeling of dynamic motion integration. *J Physiol* 101: 64-77, 2007.

Montagnini A, Spering M, Masson GS. Predicting 2D target velocity cannot help 2D motion integration for smooth pursuit initiation. *J Neurophysiol* 96: 3545-50, 2006.

Morris EJ, Lisberger SG. Different responses to small visual errors during initiation and maintenance of smooth-pursuit eye movements in monkeys. *J Neurophysiol* 58: 1351-69, 1987.

Morris JC, Mohs RC, Rogers H, Fillenbaum G, Heyman A. Consortium to establish a registry for Alzheimer's disease (CERAD) clinical and neuropsychological assessment of Alzheimer's disease. *Psychopharmacol Bull* 24: 641-52, 1988.

Morrow MJ, Sharpe JA. Deficits of smooth-pursuit eye movement after unilateral frontal lobe lesions. *Ann Neurol* 37: 443-51, 1995.

Mrotek LA, Flanders M, Soechting JF. Oculomotor responses to gradual changes in target direction. *Exp Brain Res* 172: 175-92, 2006.

Mrotek LA, Soechting JF. Target interception: hand-eye coordination and strategies. *J Neurosci* 27: 7297-309, 2007.

Munzert J, Hohmann T, Hossner E-J. Discriminating throwing distances from point-light displays with masked ball flight. *Eur J Cogn Psychol* 22: 247-264, 2010.

Nagel M, Sprenger A, Nitschke M, Zapf S, Heide W, Binkofski F, Lencer R. Different extraretinal neuronal mechanisms of smooth pursuit eye movements in schizophrenia: An fMRI study. *Neuroimage* 34: 300-9, 2007.

Nagel M, Sprenger A, Zapf S, Erdmann C, Kömpf D, Heide W, Binkofski F, Lencer R. Parametric modulation of cortical activation during smooth pursuit with and without target blanking. an fMRI study. *Neuroimage* 29: 1319-25, 2006.

Neary D, Snowden JS, Gustafson L, Passant U, Stuss D, Black S, Freedman M, Kertesz A, Robert P, Albert MS, Boone K, Miller BL, Cummings JL, Benson DF. Frontotemporal lobar degeneration: a consensus on clinical diagnostic criteria. *Neurology* 51: 1546-54, 1998.

Nelson PT, Braak H, Markesbery WR. Neuropathology and cognitive impairment in Alzheimer disease: a complex but coherent relationship. *J Neuropathol Exp Neurol* 68: 1-14, 2009.

Neri P, Morrone MC, Burr DC. Seeing biological motion. *Nature* 395: 894-6, 1998.

Newsome WT, Paré EB. A selective impairment of motion perception following lesions of the middle temporal visual area (MT). *J Neurosci* 8: 2201-11, 1988.

Newsome WT, Wurtz RH, Dursteler MR, Mikami A. Deficits in visual motion processing following ibotenic acid lesions of the middle temporal visual area of the macaque monkey'. *J Neurosci* 5: 825-840, 1985.

Newsome WT, Wurtz RH, Komatsu H. Relation of cortical areas MT and MST to pursuit eye movements. II. Differentiation of retinal from extraretinal inputs. *J Neurophysiol* 60: 604-620, 1988.

Norman JF, Payton SM, Long JR, Hawkes LM. Aging and the perception of biological motion. *Psychol Aging* 19: 219-25, 2004.

Norman JF, Ross HE, Hawkes LM, Long JR. Aging and the perception of speed. *Perception* 32: 85-96, 2003.

Nyffeler T, Rivaud-Pechoux S, Wattiez N, Gaymard B. Involvement of the supplementary eye field in oculomotor predictive behavior. *J Cogn Neurosci* 20: 1583-94, 2008.

Ono S, Mustari MJ. Extraretinal Signals in MSTd Neurons Related to Volitional Smooth Pursuit. *J Neurophysiol* : 2819-2825, 2006.

Oram MW, Perrett DI. Responses of anterior superior temporal polysensory (STPa) neurons to “Biological Motion” stimuli. *J Cogn Neurosci* 6: 99-116, 1994.

Orban de Xivry J-J, Bennett SJ, Lefèvre P, Barnes GR. Evidence for synergy between saccades and smooth pursuit during transient target disappearance. *J Neurophysiol* 95: 418-27, 2006.

Orban de Xivry J-J, Coppe S, Lefèvre P, Missal M. Biological motion drives perception and action. *J Vis* 10: 6.1-11, 2010.

Orban de Xivry J-J, Lefèvre P. Saccades and pursuit: two outcomes of a single sensorimotor process. *J Physiol* 584: 11-23, 2007.

Orban de Xivry J-J, Missal M, Lefèvre P. A dynamic representation of target motion drives predictive smooth pursuit during target blanking. *J Vis* 8: 6.1-13, 2008.

Orban de Xivry J-J, Missal M, Lefèvre P. Smooth pursuit performance during target blanking does not influence the triggering of predictive saccades. *J Vis* 9: 7.1-16, 2009.

Osborne LC, Bialek W, Lisberger SG. Time course of information about motion direction in visual area MT of macaque monkeys. *J Neurosci* 24: 3210-22, 2004.

Osborne LC, Hohl SS, Bialek W, Lisberger SG. Time course of precision in smooth-pursuit eye movements of monkeys. *J Neurosci* 27: 2987-98, 2007.

Osborne LC, Lisberger SG, Bialek W. A sensory source for motor variation. *Nature* 437: 412-6, 2005.

Pack CC, Born RT. Temporal dynamics of a neural solution to the aperture problem in visual area MT of macaque brain. *Nature* 409: 1040-2, 2001.

Paré M, Munoz DP. Saccadic reaction time in the monkey: advanced preparation of oculomotor programs is primarily responsible for express saccade occurrence. *J Neurophysiol* 76: 3666-81, 1996.

Pavlova M, Lutzenberger W, Sokolov AN, Birbaumer N, Krägeloh-Mann I. Oscillatory MEG response to human locomotion is modulated by periventricular lesions. *NeuroImage* 35: 1256-63, 2007.

Pelphrey KA, Mitchell TV, McKeown MJ, Goldstein J, Allison T, McCarthy G. Brain activity evoked by the perception of human walking: controlling for meaningful coherent motion. *J Neurosci* 23: 6819-25, 2003.

Perrett DI, Oram MW, Ashbridge E. Evidence accumulation in cell populations responsive to faces: an account of generalisation of recognition without mental transformations. *Cognition* 67: 111-45, 1998.

Perrett DI, Smith PA, Potter DD, Mistlin AJ, Head AS, Milner AD, Jeeves MA. Visual cells in the temporal cortex sensitive to face view and gaze direction. *Proc R Soc Lond B Biol Sci* 223: 293-317, 1985.

Petit L, Orssaud C, Tzourio N, Crivello F, Berthoz A, Mazoyer B. Functional anatomy of a prelearned sequence of horizontal saccades in humans. *J Neurosci* 16: 3714-26, 1996.

Peuskens H, Vanrie J, Verfaillie K, Orban GA. Specificity of regions processing biological motion. *Eur J Neurosci* 21: 2864-75, 2005.

Pierrot-Deseilligny C, Rivaud S, Gaymard B, Agid Y. Cortical control of reflexive visually-guided saccades. *Brain* 114: 1473-1485, 1991.

Pievani M, de Haan W, Wu T, Seeley WW, Frisoni GB. Functional network disruption in the degenerative dementias. *Lancet Neurol* 10: 829-843, 2011.

Piguet O, Hornberger M, Mioshi E, Hodges JR. Behavioural-variant frontotemporal dementia: diagnosis, clinical staging, and management. *Lancet Neurol* 10: 162-72, 2011.

Pola J, Wyatt HJ. Offset dynamics of human smooth pursuit eye movements: effects of target presence and subject attention. *Vision Res* 37: 2579-95, 1997.

Poliakoff E, Collins CJS, Barnes GR. Target selection for predictive smooth pursuit eye movements. *Exp Brain Res* 155: 129-33, 2004.

Poliakoff E, Collins CJS, Barnes GR. Attention and selection for predictive smooth pursuit eye movements. *Brain Res Cogn Brain Res* 25: 688-700, 2005.

Pozzo T, Papaxanthis C, Petit JL, Schweighofer N, Stucchi N. Kinematic features of movement tunes perception and action coupling. *Behav Brain Res* 169: 75-82, 2006.

Price NSC, Ono S, Mustari MJ, Ibbotson MR. Comparing acceleration and speed tuning in macaque MT: physiology and modeling. *J Neurophysiol* 94: 3451-64, 2005.

Priebe NJ, Cassanello CR, Lisberger SG. The neural representation of speed in macaque area MT/V5. *J Neurosci* 23: 5650-61, 2003.

Priebe NJ, Lisberger SG. Estimating target speed from the population response in visual area MT. *J Neurosci* 24: 1907-16, 2004.

Puce A, Perrett DI. Electrophysiology and brain imaging of biological motion. *Philos Trans R Soc Lond B Biol Sci* 358: 435-45, 2003.

Rambold H, Churchland A, Selig Y, Jasmin L, Lisberger SG. Partial ablations of the flocculus and ventral paraflocculus in monkeys cause linked deficits in smooth pursuit eye movements and adaptive modification of the VOR. *J Neurophysiol* 87: 912–924, 2002.

Rao P. Bayesian computation in recurrent neural circuits. *Neural Comput* 16:1–38, 2004.

Rasche C, Gegenfurtner KR. Precision of speed discrimination and smooth pursuit eye movements. *Vision Res* 49: 514-523, 2009.

Rashbass C. The relationship between saccadic and smooth tracking eye movements. *J Physiol* 159: 326-38, 1961.

Robinson DA, Gordon JL, Gordon SE. A model of the smooth pursuit eye movement system. *Biological cybernetics* 55: 43-57, 1986.

Robinson DA. The mechanics of human smooth pursuit eye movement. *J Physiol* 180: 569-91, 1965.

Robinson DA. Adaptive gain control of vestibuloocular reflex by the cerebellum. *J Neurophysiol* 39: 954-69, 1976.

Robinson F and Fuchs A. The role of the cerebellum in voluntary eye movements. *Annu Rev Neurosci* 24: 981–1004, 2001.

Ronsse R, Miall RC, Swinnen SP. Multisensory integration in dynamical behaviors: maximum likelihood estimation across bimanual skill learning. *J Neurosci* 29: 8419-28, 2009.

Rouleau I, Salmon DP, Butters N, Kennedy C, McGuire K. Quantitative and qualitative analyses of clock drawings in Alzheimer's and Huntington's disease. *Brain Cogn* 18: 70-87, 1992.

Rudolph K, Pasternak T. Transient and permanent deficits in motion perception after lesions of cortical areas MT and MST in the macaque monkey. *Cereb Cortex* 9: 90-100, 1999.

Rueda AD, Schmitter-Edgecombe M. Time estimation abilities in mild cognitive impairment and Alzheimer's disease. *Neuropsychology* 23: 178-88, 2009.

Sakata H, Shibutani H, Kawano K. Functional properties of visual tracking neurons in posterior parietal association cortex of the monkey. *J Neurophysiol* 49: 1364-80, 1983.

Saunier G, Papaxanthis C, Vargas CD, Pozzo T. Inference of complex human motion requires internal models of action: behavioral evidence. *Exp Brain Res* 185: 399-409, 2008.

Saygin AP, Driver J, de Sa VR. In the footsteps of biological motion and multisensory perception: judgments of audiovisual temporal relations are enhanced for upright walkers. *Psychol Sci* 19: 469-75, 2008.

Saygin AP, Wilson SM, Hagler DJ, Bates E, Sereno MI. Point-light biological motion perception activates human premotor cortex. *J Neurosci* 24: 6181-8, 2004.

Saygin AP. Superior temporal and premotor brain areas necessary for biological motion perception. *Brain* 130: 2452-61, 2007.

Schall JD. Neural basis of deciding, choosing and acting. *Nat Rev Neurosci* 2: 33-42, 2001.

Schiller PH, Haushofer J, Kendall G. How do target predictability and precueing affect the production of express saccades in monkeys? *Eur J Neurosci* 19: 1963-8, 2004.

Schlack A, Hoffmann K-P, Bremmer F. Selectivity of macaque ventral intraparietal area (area VIP) for smooth pursuit eye movements. *J Physiol* 551: 551-61, 2003.

Schmid AM, Barnes GR, Rees G, Frith CD. An fMRI study of anticipation and learning of smooth pursuit eye movements in humans. *Neuroreport* 12: 1409-14, 2001.

Schoppik D, Nagel KI, Lisberger SG. Cortical mechanisms of smooth eye movements revealed by dynamic covariations of neural and behavioral responses. *Neuron* 58: 248-60, 2008.

Schreiber C, Missal M, Lefèvre P. Asynchrony between position and motion signals in the saccadic system. *J Neurophysiol* 95: 960-9, 2006.

Schütz AC, Souto D. Adaptation of catch-up saccades during the initiation of smooth pursuit eye movements. *Exp Brain Res* 209: 537-49, 2011.

Schütz-Bosbach S, Prinz W. Perceptual resonance: action-induced modulation of perception. *Trends Cogn Sci* 11: 349-55, 2007.

Scudder CA, Kaneko CS, Fuchs AF. The brainstem burst generator for saccadic eye movements: a modern synthesis. *Exp Brain Res* 142: 439-62, 2002.

Seeley WW, Crawford RRK, Zhou J, Miller BL, Greicius MD. Neurodegenerative diseases target large-scale human brain networks. *Neuron* 62: 42-52, 2009.

Sekuler R, Hutman LP, Owsley CJ. Human aging and spatial vision. *Science* 209: 1255-6, 1980.

Sharpe JA. Neurophysiology and neuroanatomy of smooth pursuit: lesion studies. *Brain Cogn* 68: 241-54, 2008.

Shaw LM, Korecka M, Clark CM, Lee VM-Y, Trojanowski JQ. Biomarkers of neurodegeneration for diagnosis and monitoring therapeutics. *Nat Rev Drug Discov* 6: 295-303, 2007.

Shi D, Friedman HR, Bruce CJ. Deficits in smooth-pursuit eye movements after muscimol inactivation within the primate's frontal eye field. *J Neurophysiol* 80: 458-64, 1998.

Shibata T, Tabata H, Schaal S, Kawato M. A model of smooth pursuit in primates based on learning the target dynamics. *Neural Netw* 18: 213-24, 2005.

Shim J, Carlton LG, Chow JW, Chae W-S. The use of anticipatory visual cues by highly skilled tennis players. *J Mot Behav* 37: 164-75, 2005.

Singer RN, Cauraugh JH, Chen D, Steinberg GM, Frehlich SG. Visual search, anticipation, and reactive comparisons between highly-skilled and beginning tennis players. *J Appl Sport Psychol* 8: 9-26, 1996.

Smit AC, Van Gisbergen JA. An analysis of curvature in fast and slow human saccades. *Exp Brain Res* 81: 335-45, 1990.

Snowden RJ, Braddick OJ. The temporal integration and resolution of velocity signals. *Vision Res* 31: 907-914, 1991.

Soechting JF, Rao HM, Juveli JZ. Incorporating prediction in models for two-dimensional smooth pursuit. *PloS one* 5(9): e12574, 2010.

Souto D, Kerzel D. Dynamics of attention during the initiation of smooth pursuit eye movements. *J Vis* 8: 3.1-16, 2008.

Sparks DL. The brainstem control of saccadic eye movements. *Nat Rev Neurosci* 3: 952-64, 2002.

Spering M, Gegenfurtner KR, Kerzel D. Distractor interference during smooth pursuit eye movements. *J Exp Psychol Hum Percept Perform* 32: 1136-54, 2006.

Spering M, Gegenfurtner KR. Contrast and Assimilation in Motion Perception and Smooth Pursuit Eye Movements. *J Neurophysiol,* 98: 1355-1363, 2007.

Stone LS, Beutter BR, Lorenceau J. Visual motion integration for perception and pursuit. *Perception* 29: 771-787, 2000.

Stone LS, Krauzlis RJ. Shared motion signals for human perceptual decisions and oculomotor actions. *J Vis* 3: 7.725-736, 2003.

Sumi S. Upside-down presentation of the Johansson moving light-spot pattern. *Perception* 13: 283-6, 1984.

Suzuki DA, Noda H and Kase M. Visual and pursuit eye movement related activity in posterior vermis of the monkey cerebellum. *J Neurophysiol* 46: 1120–1139, 1981.

Suzuki DA and Keller EL. The role of the posterior vermis of monkey cerebellum in smooth-pursuit eye movement control. I. Eye and head movement-related activity. *J Neurophysiol* 59: 1–18, 1988a.

Suzuki DA and Keller EL. The role of the posterior vermis of monkey cerebellum in smooth-pursuit eye movement control. II. Target velocityrelated Purkinje cell activity. *J Neurophysiol* 59: 19–40, 1988b.

Tadin D, Silvanto J, Pascual-Leone A, Battelli L. Improved motion perception and impaired spatial suppression following disruption of cortical area MT/V5. *J Neurosci* 31: 1279-83, 2011.

Tanaka M, Lisberger SG. Regulation of the gain of visually guided smooth-pursuit eye movements by frontal cortex. *Nature* 409: 191-4, 2001.

Tanaka M, Lisberger SG. Role of arcuate frontal cortex of monkeys in smooth pursuit eye movements. I. Basic response properties to retinal image motion and position. *J Neurophysiol* 87: 2684-99, 2002.

Thier P, Erickson RG. Responses of Visual-Tracking Neurons from Cortical Area MST-I to Visual, Eye and Head Motion. *Eur J Neurosci* 4: 539-553, 1992.

Thier P, Ilg UJ. The neural basis of smooth-pursuit eye movements. *Curr Opin Neurobiol* 15: 645-52, 2005.

Thornton IM, Pinto J, Shiffrar M. The visual perception of human locomotion. *Cogn Neuropsychol* 15: 535-52, 1998.

Thornton IM, Rensink RA, Shiffrar M. Active versus passive processing of biological motion. *Perception* 31: 837-53, 2002.

Thornton IM, Vuong QC. Incidental processing of biological motion. *Curr Biol* 14: 1084-9, 2004.

Tian JR, Lynch JC. Slow and saccadic eye movements evoked by microstimulation in the supplementary eye field of the cebus monkey. *J Neurophysiol* 74: 2204-10, 1995.

Tian JR, Lynch JC. Functionally defined smooth and saccadic eye movement subregions in the frontal eye field of Cebus monkeys. *J Neurophysiol* 76: 2740-53, 1996a.

Tian JR, Lynch JC. Corticocortical input to the smooth and saccadic eye movement subregions of the frontal eye field in Cebus monkeys. *J Neurophysiol* 76: 2754-71, 1996b.

Todorov E, Jordan MI. Optimal feedback control as a theory of motor coordination. *Nat Neurosci* 5: 1226-35, 2002.

Treue S, Hol K, Rauber HJ. Seeing multiple directions of motion-physiology and psychophysics. *Nat Neurosci* 3: 270-6, 2000.

Troje NF, Westhoff C. The inversion effect in biological motion perception: evidence for a “life detector”? *Curr Biol* 16: 821-4, 2006.

Troje NF. Biological motion perception. In: *The senses: A comprehensive reference*, edited by Basbaum IA, Kaneko A, Shepherd G, Westheimer G, Albright T, Masland R, Dallos P, Oertel D, Firestein S, Beauchamp G, Bushnell M, Kaas J, Gardner E. Oxford: Elsevier, 2008, p. 231-238.

Tychsen L, Lisberger SG. Visual motion processing for the initiation of smooth-pursuit eye movements in humans. *J Neurophysiol* 56: 953-68, 1986.

Van der Linden M, Coyette F, Poitrenaud J, Kalafat M, Calicis F, Wyns C, Adam S. L’épreuve de rappel libre / rappel indicé à 16 items (RL/RI-16). In: *L’évaluation des troubles de la mémoire: présentation de quatre tests de mémoire épisodique (avec leur étalonnage)*. Marseille, Solal, 2004, p. 25–47.

Van Gisbergen JA, van Opstal AJ, Roebroek J. Stimulus induced midflight modification of saccades. In: *Eye Movements: From Physiology to Cognition*, edited by O’Regan J, Levy-Schoen A. Elsevier, 1987, p. 27-36.

Vaina L, Lemay M, Bienfang DC, Choi AY, Nakayama K. Intact “biological motion” and “structure from motion” perception in a patient with impaired motion mechanisms: a case study. *Vis Neurosci* 5: 353-69, 1990.

Vandenberghe R, Van Laere K, Ivanoiu A, Salmon E, Bastin C, Triau E, Hasselbalch S, Law I, Andersen A, Korner A, Minthon L, Garraux G, Nelissen N, Bormans G, Buckley C, Owenius R, Thurfjell L, Farrar G, Brooks DJ. 18F-flutemetamol amyloid imaging in Alzheimer disease and mild cognitive impairment: a phase 2 trial. *Ann Neurol* 68: 319-29, 2010.

Vanrie J, Verfaillie K. Perception of biological motion: a stimulus set of human point-light actions. *Behav Res Meth* 36: 625-9, 2004.

Vaziri S, Diedrichsen J, Shadmehr R. Why does the brain predict sensory consequences of oculomotor commands? Optimal integration of the predicted and the actual sensory feedback. *J Neurosci* 26: 4188-97, 2006.

Vemuri P, Simon G, Kantarci K, Whitwell JL, Senjem ML, Przybelski SA, Gunter JL, Josephs KA, Knopman DS, Boeve BF, Ferman TJ, Dickson DW, Parisi JE, Petersen RC, Jack CR. Antemortem differential diagnosis of dementia pathology using structural MRI: Differential-STAND. *Neuroimage* 55: 522-31, 2011.

Verfaillie K. Perceiving human locomotion: priming effects in direction discrimination. *Brain and cognition* 44: 192-213, 2000.

Viviani P, Berthoz A, Tracey D. The curvature of oblique saccades. *Vision Res* 17: 661-4, 1977.

Wallace JM, Stone LS, Masson GS. Object motion computation for the initiation of smooth pursuit eye movements in humans. *J Neurophysiol* 93: 2279-93, 2005.

Warren WH, Blackwell A, Morris MW. Age differences in perceiving the direction of self-motion from optical flow. *J Gerontol* 44: P147-53, 1989.

Watamaniuk SNJ, Heinen SJ. Human smooth pursuit direction discrimination. *Vision Res* 39: 59-70, 1999.

Wells SG, Barnes GR. Fast, anticipatory smooth-pursuit eye movements appear to depend on a short-term store. *Exp Brain Res* 120: 129-33, 1998.

Wells SG, Barnes GR. Predictive smooth pursuit eye movements during identification of moving acuity targets. *Vision Res* 39: 2767-2775, 1999.

Westheimer G, McKee SP. Visual acuity in the presence of retinal-image motion. *J Opt Soc Am A Opt Image Sci Vis* 65: 847-50, 1975.

Westheimer G. Eye movement responses to a horizontally moving visual stimulus. *AMA Arch Ophthalmol* 52: 932-41, 1954.

Whittaker SG, Eaholtz G. Learning patterns of eye motion for foveal pursuit. *Invest Ophthalmol Vis Sci* 23: 393-7, 1982.

Wiener M, Coslett HB. Disruption of temporal processing in a subject with probable frontotemporal dementia. *Neuropsychologia* 46: 1927-39, 2008.

Wilmer JB, Nakayama K. Two distinct visual motion mechanisms for smooth pursuit: evidence from individual differences. *Neuron* 54: 987-1000, 2007.

Wolpert DM, Ghahramani Z, Jordan MI. An internal model for sensorimotor integration. *Science* 269: 1880-1882, 1995.

Wu W, Gao Y, Bienenstock E, Donoghue JP, Black MJ. Bayesian population decoding of motor cortical activity using a Kalman filter. *Neural Comput* 18: 80-118, 2006.

Wyatt HJ, Pola J. Smooth pursuit eye movements under open-loop and closed-loop conditions. *Vision Res* 23: 1121-1131, 1983.

Xiao Q, Barborica A, Ferrera VP. Modulation of visual responses in macaque frontal eye field during covert tracking of invisible targets. *Cereb Cortex* 17: 918-28, 2007.

Yarrow K, Brown P, Krakauer JW. Inside the brain of an elite athlete: the neural processes that support high achievement in sports. *Nat Rev Neurosci* 10: 585-96, 2009.

Young LR, Forster J, Van Houtte N. A revised stochastic sampled data model for eye tracking movements. *Fourth Ann NASA - University conference on manual control, University of Michigan, Ann Arbor Michigan*. .

Zee DS, Robinson DA. A hypothetical explanation of saccadic oscillations. *Ann Neurol* : 405-414, 1979.

Zhou J, Greicius MD, Gennatas ED, Growdon ME, Jang JY, Rabinovici GD, Kramer JH, Weiner MW, Miller BL, Seeley WW. Divergent network connectivity changes in behavioural variant frontotemporal dementia and Alzheimer's disease. *Brain* 133: 1352-67, 2010.